

We thank all three reviewers for their comments. We have revised the manuscript based on their comments and queries and provided a point-by-point response below. Reviewer comments are in regular black, our response is in blue, text from the manuscript is in red, and additions/updates are in *italic magenta*.

Reviewer 1

This manuscript describes application of the statistical oxidation model (SOM) to predict OA concentrations in a regional chemical transport model. The modeling focuses primarily on the time period for the 2005 SOAR campaign, though there are also some comparisons to the 2010 CalNex campaign. This is the third in a series of papers regarding application of SOM to regional models, and focuses primarily on impacts of I/SVOCs and NO_x on predicted OA concentrations. Overall the manuscript is appropriate for ACP. However, before publication the authors should work to improve the clarity of presentation. As described in my comments below, the manuscript is at times hard to follow.

1. One note on the manuscript format: I can't use the line numbers. The pdf I can see has line numbers from 0-9 that repeat. Thus in my comments I try to cite the page number and quote the relevant text where possible.

We apologize that the line numbers did not translate well when converting the .docx file to a .pdf file.

2. The manuscript is long and at times hard to follow. While the various topics (e.g., POA partitioning, NO_x effects, model-measurement comparison) are placed into organized subsections, there is still a lot of information that the reader needs to keep track of throughout the manuscript. There are nine different case studies (Table 3), each at high and low NO_x, and a number of SOA pseudo-species (aI-SOA, aV-SOA_aromatic, etc.). Maybe his level of complexity is unavoidable because of the scope of the study. Nonetheless, I found myself having to go back and forth between the Methods and Results sections.

While we agree with the reviewer that the paper is long, the length and complexity of the paper stems from the detail in describing and providing context to the model predictions and the model evaluation. As the reviewer points out, the length to a certain extent is unavoidable. In the reviewed version of the manuscript, we have already summarized the findings from the model in the summary and discussion section (Section 5). To help the reader navigate the paper, we have added a glossary early in the manuscript for reference and have added the following text at the end of the introduction: *“To help the reader, we provide a brief overview of the different sections in this manuscript. Section 2 discusses details of the chemical transport model (2.1), organic aerosol model (2.2), simulations performed (2.3), and measurements used for model evaluation (2.4). In Section 3, we first describe the emissions (3.1), spatial distribution (3.2), and precursor contributions to OA (3.3), followed by the influence of vapor wall losses (3.4) and NO_x (3.6) on SOA formation. In the same section, we describe results from sensitivity simulations performed on the most sensitive inputs (3.5). Next, we compare model predictions of SOA precursors (4.1), OA (4.2), POA, and SOA (4.3) mass concentrations, and OA elemental composition (4.4) against measurements in southern California. Finally, we highlight key findings from this work in the summary and discussion section (5).”*.

3. It's not clear to me what the take-home message of this manuscript is. The most striking result, in my opinion, is shown in Figure 3. This figure shows that vapor wall losses are the largest available "knob" for changing SOA predictions. Including vapor wall losses has a bigger impact on SOA predictions than NO_x effects or the inclusion of I/SVOC SOA. Maybe this issue is addressed in more detail in Cappa (2016), but it seems like it deserves more attention in this manuscript. The fact that the SOA predictions are strongly dependent on what amounts to an uncertainty in smog chamber data (because the vapor wall loss is calculated rather than directly sampled) is potentially troubling.

As summarized in Section 5, there are several take-home messages from this manuscript, many of which agree with findings in previous literature: (i) treating the POA as semi-volatile will reduce ambient POA mass concentrations, (ii) parameterizations that have been corrected for vapor wall losses will increase ambient SOA mass concentrations, (iii) S/IVOCs, after accounting for the influence of vapor wall losses, do not contribute as much to the SOA burden as traditional VOC precursors (e.g., aromatics), (iv) accounting for the influence of NO_x may increase SOA mass concentrations in high NO_x/urban regions and (v) updates included in this work seem to improve the model-measurement comparison for OA mass and composition in southern California. As the reviewer points out, the SOA mass concentrations were substantially enhanced after accounting for the influence of vapor wall losses and this was previously discussed in our previous publication (Cappa et al., 2016). But the vapor wall loss finding does not diminish the importance of the other findings surrounding S/IVOCs and NO_x.

4. Emissions: I would suggest toning down the rhetoric on whether certain gasoline and diesel vehicle emission profiles are representative for use in chemical transport models. On both page 3 and pages 20-21 the authors are critical of using either the Schauer et al emissions profiles or of scaling POA emissions to estimate IVOCs. It is a fair criticism that the Schauer emissions profiles are dated (though maybe not too out of date for the 2005 modeling period for SOAR), and that there seem to be better IVOC estimates than scaling POA emissions. However, the authors use the May et al emissions profiles, which include gasoline vehicles up through model year 2010 and DPF-equipped diesel vehicles, and offer no comment on how those profiles might also be inappropriate for a 2005 modeling period. At the very least, it seems like the diesel emissions profile in the model should not include the DPF vehicles tested by May et al, unless there is evidence of significant DPF diesel traffic in California prior to the 2007 change in federal emissions limits for diesels.

We agree with the reviewer that our criticism with the old data came out too strong. We have updated the text in the introduction (Section 1) and the results (Section 3.3) as follows.

Section 1: *"Models have assumed that these data are representative of emissions from modern diesel-powered sources and the POA/IVOC properties from diesel sources are similar to those from other sources. New source data are now available to update the POA and IVOC emissions estimates in chemical transport models."*

Section 3.3: Added the qualifier *"likely to be less representative"* instead of *"very likely to be unrepresentative"* and *"performed on more representative sources"* instead of *"performed on representative sources"*.

The reviewer raises an important point of the compatibility of using the May et al. (2013a, 2013b) data that has sources manufactured after 2005 to inform the POA and IVOC emissions estimates for the vehicle/engine fleet in 2005. For all the data used in this work, there is either no

evidence or very little data to suggest that any of the inputs used in this work were different for sources manufactured before and after 2005. This is now made clear with the following additions in Section 2.2:

- *“Almost three-quarters of the light-duty gasoline vehicles used in May et al. (2013a) were manufactured in or prior to 2005 (the year modeled in this work) and they did not find the POA volatility distribution data to be sensitive to the model year of the vehicle. Hence, the volatility distribution used in this work should still be representative of the vehicle fleet in 2005.”*
- *“May et al. (2013b) did not report on differences in the POA volatility distribution between vehicles that did or did not use a modern emissions control system (diesel particulate filter (DPF) and/or diesel oxidation catalyst (DOC)). Hence, we assumed that the volatility distribution used here was still representative of the mostly non-DPF and non-DOC vehicle fleet in 2005.”*
- *“The IVOC:NMOG fractions did not appear to be statistically different for the gasoline and diesel sources manufactured before or after 2005 and hence those fractions were assumed to be representative of the source fleet in 2005.”*

5. NO_x effects are included in the final model prediction using equations 1-4. These equations are introduced in the Methods section, but the implications of the various corrections are not discussed. Then on page 16 it is noted that a logarithmic function is used. Since NO_x effects are a major focus of this paper, the choice of the logarithmic function needs to be discussed in more detail. For instance, why is a logarithmic function used? Is there a physical basis for using this functional form?

We have cited previous work to justify our choice for the use of VOC:NO_x and NO_x to model the NO_x dependence on SOA formation and provided explanations for the use of linear and logarithmic formulations. The text in Section 2.2.3 was modified as follows: *“Presto et al. (2006) found that the SOA from α -pinene ozonolysis under varying NO_x conditions could be estimated by interpolating the SOA formed between the low and high NO_x conditions using the VOC:NO_x ratio. Hence, in the first method, we used the VOC:NO_x ratios from the low and high NO_x chamber experiments as our bounds and used the 3D model predicted VOC:NO_x ratio to interpolate between the minimum and maximum SOA mass concentrations predicted from the low and high NO_x simulations. Previous work (e.g., Camredon et al. (2007), Xu et al. (2015)) has also found SOA formation to vary along a NO_x scale and hence, in the second method, we used NO_x concentrations from the low and high NO_x chamber experiments and the 3D model predictions to perform the interpolation. For each method, we performed the interpolation on the SOA mass concentrations assuming a linear or logarithmic dependence on the VOC:NO_x ratios and NO_x concentrations. The linear dependency was chosen for simplicity while the logarithmic dependency was chosen to mimic the visual trends in SOA and VOC:NO_x or NO_x reported in previous work.”* The choice of equation 2 (i.e., logarithmic dependence of VOC:NO_x on SOA) for Sections 4 and 5 was based on the SOA being most sensitive to that formulation. None of the equations proposed in Section 2.2.3 have been validated and we added the following sentence to Section 3.6 to make that clear: *“The validity of equation 2 needs to be examined in future work.”*

6. Abstract: "IVOCs did not contribute significantly to SOA mass concentrations in the urban areas" A 15% contribution of IVOCs to SOA does not seem insignificant.

We have reworded the text in the abstract to: *“Model predictions suggested that both SVOCs (evaporated POA vapors) and IVOCs did not contribute as much as other anthropogenic*

precursors (e.g., alkanes, aromatics) to SOA mass concentrations in the urban areas (<5% and <15% of the total SOA respectively) as the timescales for SOA production appeared to be shorter than the timescales for transport out of the urban airshed.”.

7. Page 6 "Seven SOM grids were used" I think this means that the SOA from the 9 classes were tracked separately. Please clarify.

SOA from 9 different precursor types or classes was modeled but tracked in 7 different SOM grids. Monoterpenes and sesquiterpenes were tracked on the same grid since they both used the same SOM parameters to model SOA formation. Similarly, SVOCs and IVOCs were tracked on the same grid. The following text is reproduced from the paper that describes the SOM grid setup: “Seven SOM grids were used to represent SOA formation from nine different precursor classes: (i) long alkanes, (ii) benzene, (iii) high-yield aromatics, (iv) low-yield aromatics, (v) isoprene, (vi) monoterpenes, (vii) sesquiterpenes, (viii) semi-volatile POA (SVOC), and (ix) IVOCs. Classes (i) through (vii) have been included in previous applications of the SOM and we refer the reader to our earlier publications for more details (Cappa et al., 2016; Jathar et al., 2015, 2016). Classes (viii) and (ix) were included in this work for the first time. The SOA formation from monoterpenes and sesquiterpenes (classes vi and vii) was modeled in the same SOM grid since both precursors used the SOM parameter sets for α -pinene. Similarly, the SOA formation from SVOCs and IVOCs was modeled in the same SOM grid and both used the SOM parameter sets for n-dodecane; sensitivity simulations were performed using the SOM parameter set for toluene.”.

8. What are units of Δ LVP in Table 1?

Δ LVP has units of $[\log_{10}] \mu\text{g}/\text{m}^3$. It is the change in vapor pressure with the addition of one oxygen to the carbon backbone. To link the SOM parameters in Table 1 to the text, we have updated the text as follows: “Six precursor-specific adjustable parameters are assigned for each SOM grid: four parameters that define the molar yields of the four functionalized, oxidized products (P_{func}), one parameter that determines the probability of functionalization or fragmentation (m_{frag}) and one parameter that describes the relationship between N_{C} , N_{O} and volatility (Δ LVP).”.

9. Bottom of page 7 - alkane seems to be mistyped as "alke"

We have corrected the ‘alke’ to ‘*alkane*’.

10. Page 9 - IVOCs are modeled as either a C13 or C15 alkane, but above and in Table 1 it is stated that IVOCs are modeled as a C12 hydrocarbon. Please clarify.

Following Jathar et al. (2014), IVOCs from the three combustion sources (gasoline exhaust, diesel exhaust, and biomass burning) are modeled as a C₁₃ or C₁₅ alkane. However, the SOM parameters to model the oxidation chemistry for C₁₃ or C₁₅ (or any other alkane for that matter) are based on fits from chamber experiments performed on a C₁₂ alkane. As the SOM informs the general oxidation scheme and trajectory through the carbon-oxygen grid, the SOA mass yields for C₁₂, C₁₃, and C₁₅ on using the same parameter set for C₁₂ could be different. We have reproduced text from the manuscript that explains this point for SVOCs but one that is equally applicable to IVOCs: “The reactive behavior of POA was modeled by assuming that the POA vapors (i.e. SVOCs) (represented as a hydrocarbon distribution) and their products participated

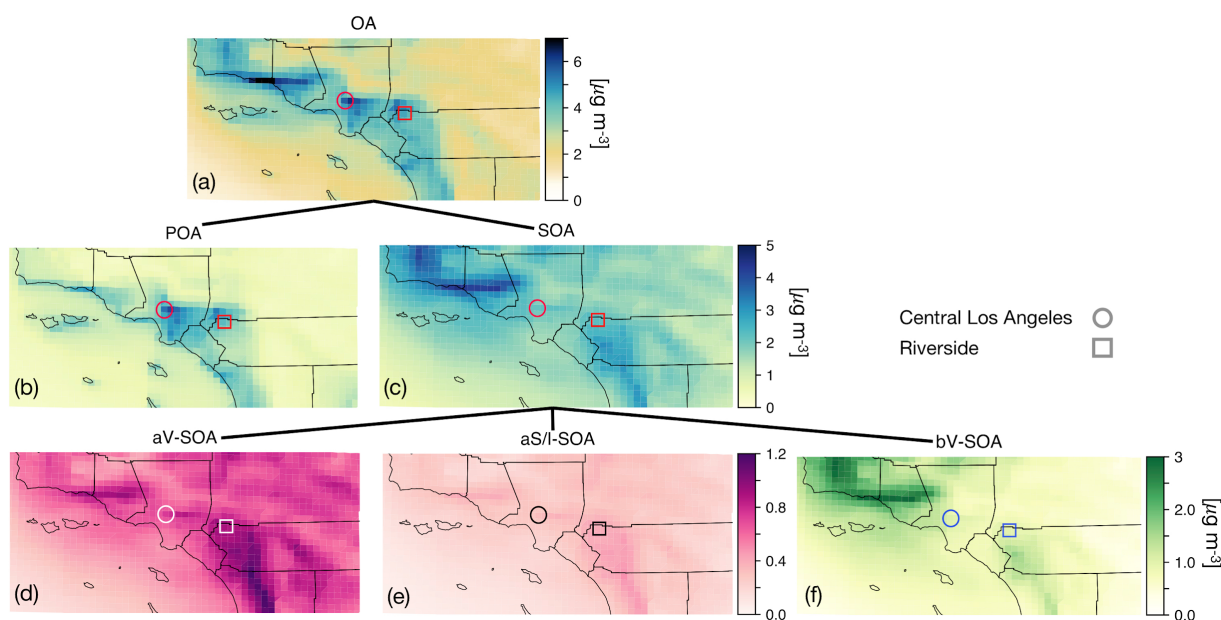
in gas-phase oxidation and formed SOA similar to linear alkanes and utilized the SOM parameter set for n-dodecane. The surrogate, in this case n-dodecane, only informs the multi-generational oxidation chemistry of the precursor and the actual compound of interest (e.g., a C_{15} linear alkane) can have a different SOA mass yield than that of n-dodecane.”. For completeness, however, we have added the following text when describing the methods to model SOA formation from IVOCs: *“As mentioned earlier, n-dodecane, only informs the multi-generational oxidation chemistry of the precursor and the actual compound of interest (e.g., a C_{13} or C_{15} linear alkane) can have a different SOA mass yield than that of n-dodecane.”.*

11. VOC speciation from May et al - is this only for vehicles relevant to the 2005 fleet?

May et al. (2014) did not find the VOC speciation to differ substantially with the vehicle model year and hence the VOC speciation used in this work was representative of the 2005 vehicle fleet.

12. Figure 2 - It would help to label locations of LA and Riverside.

We have added labels denoting the two sites to Figure 2.



13. Page 16 - "In central Los Angeles" - how many grid cells are covered by "central" LA and the whole of LA?

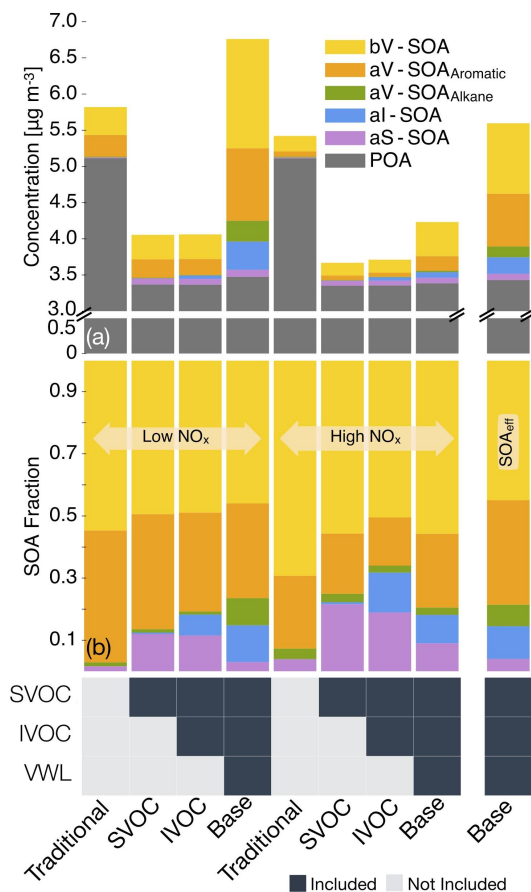
The central Los Angeles site is not referring to an area/region but rather to an EPA CSN (chemical speciation network) site located in ‘central’ Los Angeles. We have added the following text in parentheses in a few instances where we refer to the central Los Angeles site *“(grid cell containing the CSN site)”*.

14. Page 17 compares SOA concentrations in LA and Riverside, and states that a difference of $0.2 \mu\text{g}/\text{m}^3$ of SOA between Riverside and LA is evidence of higher SOA in downwind areas. What is the resolving power of the model (if this were a measurement I would think of the

minimum detection limit or precision)? What is the minimum concentration difference that can be claimed as meaningfully different between two locations?

The resolving power of the model, purely from a numerical perspective, should be quite high (say less than $0.001 \mu\text{g m}^{-3}$). The resolving power of the model should be lower as we consider the uncertainty associated with representing the emissions, chemistry, transport, and deposition in the chemical transport model, all of which will tend to affect the spatial distribution of SOA. We have not done any systematic model experiments to study the resolving power of the model so, as the reviewer points out, we do not know if the $0.2 \mu\text{g m}^{-3}$ difference between the LA and Riverside sites is evidence for higher SOA in downwind areas. However, we should note that the SOA differences between LA and Riverside are retained across our suite of sensitivity simulations. We have altered the text to reflect the reviewer's comment: "SOA mass concentrations, *in contrast to POA*, had a more regional presence *with lesser differences between the upwind and downwind regions* (e.g., $2.4 \mu\text{g m}^{-3}$ in Riverside versus $2.2 \mu\text{g m}^{-3}$ in central Los Angeles) or in regions with high emissions of biogenic VOCs (e.g., $2.5 \mu\text{g m}^{-3}$ inside the Los Padres National Forest).".

15. Figure 3 - panels are not labeled as (a) and (b) as noted in the caption.



This has been corrected.

16. Last line of page 18, the POA reductions between the Traditional and SVOC model case are "more realistic." More realistic than what? The expected POA reduction from May et al (which was not a modeling study)? It seems like the appropriate comparison for how realistic the model

predicted POA concentration is comes from comparing to something like AMS data, not by the fractional evaporation in nonvolatile versus semivolatile POA cases.

The word ‘realistic’ was used here to indicate that we have only considered POA to be semi-volatile from sources where there is evidence for such (i.e., gasoline, diesel, biomass burning, and food cooking sources) and kept the POA from other sources as non-volatile. We have rephrased the sentence as follows: “*The POA mass reductions shown here are conservative and might have been larger if there was evidence that sources other than those considered here (e.g., marine, dust) produced POA that was semi-volatile too.*”. The model predicted POA was compared to the AMS measurements in Section 4.3 to assess how realistic the predictions are.

17. The top of page 30 suggests that missing VOCs from consumer products might be a reason for low predictions at CSN sites. I don’t find this explanation very convincing for several reasons. First, the IMPROVE sites are also under predicted (negative bias for both CSN and IMPROVE), so it’s not clear there is a missing source of urban VOCs. Figure 3 shows that SOA predictions are most sensitive to vapor wall losses, which could easily account for SOA under predictions. Since adding 80 tons/day of IVOC emissions (Figure 1) barely impacts SOA formation (in the case without vapor wall loss), the corresponding source associated with personal care products would need to be huge to make up for the missing SOA.

For the ‘Base-Effective’ model results (and the ‘Base-Low NO_x’ model results), the model-measurement comparison at the IMPROVE sites is better (fractional bias of -16.6%) than at the CSN sites (fractional bias of -53.4%). So, it is possible that the difference in the model-measurement comparison can be attributed to an urban source of SOA. We cite the McDonald et al. (2018) paper because this recent paper makes strong arguments that atmospheric models are missing an important source of SOA in urban areas. We do not think it is the only explanation for the urban-rural differences in the model-measurement comparison and we state in the same paragraph that, “*It is also possible that the urban versus rural/remote continental difference is an artifact of how the SOM models the oxidation chemistry and/or accounts for the influence of vapor wall losses.*”. Furthermore, as the reviewer would agree, there are large uncertainties surrounding the IVOC emissions and their potential to form SOA from volatile chemical products (VCP) so it might be premature to say that the differences observed in this work stem from not including SOA formation from VCP-IVOCs. Accordingly, we have added rearranged the text in that paragraph to give the impression that VCP-IVOCs might be one reason to explaining the urban-rural differences in the model-measurement comparison: “*Given the differences in the model-measurement comparison between the CSN (or urban) and IMPROVE (rural/remote continental) sites, the underprediction at the CSN sites might be indicative of a missing urban source or pathway of OA formation. Recently, McDonald et al. (2018) found that volatile chemical products such as pesticides, coatings, cleaning agents, and personal care products may contribute substantially to IVOC emissions and account for more than half of the anthropogenic SOA formation in southern California. Our underprediction at urban sites might be evidence of missing SOA from volatile chemical product-related IVOC emissions. However, it is also possible that the urban versus rural/remote continental difference is an artifact of how the SOM models the oxidation chemistry and/or accounts for the influence of vapor wall losses.*”.

18. Page 33 "under and over predicted the H:C and O:C" I think this is reversed. O:C is under predicted.

This has been corrected.

Reviewer 2

The manuscript describes the update of a chemical transport model, specifically the UCD/CIT model in which the SOM model has been embedded, to predict OA and SOA in California. The modeling period studied is 14 days during late July and early August 2005. The major advance in this work, compared to previous work published by same group, is the addition of primary IVOCs and SVOCs to the model including treating POA as semi-volatile, while accounting for vapor wall losses during chamber experiments and molecular fragmentation. The authors also examine how NO_x levels impact SOA predictions in the updated model.

The paper is well written, of interest to ACP readers, and appropriate for publication once the following comments have been addressed. I have listed one general comment immediately below followed by more specific and minor comments. Lastly, there is a problem with the manuscript formatting and the line numbers are not displayed correctly in the pdf document. I have thus used the page number and paragraph to indicate the relevant sections of the text. Length of manuscript: I found the manuscript very long to read, but well-written and clear. I think the scope of the research mostly justifies the length of the manuscript.

1. The sole exception is the section regarding future OA concentrations in 2035. This section felt very much like it was “tacked-on” and it is not well developed. Given the uncertainties in the model, how accurate is the model when projected to 30 years into the future? Sensitivity studies should be run to identify how the predictions vary with different model assumptions as was done for the 2005 simulations. Furthermore, what is the value of running a simulation for only a two week period in 2035? If one wants to inform future policy decisions, it would be better to run the simulation for a much longer period (e.g. a few months). Ultimately, it seems like this work is best left for another manuscript, and deleting this part would also shorten the length of the current manuscript.

The primary motivation to perform the future air quality modeling was to raise awareness in the research and regulatory community that SOA formation in the future may be influenced not only by changes in VOC emissions and VOC:NO_x ratios but also by changes in oxidant (e.g., OH) concentrations. Zhao et al. (2017) recently contended that SOA formation in southern California may increase in the future with changes in the VOC:NO_x ratios, despite decreases in SOA precursor emissions. They used a box model to draw those conclusions. Through the use of the air quality model developed in this work, we imply that increases in the OH concentrations from reductions in NO_x could be much more important in determining ambient SOA mass concentrations than changes in the VOC:NO_x ratios. Our future air quality modeling results are not intended to accurately capture the absolute concentrations in a future world but rather to communicate the sensitivity of future SOA to changes in emissions, chemical regimes, and oxidant loadings. Sensitivity simulations similar to those performed for the 2005 episode would not change the percentage changes in OA-POA-SOA mass concentrations. Our model results contribute to this evolving discussion since they include the latest knowledge about SOA formation in a 3D model framework.

2. Introduction, page 3, paragraph 2: The text here stating that SOA formation schemes have been rarely validated against experimental data is too strong or needs to be nuanced. One can, for example, cite the following modeling studies where P-S/IVOCs are treated and models are compared against measurements.

Fountoukis et al. Atmos. Chem. Phys. 2016, 16, 3727-3741.

Murphy et al. Atmos. Chem. Phys. 2017, 17, 11107-11133.

Zhang et al. Atmos. Chem. Phys. 2015, 15, 13973-13992.

We agree with the reviewer. We have revised the text to say that some studies have validated the SOA formation schemes against experimental data and included the recommended citations:

“While some of these schemes have been validated against experimental data (Fountoukis et al., 2016; Hodzic and Jimenez, 2011; Murphy et al., 2017; Zhang et al., 2015), most have assumed that all sources have the same rate and potential to form SOA and, in some cases, ignore fragmentation reactions tied to multigenerational chemistry.”.

3. Page 8, second paragraph: what is meant by “carbon-equivalent linear alkane”?

‘Carbon-equivalent’ here means that the POA hydrocarbon included in the model has the same reaction rate constant with OH as a linear alkane with the same number of carbon atoms.

4. Is it reasonable to assume that linear alkanes can be used to estimate OH reaction rate constants of SVOCs, given that branched alkanes represent a large portion of POA mass?

The reviewer is right to point out that if the POA mass is mostly comprised of branched/cyclic alkanes (and perhaps even aromatics), as we point out later in that paragraph, the reaction rate constants with OH would be larger than the carbon-equivalent linear alkane. We acknowledge this limitation in the following sentence: *“We should note that the presence of branched/cyclic alkane and aromatic compounds in the SVOCs would require the use of a higher reaction rate constant with OH as these compounds are more reactive with OH than carbon-equivalent linear alkanes.”.*

5. Section 2.2.2, last paragraph: Is it correct to state that the model is consistent with Gordon et al.? From the text, it seems that the yields in the model are different versus the Gordon et al. smog chamber studies, but it is expected that the difference in SOA yields will be compensated for by the fact that emissions are different relative to work of Zhao et al.

Based on the work of Jathar et al. (2014), the linear alkane surrogate used to model the IVOCs from gasoline, diesel, and biomass burning sources was chosen to reproduce the SOA formation observed in chamber data (Gordon et al., 2014a, 2014b; Hennigan et al., 2011). This was stated earlier through the following sentence: *“The equivalent linear alkane to model SOA formation from IVOCs in Jathar et al. (2014) was based on fitting the SOA formation observed in chamber experiments (Gordon et al., 2014a; Gordon et al., 2014b; Hennigan et al., 2011) and hence the choice of the hydrocarbon in this work was experimentally constrained.”.* We have added the citations for the chamber studies to be clear. The two subsequent paragraphs describe the differences of our IVOC-SOA model with the work of Zhao et al. (2015, 2016).

6. Section 2.2.3: It would improve the manuscript if the choice of the equation where there is a logarithmic dependence on the VOC/NO_x ratio, among the four equations presented, were better

justified based on chemical reasons. Currently, the justification is essentially based on the observation that this equation results in the highest SOA prediction.

We have cited previous work to justify our choice for the use of VOC:NO_x and NO_x to model the NO_x dependence on SOA formation and provided explanations for the use of linear and logarithmic formulations. The text in Section 2.2.3 was modified as follows: “*Presto et al. (2006) found that the SOA from α -pinene ozonolysis under varying NO_x conditions could be estimated by interpolating the SOA formed between the low and high NO_x conditions using the VOC:NO_x ratio.* Hence, in the first method, we used the VOC:NO_x ratios from the low and high NO_x chamber experiments as our bounds and used the 3D model predicted VOC:NO_x ratio to interpolate between the minimum and maximum SOA mass concentrations predicted from the low and high NO_x simulations. *Previous work (e.g., Camredon et al. (2007), Xu et al. (2015)) has also found SOA formation to vary along a NO_x scale and hence, in the second method, we used NO_x concentrations from the low and high NO_x chamber experiments and the 3D model predictions to perform the interpolation. For each method, we performed the interpolation on the SOA mass concentrations assuming a linear or logarithmic dependence on the VOC:NO_x ratios and NO_x concentrations. The linear dependency was chosen for simplicity while the logarithmic dependency was chosen to mimic the visual trends in SOA and VOC:NO_x or NO_x reported in previous work and also to produce the highest response in the SOA formation with NO_x.”. The choice of equation 2 (i.e., logarithmic dependence of VOC:NO_x on SOA) for Sections 4 and 5 was based on the SOA being most sensitive to that formulation. None of the equations proposed in Section 2.2.3 have been validated and we added the following sentence to Section 3.6 to make that clear: “*The validity of equation 2 needs to be examined in future work.*”.*

7. Table 3: A clarifying question: were the vapor wall losses corrected for VOCs in all the simulations? Even in the traditional case? This is what is indicated by the table, but in the text below it is simply stated “no correction for chamber vapor wall losses”, which would seem to exclude also the application of the correction to the VOCs.

The vapor wall loss corrected SOM parameterizations were either applied for all SOA precursors or not at all. This is now clarified in the caption for Table 3.

8. Page 19, last sentence: using a 20% yield as an approximate SOA mass yield seems too low, given that earlier in the same paragraph estimated yields for SVOC oxidation ranged from 33% to 86%. I also think the oxidation rate constant is a little low, given that octadecane and nonadecane (for example) have rate constants that are greater than 2e-11 cm³ molecules⁻¹ s⁻¹, and these compounds likely represent a lower limit as oxidation rates increase with alkane branching. Also, how was the wind speed of 5 miles per hour chosen?

We thank the reviewer for this comment. The reviewer is correct to point out that we need to use a higher SOA mass yield. The way the calculation was done assumed that all of the SOA from SVOC oxidation in the Los Angeles grid cell was from 20 miles away. As the central Los Angeles site is only 10 miles from the coast and the prevailing winds are from west to east, our calculation represented an upper bound on the chemical conversion efficiency. We have revised our calculation and the text to represent the minimum and maximum chemical conversion efficiencies assuming that the SOA from SVOC oxidation arose from SVOC emissions in the same grid cell to up to 2 grid cells away (up to 12.5 miles away). The wind speed of 5 miles per hour was based on the average wind speed in central Los Angeles in the month of July. In our

revised calculation and updated text, we have updated the wind speed to 5.4 miles per hour based on data gathered from Weather Spark (a website that collates meteorological information). The update text is as follows: *“If we assume that most of the sS-SOA in the grid cell that contains the Los Angeles site was from the oxidation of SVOCs released in that grid cell and from grid cells that are up to two grid cells away, our results do not appear unrealistic. For example, for an SOA precursor with an OH reaction rate constant of $2.4 \times 10^{-11} \text{ cm}^3 \text{ molecules}^{-1} \text{ s}^{-1}$ (average value from a C₁₈ and C₂₀ linear alkane) and an SOA mass yield of 60% (average from the SOA mass yield range described earlier for a C₁₈ and C₂₀ linear alkane), the chemical conversion efficiency would be 3.5-15% with a daily-averaged OH concentration of $1.5 \times 10^6 \text{ molecules cm}^{-3}$ and a reaction time of 0.5-2.3 hours. A reaction time of 0.5 to 2.3 hours corresponds to a transport of 2.5 (half a grid cell) and 12.5 (2.5 grid cells) miles at an average wind speed of 5.4 miles per hour (Weather Spark).”*.

9. Page 20: The statement saying IVOCs as a bulk class of SOA precursors may not contribute substantially to ambient SOA levels is too strong. There is an important contribution, especially if one only considers anthropogenic SOA, even though that contribution may be less than that from traditional VOCs.

The sentence the reviewer mentions and the following sentence have been combined to change the tone as follows: *“Our simulations imply that IVOCs might be as influential as SVOCs as a bulk class of SOA precursors but they were still less important than the traditional SOA precursors (that included long alkanes and aromatics) in contributing to ambient SOA levels.”*.

10. Page 21, first paragraph, last sentence: I don’t disagree with the value of the work presented in the manuscript, but, in my opinion, what is really unique is the incorporation of these 4 elements into a chemical transport model. It seems that should be mentioned somewhere in this sentence.

We agree with the reviewer on this point and have updated the sentence as follows: *“In this work, we (i) rely on a comprehensive set of IVOC emissions estimates made from measurements performed on representative sources, (ii) model fragmentation reactions during IVOC oxidation, (iii) to some degree constrain SOA formation from IVOCs with chamber experiments, (iv) to some degree account for the influence of vapor wall losses in chamber experiments, and (v) include all of the previously mentioned updates in a chemical transport model.”*.

11. Page 32, Line 3: I think there is a typo here and the measured value given is incorrect and should be 1.9 rather than 2.2.

This has been corrected.

12. Page 32, first paragraph, last sentence: The comparison of HOA to POA from mobile sources is rather good. It would be worthwhile to point that out.

The wording was changed to: *“We did not model POA from mobile sources separately but if we assumed that mobile sources only accounted for about a quarter of the partitioned POA mass in southern California (based on Figure 1), our estimated Base model predictions of POA mass concentrations from mobile sources of $0.85 \mu\text{g m}^{-3}$ ($=3.4 \times 0.25$) would compare reasonably with the measured HOA mass concentrations of $1.20 \mu\text{g m}^{-3}$.”*.

13. Figure S5: Why do the b-alkanes have an enhancement of less than 1 under high NO_x conditions? Doesn't correcting for the wall losses always increase the SOA yield?

The SOM parameters for branched alkanes were based on chamber experiments performed on methylundecane. These parameters, relatively speaking, indicate a higher propensity to fragment since the P_{frag} value is lower and the functionalized products have more oxygens added to the carbon backbone per reaction step. This suggests that in the absence of vapor losses to the chamber wall fragmentation will become progressively more important during a chamber experiment. Hence, the most likely explanation for an enhancement less than 1 for smaller carbon number branched alkanes is that the chamber wall absorbs and protects some of the oxidation products from being fragmented.

Minor comments:

14. Table 1: Simply for the sake of clarity, the order of the molar yields should be indicated. Do they progress (left to right) from the addition of 1 to 4 oxygen atoms per reaction, or is it the opposite order?

Thanks for the comment. We have added the labels P_{f1} through P_{f4} below the label P_{func} to the make this clear. We have also added this detail in the caption.

15. Table 2: There is an "&" symbol in the footnotes of the table, but I cannot find the matching symbol in the table or table caption.

The '&' applies to the calculation of the VOC:NO_x ratio for all low NO_x experiments. The table reproduced below captures that change.

Table 2: Low and high VOC:NO_x ratios in ppb ppb⁻¹ from chamber experiments used to model the influence of NO_x on SOA formation.

SOM surrogate	(VOC:NO _x) _{low} NO _x	NO _{x,low} NO _x	(VOC:NO _x) _{high} NO _x	NO _{x,high} NO _x	Reference
<i>n</i> -dodecane	17.0 ^{&}	<2 ppbv	0.09	343	Loza et al.(2014)
benzene	207 ^{&}	<2 ppbv	1.98	169	Ng et al.(2007)
toluene	46.3 ^{&*}	<0.8 ppbv	0.76 [*]	50	Zhang et al.(2014)
<i>m</i> -xylene	12.1 ^{&#}	<2 ppbv	0.10	943	Ng et al.(2007)
isoprene	24.5 ^{&}	<2 ppbv	0.29	937	Chhabra et al.(2010)
α-pinene	33.1 ^{&}	<2 ppbv	0.05	844	Chhabra et al.(2010)

[&]minimum VOC:NO_x ratios since these assume a NO_x concentration of 0.8 ppbv in the chamber

^{*}average of six experiments performed by Zhang et al.(2014)

[#]average of two experiments performed by Ng et al.(2007)

16. Page 7: There appears to be a typo on the last line of this page.

The typo has been corrected.

17. Section 2.2.3: Were the IVOCs and gas phase SVOCs used to calculate the modeled VOC:NO_x ratios? These compounds would contribute to the HO₂ budget, although likely less than the VOCs.

Yes, the gas-phase IVOCs and SVOCs were used to calculate the modeled VOC:NO_x ratios. We have added this detail to the text: “For the VOC:NO_{x,model} ratio, the VOC is the sum of all organic species tracked in the SAPRC-11 gas-phase chemical mechanism, including all IVOCs and gas-phase SVOCs.”.

18. Page 16, last paragraph: a reference should be provided for the measured mass concentrations of POA over the open ocean west of California.

The correct reference for this Hayes et al. (2013) and this has been added to the end of that sentence.

19. Page 28: What was the measured aromatic concentration ratio between 2005 and 2010 at the Los Angeles-North Main Street site?

As stated in the parentheses, the measured aromatic concentration ratio between 2005 and 2010 at the Los Angeles-North Main Street site was 1.67. This ratio was consistent with the 2005(modeled)-to-2010(measured) ratio of aromatic concentrations of 2 at Pasadena.

20. Page 29, last sentence: it should be clarified that the 27 measurements available for comparison are measurements taken at IMPROVE sites. (At least I think that is the case, it is not entirely clear from the manuscript.)

This is now made clear that the 27 measurements are at the IMPROVE sites: “Of the 27 IMPROVE measurements available for comparison, 22 or ~80% of the model predictions corrected for NO_x were within a factor of two of measurements with little bias (fractional bias=-16.63%).”.

21. Page 34, lines 1 – 2: There may be a typo here. I thought the argument was the timescales for SOA formation are LONGER than the timescales for transport out of the urban airshed.

Yes, that is correct. The sentence has been corrected.

22. Page 36, references: The reference from the American Lung Association doesn’t seem to be correct as it contains a link to a website about air quality in Fort Collins, Colorado. In addition, the organization name is shortened as if it is an author’s name.

We apologize for this oversight. This has been corrected.

23. Supporting information: Some of the tables and figures and their matching captions are split across different pages. For readability, each figure and table should appear entirely on one page with its caption.

This has been fixed.

Reviewer 3

Reviewer comments on "Simulating secondary organic aerosol in a regional 1 air quality model using the statistical oxidation model – Part 3: Assessing the influence of semi-volatile and

intermediate volatility organic compounds and NOX," acp-2018-616 This work describes an update to the UCD/CIT chemical transport model, specifically by the inclusion of the SOM organic aerosol model. The impacts of various improvements are described and investigated, such as the inclusion of SVOC and IVOC oxidation. In general, the methods are well described, and the results are reasonable. The manuscript is well within the scope of the journal, and warrants publication with minor revisions as described below.

Major comments:

1. The manuscript is fairly lengthy and detailed. While this is reasonable for a detailed description of model improvements, it can make it difficult to keep track of the main points at times. I wonder if some of the results could be boiled down to really the key points, and some of the subtleties moved to the supplement.

While we agree with the reviewer that the manuscript is lengthy, the length was dictated by the breadth of findings discussed. The key findings are brought together and summarized in the 'Discussion' section, alongside its implications for the atmospheric modeling of OA in urban environments. The 'Discussion' section hence provides an overview of the key results of this study. To help the reader navigate the manuscript, we have added the following text at the end of the introduction: *"To help the reader, we provide a brief overview of the different sections in this manuscript. Section 2 discusses details of the chemical transport model (2.1), organic aerosol model (2.2), simulations performed (2.3), and measurements used for model evaluation (2.4). In Section 3, we first describe the emissions (3.1), spatial distribution (3.2), and precursor contributions to OA (3.3), followed by the influence of vapor wall losses (3.4) and NOX (3.6) on SOA formation. In the same section, we describe results from sensitivity simulations performed on the most sensitive inputs (3.5). Next, we compare model predictions of SOA precursors (4.1), OA (4.2), POA, and SOA (4.3) mass concentrations, and OA elemental composition (4.4) against measurements in southern California. Finally, we highlight key findings from this work in the summary and discussion section (5)."*

2. As a chemistry-minded member of our community, a frequent point of confusion for me is in discussion of IVOC with lack of precision around the chemical composition being represented. In this case, IVOC is being used to mean non-speciated intermediate volatility combustion emissions, which are primarily branched and cyclic aliphatics and some aromatics. Yet they are represented by n-alkanes (which likely differ in their SOA yields), and are somehow grouped separately than "long alkanes and aromatics", despite this being a reasonable description of these IVOCs (I presume the latter refers to speciated emissions?). It would be helpful to be more precise in the language and consider in the discussion what these emissions likely are.

We agree with the reviewer. We have added more detail in Section 2.2.2 to be clear about we define, add, and model IVOCs in this work as a new SOA precursor and how the IVOCs added to the model in this work are distinct from the speciated long alkane and aromatic precursors already present in the emissions inventory. We reproduce part of that section with updates here: *"In Jathar et al. (2014), IVOC emissions, defined as the sum of all unspeciated compounds, were determined as a mass fraction of the total non-methane organic gas (NMOG) emissions for three different source categories: gasoline vehicles, diesel vehicles, and biomass burning. Here, the IVOCs, as unspeciated organic compounds, are new SOA precursors added to the emissions inventory and regardless of their chemical makeup are distinct from the speciated precursors*

such as long alkanes and aromatics already present in existing emissions inventories. ... The equivalent linear alkane to model SOA formation from IVOCs in Jathar et al. (2014) was based on fitting the SOA formation observed in chamber experiments and hence the choice of the hydrocarbon in this work was experimentally constrained. Jathar et al. (2014) used linear alkanes as a surrogate as the SOA formation from linear alkanes was well studied when they developed the parameterization and the SOA mass yields increased predictably with the carbon number of the precursor. Recent application of gas-chromatography mass-spectrometry to combustion emissions has found that IVOCs are mostly composed of branched/cyclic alkane and aromatic compounds (Gentner et al., 2012; Koss et al., 2018; Zhao et al., 2016, 2017). So while it would have been more appropriate to model the IVOCs as an alkane-aromatic mixture, this choice would not have substantially changed the model predictions in the work as the SOA formation from this alkane-aromatic mixture would still be constrained to the same chamber experiments. We will consider the recent detailed speciation work surrounding IVOCs in future applications of this model. In this work, we also investigated the sensitivity in model predictions to the use of an aromatic compound (i.e., toluene) as a surrogate instead of an alkane (i.e., n-dodecane) to model SOA formation from IVOCs (see rationale in Section 2.4).”.

The following text was added to Section 5 to motivate future work with detailed speciation now available for IVOCs from some combustion sources: *“The IVOCs in this work were modeled using a linear alkane surrogate despite recent evidence that IVOCs in combustion emissions are a mixture of branched and cyclic alkanes, aromatics, and oxygenated compounds with very few linear alkanes (Koss et al., 2018; Zhao et al., 2016, 2017). A more chemically appropriate representation of the IVOCs would not have substantially changed the findings in this work since the linear alkane surrogates were chosen to reproduce the SOA formation in chamber experiments performed on combustion emissions. However, future work should incorporate the more detailed speciation available to model the emissions and SOA formation from IVOCs.”.*

3. This line numbering approach is maddening bordering on useless. Please in the future use unique line numbers for all lines on a given page, or better yet use continuous line numbers throughout the document. When I copy and paste into notepad, I see digits before the final appear and are continuous, so perhaps this is just a conversion issue?

We apologize that the line numbers did not translate well when converting the .docx file to a .pdf file.

4. Page 1, paragraph 1: extra space before "gas/particle"

This has been corrected.

5. Page 3, line 3: remove comma after "formed"

This has been corrected.

6. Page 3, paragraph 1: IVOCs are not necessarily unique from "aromatics and long alkanes", in fact as the authors point out that is in large part what they contain (plus cyclic and polycyclic aliphatics), so the wording seems a bit off. I would also direct the authors to Gentner et al., PNAS, 2012 (doi: 10.1073/pnas.1212272109), for a detailed analysis of the composition of combustion emissions in the IVOC range (e.g. diesel fuels), and that work in general that

suggested substantial OA formation from diesel fuel components (i.e. IVOCs). Similarly Worton et al. (ES&T, 2014, doi: 10.1021/es405375) found POA from all sources to "look like" motor oil, which was heavily cyclized and branched.

The reviewer is right to point out that the sentences were not consistent. They have been corrected as follows and now include a citation to Gentner et al. (2012): “In addition, all combustion processes are now believed to include emissions of an important additional class of SOA precursors: intermediate-volatility organic compounds (IVOCs) (Jathar et al., 2014). Gas-chromatography mass-spectrometry applications have suggested that they are primarily composed of high molecular weight *linear, branched, and cyclic* alkanes (carbon numbers greater than 12) and aromatics (Gentner et al., 2012; Zhao et al., 2014, 2017).”. Thank you for mentioning the Worton et al. (2014) study. It has already been mentioned later (Section 2.2.2) when explaining the rationale of using alkanes as a surrogate to model the chemistry and gas/particle partitioning of POA/SVOCs.

7. Page 4, paragraph 2: 500 ppbv is very high NO_x indeed - are these general trends applicable to more ambient-relevant conditions?

We apologize for the error but the parentheses should have read ‘>50 ppbv’ instead of ‘>500 ppbv’. Previous ‘high NO_x’ chamber experiments have been performed across a range of initial NO_x values spanning from 50 ppbv to 1 ppmv. We have modified the text in the parentheses to ‘>50 ppbv and up to ~1 ppmv’. To answer the reviewer’s question, the trends in SOA mass yields with NO_x seem applicable to even atmospherically-relevant concentrations of NO_x since chamber experiments performed at even modestly high NO_x concentrations (~100 ppbv) produce differences in SOA mass yields between low and high NO_x experiments (e.g., for toluene as shown in Zhang et al. (2014)). What still remains unclear, however, is how the SOA mass yields vary over a continuous range of initial NO_x concentrations and how changes in the NO_x concentrations during the chamber experiment or transport from high NO_x to low NO_x environments affect the SOA mass yield.

8. Page 4, paragraph 3: Should be "i.e., Henze", because the authors mean "in other words", not "for example".

This has been corrected.

9. Page 6, paragraph 2: Though dodecane probably has an approximately appropriate volatility and chain-length, the true chemical composition of combustion related I/SVOCs contains much for branching and cyclization. For future work I would recommend generating an SOM grid for a branched alkylcyclohexane or some similar such compound, if possible.

We agree with the reviewer’s comment that S/IVOCs, based on previous emissions characterization work, are more likely to be branched or cyclic alkanes rather than linear alkanes and that parameterizations based on a branched/cyclic alkane would have been more appropriate for use in our work. We accept this to be a limitation of the current work and in future work we will plan to use parameterizations for branched/cyclic alkanes (e.g., SOM parameters developed for methylundecane and hexylcyclohexane by Cappa et al. (2013)) to model the SOA formation from SVOCs. We have added some more detail to Section 2.2.2 and Section 5 based on the reviewer comment here and earlier (#2) to articulate the motivation for using linear alkanes

instead of branched/cyclic alkanes and how they will not affect the findings from this work. To review the exact additions to the manuscript, see response to comment #2.

10. Page 7, last line: misspelled alkane

This has been corrected.

11. Page 8, paragraph 2: Gentner et al. (2012) estimated that branching and cyclization, which likely dominate I/SVOCs decrease SOA yields by a factor of around 3 (based on compiled chamber data available at that time). The assumption of a linear alkane SOM grid could consequently have a significant impact on SOA produced in this work. The authors point to Gentner and Caravaggio to justify that "alkanes" are the substantial fraction, but this somewhat obscures the fact that these alkanes are not linear, which may be important.

We completely agree with the reviewer on this comment, which is similar to those raised earlier (comments #2 and #9). The choice of a linear alkane to model the SOA formation from IVOCs should not have an effect on the model predictions in this work since the linear alkane choice was constrained to results from chamber experiments performed on combustion emissions from gasoline, diesel, and biomass burning sources. We have updated the text in Sections 2.2.2 and 5 to make this clear. To review the exact changes, we refer the reviewer/editor to our response to comment #s 2 and 9.

12. Page 14, paragraph 1: I'm a bit confused, if measured OA:OC is 1.8-2.1, but are the authors using 1.6?

An OA:OC ratio of 1.6 was used for the OC measured at the CSN (more urban) sites and an OA:OC ratio of 2.1 was used for the OC measured at the IMPROVE (more rural/remote) sites. The OA:OC ratio measured by Docherty et al. (2011) was 1.77, which was close to the value we used for the OC measured at the CSN site.

13. Figure 1 and discussion therefore: The terminology of splitting "IVOC" and "long alkane and aromatics" is a bit confusing, since the IVOCs are being modeled as long alkanes, and is comprised of alkanes and aromatics. I would recommended something more like "speciated" and "unspeciated", or "lumped". It's not totally clear to me what is a long alkane, and what is an IVOC, but perhaps I missed it in the methods?

IVOCs, as defined and described in Section 2.2.2, are unspciated organic compounds found in combustion emissions with C^* values mostly smaller than $10^6 \mu\text{g m}^{-3}$. In this work, the SOA formation from these IVOCs, regardless of their actual chemical makeup, was modeled by using a linear alkane as a surrogate, based on the work of Jathar et al. (2014). It is a separate matter that recent work with mobile source emissions has suggested that the IVOCs may in fact be a combination of branched/cyclic alkanes and aromatic compounds (e.g., for gasoline vehicle emissions suggested by Zhao et al. (2016)). Long alkanes, on the other hand, are emissions of alkanes that are currently in the emissions inventory but rarely include emissions of alkanes with C^* values smaller than $10^6 \mu\text{g m}^{-3}$ (Pye and Pouliot, 2012). Given that the IVOCs and long alkanes are approximately separated in C^* space (above and below $10^6 \mu\text{g m}^{-3}$) and treated separated in the emissions inventory, the IVOC label used in Figure 1 and throughout this work does not conflict with that of long alkanes. We agree with the reviewer that this needs to be made

clear in the manuscript. We have added some clarification in Section 2.2.1: *“Long alkanes as a precursor class includes linear, branched, and cyclic alkanes roughly up to a carbon number of C₁₃ and represent speciated alkanes present in existing emissions inventories. These long alkanes are distinct from the alkanes that might be present in SVOC and IVOCs. High-yield and lower-yield aromatics include all speciated aromatic compounds present in existing emissions inventories and, similar to the long alkanes precursor class, are distinct from the aromatics that might be present in SVOC and IVOCs.”*. We have also added the following text in Section 2.2.2: *“Here, the IVOCs, as unspeciated organic compounds, are new SOA precursors added to the emissions inventory and regardless of their chemical makeup are distinct from the speciated precursors such as long alkanes and aromatics already present in existing emissions inventories.”*.

14. Page 17, end of paragraph 1: What might explain this underestimation in SOA? Particularly given that the use of linear alkanes as proxies likely overestimates the SOA yield of some of these groups? Do the later changes to the model fix this regional underestimation?

The final version of the model used in this work (Base) still underestimates the SOA mass concentrations in southern California. The use of linear alkanes does not overestimate the SOA mass yield from IVOCs since the choice of the linear alkanes was constrained to chamber experiments (see earlier response to comments #2). As discussed in Section 5, the most likely reason for the underestimation might be a missing urban source or chemical pathway of SOA. It is also possible that the underestimation might be from the use of lower vapor loss rates in chambers than those recently suggested by Huang et al. (2018). We have added the following text in Section 5 to highlight the implications of this recent work: *“Recent work suggests that the vapor wall loss rates to the Teflon wall might be two or more times larger than the rates used in this work to develop the SOM parameters (Huang et al., 2018; Krechmer et al., 2016). The use of these faster rates will tend to increase the model predicted SOA mass concentrations and help explain the underpredictions with ambient measurements.”*.

15. Page 17, end of paragraph 1: missing a period

This has been corrected.

16. Page 20, paragraph 3: "Our simulations imply that IVOCs as a bulk class of SOA precursors may not contribute substantially to ambient SOA levels." Again, I'm not quite sure what to make of this statement, as long alkanes may include species that would be considered IVOCs, so I'm a bit confused by imprecision in language around these compound classes.

The distinction between long alkanes, aromatics, and IVOCs has been made clear in the revised manuscript. See responses to reviewer comment #2 and #13. We have revised the statement the reviewer is referring to as follows: *“Our simulations imply that IVOCs might be as influential as SVOCs as a bulk class of SOA precursors but they were still less important than the traditional SOA precursors (that included long alkanes and aromatics) in contributing to ambient SOA levels.”*.

17. Page 22: The authors discuss the impact of faster reaction times, but what about the impact of high volatility preventing wall loss. Does a C₆ compound really suffer substantial wall loss,

given its ability to re-partition to the gas phase? I would expect most losses to be centered in the IVOC range (less reversibly absorbing to the walls).

It is important to remember that vapor wall losses affect both the precursor and the intermediate oxidation products that are still in the gas/vapor phase. Volatile precursors (such as the C₆ compound that the reviewer mentions) are not irreversibly lost to the walls but the oxidation products from the first few generations of chemistry might be in the gas/vapor phase as they are still too volatile to partition to the particle phase (with possibly in the IVOC range) and hence susceptible to loss to the chamber walls. In contrast, intermediate-volatility precursors have shorter chemical lifetimes and go through fewer steps of oxidation to form SOA, which makes them less susceptible to vapor wall losses.

18. Page 26, paragraph 2: The discussion of equations 1-4 is a bit unclear. It would be helpful to remind the reader of the implications of each equation.

We have added the following sentence to remind the reader of the functional form of the equation: *“To remind the reader, equations (1) and (2) assume a linear and logarithmic dependence respectively between the SOA mass concentration and the VOC:NO_x ratio. Equations (3) and (4) assume a linear and logarithmic dependence respectively between the SOA mass concentration and the NO_x concentration.”*.

19. Figure 8, Table 4 and discussion thereof: What does it mean from a practical sense that the correlations here are so poor. While I acknowledge the biases and averages are not unreasonable, the model appears unable to capture the temporal variability of these measurements - is that simply due to poor resolution in emissions databases, or is there additional important complexity being ignored? The concern of course is that it might be telling us something more fundamental about the assumptions or applications of the model.

This is an important discussion point and we thank the reviewer for the comment. To expand on what the reviewer is suggesting, the poor correlations are indicative of poor model skill where the model is unable to accurately capture the temporal or spatial variability in the measurements. However, the model skill showcased here, particularly for OA, is not very different than that produced by other models in the literature. For example, Baker et al. (2015) in an application of the Community Multiscale Air Quality (CMAQ) model reported an R² of 0.0036 for their base model and an R² of 0.10 for a sensitivity simulation for OA over all CSN and IMPROVE sites in southern California. In this work, we report R² values of 0.13 and 0.079 over the CSN and IMPROVE networks respectively, which are slightly better than those reported by Baker et al. (2015) in the same geographical area but a different time period. However, Murphy et al. (2017) in an application of a similar CMAQ model over the contiguous United States reported an higher R² of 0.26 for OA over all CSN and IMPROVE sites. Similarly, Ahmadov et al. (2012) in an application of the Weather Research and Forecasting - Chemistry (WRF-Chem) model reported an R² between 0.30 and 0.37 for OA over CSN and IMPROVE sites in the eastern United States. If representative, the Murphy and Ahmadov results suggest that the emissions and chemistry of OA (and perhaps even the meteorology) are not well represented by models in the southern California region. There are numerous reasons for why the model skill may be so poor in this region. One of the reasons, as the reviewer suggests, could be the poor spatial and temporal resolution offered in the emissions inventory. But we have not explored this aspect in our work. The reviewer's comment about model skill is discussed in Section 4.2: *“The model skill,*

captured by the R^2 values, for all model simulations at both the CSN and IMPROVE sites was quite poor, but still slightly better than that found in earlier work for the southern California region with the CMAQ model (Baker et al., 2015). However, the model skill was much worse than that reported in earlier work with CMAQ (e.g., Murphy et al. (2017)) and WRF-Chem (e.g., Ahmadov et al. (2012)) over regions other than southern California, suggesting that there might be missing emissions sources and/or chemical pathways or meteorological considerations that contribute to the poor model skill in southern California.”.

20. Figure 9: It’s not clear why an O:C of 0.078 was chosen. I imagine it comes from the measurements, but it’s not obvious where this is stated. Update: I see it is stated later, this should be brought forward to discussion of the figure or the caption.

We have added the necessary citation to the caption of Figure 9: *”The three different predictions show results from the Base simulations for OA assuming no change, the POA O:C was fixed to 0.078 based on the measurements of Docherty et al. (2011), and no POA.”.* We also added detail to Section 4.4 to link the various model predictions discussed in the text to those in Figure 9. For example, *“For the Base simulations (shown as orange box plots), model predictions of H:C were significantly overpredicted and those for O:C were significantly underpredicted although the predictions did capture dips in the H:C and the peaks in the O:C ratios in the mid-afternoon, coincident with peak photochemical activity.”.* Similar changes were made elsewhere in Section 4.4. when referencing the predictions in Figure 9.

21. Page 34 paragraph 3: Given how big a role vapor wall loss correction plays in the model, it would be helpful to have some discussion of how exactly it is being corrected for. This manuscript just references previous studies, but it warrants some overview here.

We rely on the SOM parameters developed in Cappa et al. (2016) based on the methods described in Zhang et al. (2014), to account for the influence of vapor wall losses in Teflon chambers. As these methods have been previously described in the earlier work, we do not feel the need to include a detailed description of how the wall losses were modeled, at the expense of increasing the length of this manuscript. We have added the following text in Section 2.2.1 when describing the wall loss-corrected SOM parameters for the first time: *“Details about how the vapor wall losses were modeled are described in Zhang et al. (2014) and Cappa et al. (2016). Briefly, loss of vapors to the Teflon walls of the chamber was modeled reversibly where the first-order uptake to the walls was assumed to be $2.5 \times 10^{-4} \text{ s}^{-1}$ and the release of vapors from the walls was modeled using absorptive partitioning theory with the Teflon wall serving as an absorbing mass with an effective mass concentration of 10 mg m^{-3} . Recent work has argued that vapor wall loss rates in Teflon chambers are much higher (larger than a factor of 5) than those used by Cappa et al. (2016) to derive the SOM parameterizations (Huang et al., 2018; Krechmer et al., 2016; Sunol et al., 2018). The use of a higher wall loss rate will tend to increase SOA aerosol mass yields further. This new understanding will need to be considered in the future.”.* We also added the following to provide context to our results in the discussion section: *“Loss of vapors to the Teflon walls has been shown to significantly bias SOA formation in environmental chamber experiments (Krechmer et al., 2016; 2014). Cappa et al. (2016) studied the effect of correcting for these vapor wall loss artifacts on ambient SOA mass concentrations from VOC precursors. In this work, we extended the work of Cappa et al. (2016) by considering additional precursors of SOA, i.e., S/IVOCs.”.*

References

- Ahmadov, R., McKeen, S. A., Robinson, A. L., Bahreini, R., Middlebrook, A. M., de Gouw, J. A., Meagher, J., Hsie, E.-Y., Edgerton, E., Shaw, S. and Trainer, M.: A volatility basis set model for summertime secondary organic aerosols over the eastern United States in 2006, *J. Geophys. Res.*, 117(D6), D06301, 2012.
- Baker, K. R., Carlton, A. G., Kleindienst, T. E., Offenberg, J. H., Beaver, M. R., Gentner, D. R., Goldstein, A. H., Hayes, P. L., Jimenez, J. L., Gilman, J. B., Gouw, J. A. de, Woody, M. C., Pye, H. O. T., Kelly, J. T., Lewandowski, M., Jaoui, M., Stevens, P. S., Brune, W. H., Lin, Y.-H., Rubitschun, C. L. and Surratt, J. D.: Gas and aerosol carbon in California: comparison of measurements and model predictions in Pasadena and Bakersfield, *Atmos. Chem. Phys.*, 15(9), 5243–5258, 2015.
- Camredon, M., Aumont, B., Lee-Taylor, J. and Madronich, S.: The SOA/VOC/NO_x system: an explicit model of secondary organic aerosol formation, *Atmos. Chem. Phys.*, 7(21), 5599–5610, 2007.
- Cappa, C. D., Zhang, X. and Loza, C. L.: Application of the Statistical Oxidation Model (SOM) to Secondary Organic Aerosol formation from photooxidation of C₁₂ alkanes, *Atmospheric* [online] Available from: <https://authors.library.caltech.edu/37818/>, 2013.
- Cappa, C. D., Jathar, S. H., Kleeman, M. J., Docherty, K. S., Jimenez, J. L., Seinfeld, J. H. and Wexler, A. S.: Simulating secondary organic aerosol in a regional air quality model using the statistical oxidation model--Part 2: Assessing the influence of vapor wall losses, *Atmos. Chem. Phys.*, 16(5), 3041–3059, 2016.
- Chhabra, P. S., Flagan, R. C. and Seinfeld, J. H.: Elemental analysis of chamber organic aerosol using an aerodyne high-resolution aerosol mass spectrometer, *Atmos. Chem. Phys.*, 10(9), 4111–4131, 2010.
- Docherty, K. S., Aiken, A. C., Huffman, J. A., Ulbrich, I. M., DeCarlo, P. F., Sueper, D., Worsnop, D. R., Snyder, D. C., Peltier, R. E., Weber, R. J., Grover, B. D., Eatough, D. J., Williams, B. J., Goldstein, A. H., Ziemann, P. J. and Jimenez, J. L.: The 2005 Study of Organic Aerosols at Riverside (SOAR-1): instrumental intercomparisons and fine particle composition, *Atmospheric Chemistry and Physics*; Katlenburg-Lindau, 11(23), 12387, 2011.
- Fountoukis, C., Megaritis, A. G., Skyllakou, K., Charalampidis, P. E., Denier van der Gon, H. A. C., Crippa, M., Prévôt, A. S. H., Fachinger, F., Wiedensohler, A., Pilinis, C. and Pandis, S. N.: Simulating the formation of carbonaceous aerosol in a European Megacity (Paris) during the MEGAPOLI summer and winter campaigns, *Atmos. Chem. Phys.*, 16(6), 3727–3741, 2016.
- Gentner, D. R., Isaacman, G., Worton, D. R., Chan, A. W. H., Dallmann, T. R., Davis, L., Liu, S., Day, D. A., Russell, L. M., Wilson, K. R., Weber, R., Guha, A., Harley, R. A. and Goldstein, A. H.: Elucidating secondary organic aerosol from diesel and gasoline vehicles through detailed characterization of organic carbon emissions, *Proc. Natl. Acad. Sci. U. S. A.*, 109(45), 18318–18323, 2012.
- Gordon, T. D., Presto, A. A., May, A. A., Nguyen, N. T., Lipsky, E. M., Donahue, N. M.,

Gutierrez, A., Zhang, M., Maddox, C., Rieger, P. and Others: Secondary organic aerosol formation exceeds primary particulate matter emissions for light-duty gasoline vehicles, *Atmos. Chem. Phys.*, 14(9), 4661–4678, 2014a.

Gordon, T. D., Presto, A. A., Nguyen, N. T., Robertson, W. H., Na, K., Sahay, K. N., Zhang, M., Maddox, C., Rieger, P., Chattopadhyay, S., Maldonado, H., Maricq, M. M. and Robinson, A. L.: Secondary organic aerosol production from diesel vehicle exhaust: impact of aftertreatment, fuel chemistry and driving cycle, *Atmos. Chem. Phys.*, 14(9), 4643–4659, 2014b.

Hayes, P. L., Ortega, A. M., Cubison, M. J., Froyd, K. D., Zhao, Y., Cliff, S. S., Hu, W. W., Toohey, D. W., Flynn, J. H., Lefer, B. L. and Others: Organic aerosol composition and sources in Pasadena, California, during the 2010 CalNex campaign, *J. Geophys. Res. D: Atmos.*, 118(16), 9233–9257, 2013.

Hennigan, C. J., Miracolo, M. A., Engelhart, G. J., May, A. A., Presto, A. A., Lee, T., Sullivan, A. P., McMeeking, G. R., Coe, H., Wold, C. E., Hao, W.-M., Gilman, J. B., Kuster, W. C., Gouw, J. de, Schichtel, B. A., Collett, J. L., Jr., Kreidenweis, S. M. and Robinson, A. L.: Chemical and physical transformations of organic aerosol from the photo-oxidation of open biomass burning emissions in an environmental chamber, *Atmos. Chem. Phys.*, 11(15), 7669–7686, 2011.

Hodzic, A. and Jimenez, J. L.: Modeling anthropogenically controlled secondary organic aerosols in a megacity: a simplified framework for global and climate models, *Geoscientific Model Development*, 4(4), 901–917, 2011.

Huang, Y., Zhao, R., Charan, S. M., Kenseth, C. M., Zhang, X. and Seinfeld, J. H.: Unified Theory of Vapor–Wall Mass Transport in Teflon-Walled Environmental Chambers, *Environ. Sci. Technol.*, 52(4), 2134–2142, 2018.

Jathar, S. H., Gordon, T. D., Hennigan, C. J., Pye, H. O. T., Pouliot, G., Adams, P. J., Donahue, N. M. and Robinson, A. L.: Unspeciated organic emissions from combustion sources and their influence on the secondary organic aerosol budget in the United States, *Proc. Natl. Acad. Sci. U. S. A.*, 111(29), 10473–10478, 2014.

Jathar, S. H., Cappa, C. D., Wexler, A. S., Seinfeld, J. H. and Kleeman, M. J.: Multi-generational oxidation model to simulate secondary organic aerosol in a 3-D air quality model, *Geoscientific Model Development; Katlenburg-Lindau*, 8(8), 2553–2567, 2015.

Jathar, S. H., Cappa, C. D., Wexler, A. S., Seinfeld, J. H. and Kleeman, M. J.: Simulating secondary organic aerosol in a regional air quality model using the statistical oxidation model--Part 1: Assessing the influence of constrained multi-generational ageing, *Atmos. Chem. Phys.*, 16(4), 2309–2322, 2016.

Koss, A. R., Sekimoto, K., Gilman, J. B., Selimovic, V., Coggon, M. M., Zarzana, K. J., Yuan, B., Lerner, B. M., Brown, S. S., Jimenez, J. L., Krechmer, J., Roberts, J. M., Warneke, C., Yokelson, R. J. and Gouw, J. de: Non-methane organic gas emissions from biomass burning: identification, quantification, and emission factors from PTR-ToF during the FIREX 2016 laboratory experiment, *Atmos. Chem. Phys.*, 18(5), 3299–3319, 2018.

Krechmer, J. E., Pagonis, D., Ziemann, P. J. and Jimenez, J. L.: Quantification of Gas-Wall Partitioning in Teflon Environmental Chambers Using Rapid Bursts of Low-Volatility Oxidized Species Generated in Situ, *Environ. Sci. Technol.*, 50(11), 5757–5765, 2016.

Loza, C. L., Craven, J. S., Yee, L. D., Coggon, M. M., Schwantes, R. H., Shiraiwa, M., Zhang, X., Schilling, K. A., Ng, N. L., Canagaratna, M. R., Ziemann, P. J., Flagan, R. C. and Seinfeld, J. H.: Secondary organic aerosol yields of 12-carbon alkanes, *Atmos. Chem. Phys.*, 14(3), 1423–1439, 2014.

May, A. A., Presto, A. A., Hennigan, C. J., Nguyen, N. T., Gordon, T. D. and Robinson, A. L.: Gas-particle partitioning of primary organic aerosol emissions: (1) Gasoline vehicle exhaust, *Atmos. Environ.*, 77, 128–139, 2013a.

May, A. A., Presto, A. A., Hennigan, C. J., Nguyen, N. T., Gordon, T. D. and Robinson, A. L.: Gas-particle partitioning of primary organic aerosol emissions: (2) diesel vehicles, *Environ. Sci. Technol.*, 47(15), 8288–8296, 2013b.

May, A. A., Nguyen, N. T., Presto, A. A., Gordon, T. D., Lipsky, E. M., Karve, M., Gutierrez, A., Robertson, W. H., Zhang, M., Brandow, C., Chang, O., Chen, S., Cicero-Fernandez, P., Dinkins, L., Fuentes, M., Huang, S.-M., Ling, R., Long, J., Maddox, C., Massetti, J., McCauley, E., Miguel, A., Na, K., Ong, R., Pang, Y., Rieger, P., Sax, T., Truong, T., Vo, T., Chattopadhyay, S., Maldonado, H., Maricq, M. M. and Robinson, A. L.: Gas- and particle-phase primary emissions from in-use, on-road gasoline and diesel vehicles, *Atmos. Environ.*, 88, 247–260, 2014.

McDonald, B. C., de Gouw, J. A., Gilman, J. B., Jathar, S. H., Akherati, A., Cappa, C. D., Jimenez, J. L., Lee-Taylor, J., Hayes, P. L., McKeen, S. A., Cui, Y. Y., Kim, S.-W., Gentner, D. R., Isaacman-VanWertz, G., Goldstein, A. H., Harley, R. A., Frost, G. J., Roberts, J. M., Ryerson, T. B. and Trainer, M.: Volatile chemical products emerging as largest petrochemical source of urban organic emissions, *Science*, 359(6377), 760–764, 2018.

Murphy, B. N., Woody, M. C., Jimenez, J. L., Carlton, A. M. G., Hayes, P. L., Liu, S., Ng, N. L., Russell, L. M., Setyan, A., Xu, L., Young, J., Zaveri, R. A., Zhang, Q. and Pye, H. O. T.: Semivolatile POA and parameterized total combustion SOA in CMAQv5.2: impacts on source strength and partitioning, *Atmos. Chem. Phys.*, 17(18), 11107–11133, 2017.

Ng, N. L., Kroll, J. H., Chan, A. W. H., Chhabra, P. S., Flagan, R. C. and Seinfeld, J. H.: benzene, *Atmos. Chem. Phys.*, 7, 3909–3922, 2007.

Presto, A. A. and Donahue, N. M.: Investigation of α -pinene+ ozone secondary organic aerosol formation at low total aerosol mass, *Environ. Sci. Technol.* [online] Available from: <https://pubs.acs.org/doi/abs/10.1021/es052203z>, 2006.

Pye, H. O. T. and Pouliot, G. A.: Modeling the role of alkanes, polycyclic aromatic hydrocarbons, and their oligomers in secondary organic aerosol formation, *Environ. Sci. Technol.*, 46(11), 6041–6047, 2012.

Sunol, A. M., Charan, S. M. and Seinfeld, J. H.: Computational simulation of the dynamics of secondary organic aerosol formation in an environmental chamber, *Aerosol Sci. Technol.*, 52(4),

470–482, 2018.

Worton, D. R., Isaacman, G., Gentner, D. R., Dallmann, T. R., Chan, A. W. H., Ruehl, C., Kirchstetter, T. W., Wilson, K. R., Harley, R. A. and Goldstein, A. H.: Lubricating oil dominates primary organic aerosol emissions from motor vehicles, *Environ. Sci. Technol.*, 48(7), 3698–3706, 2014.

Xu, L., Guo, H., Boyd, C. M., Klein, M., Bougiatioti, A., Cerully, K. M., Hite, J. R., Isaacman-VanWertz, G., Kreisberg, N. M., Knote, C., Olson, K., Koss, A., Goldstein, A. H., Hering, S. V., de Gouw, J., Baumann, K., Lee, S.-H., Nenes, A., Weber, R. J. and Ng, N. L.: Effects of anthropogenic emissions on aerosol formation from isoprene and monoterpenes in the southeastern United States, *Proc. Natl. Acad. Sci. U. S. A.*, 112(1), 37–42, 2015.

Zhang, Q. J., Beekmann, M., Freney, E., Sellegri, K., Pichon, J. M., Schwarzenboeck, A., Colomb, A., Bourrienne, T., Michoud, V. and Borbon, A.: Formation of secondary organic aerosol in the Paris pollution plume and its impact on surrounding regions, *Atmos. Chem. Phys.*, 15(24), 13973–13992, 2015.

Zhang, X., Cappa, C. D., Jathar, S. H., McVay, R. C., Ensberg, J. J., Kleeman, M. J. and Seinfeld, J. H.: Influence of vapor wall loss in laboratory chambers on yields of secondary organic aerosol, *Proc. Natl. Acad. Sci. U. S. A.*, 111(16), 5802–5807, 2014.

Zhao, Y., Nguyen, N. T., Presto, A. A., Hennigan, C. J., May, A. A. and Robinson, A. L.: Intermediate volatility organic compound emissions from on-road diesel vehicles: chemical composition, emission factors, and estimated secondary organic aerosol production, *Environ. Sci. Technol.*, 49(19), 11516–11526, 2015.

Zhao, Y., Nguyen, N. T., Presto, A. A., Hennigan, C. J., May, A. A. and Robinson, A. L.: Intermediate Volatility Organic Compound Emissions from On-Road Gasoline Vehicles and Small Off-Road Gasoline Engines, *Environ. Sci. Technol.*, 50(8), 4554–4563, 2016.

Zhao, Y., Saleh, R., Saliba, G., Presto, A. A., Gordon, T. D., Drozd, G. T., Goldstein, A. H., Donahue, N. M. and Robinson, A. L.: Reducing secondary organic aerosol formation from gasoline vehicle exhaust, *Proc. Natl. Acad. Sci. U. S. A.*, 114(27), 6984–6989, 2017.

Simulating secondary organic aerosol in a regional air quality model using the statistical oxidation model – Part 3: Assessing the influence of semi-volatile and intermediate volatility organic compounds and NO_x

Ali Akherati¹, Christopher D. Cappa², Michael J. Kleeman², Kenneth S. Docherty³, Jose L. Jimenez⁴, Stephen M. Griffith⁵, Sebastien Dusanter⁶, Philip S. Stevens⁵, and Shantanu H. Jathar¹

¹Department of Mechanical Engineering, Colorado State University, Fort Collins, CO, USA

²Department of Civil and Environmental Engineering, University of California Davis, Davis, CA, USA

³Jacobs Technology, Raleigh, NC, USA

⁴Department of Chemistry and Cooperative Institute for Research in Environmental Sciences (CIRES), University of Colorado, Boulder, CO, USA

⁵School of Public and Environmental Affairs and Department of Chemistry, Indiana University, Bloomington, IN, USA

⁶IMT Lille Douai, Univ. Lille, SAGE - Département Sciences de l'Atmosphère et Génie de l'Environnement, 59000 Lille, France

Correspondence to: Shantanu H. Jathar (shantanu.jathar@colostate.edu)

Abstract

Semi-volatile and intermediate-volatility organic compounds (SVOCs and IVOCs) from anthropogenic sources are likely to be important precursors of secondary organic aerosol (SOA) in urban airsheds yet their treatment in most models is based on limited and obsolete data, or completely missing. Additionally, gas-phase oxidation of organic precursors to form SOA is influenced by the presence of nitric oxide (NO), but this influence is poorly constrained in chemical transport models. In this work, we updated the organic aerosol model in the UCD/CIT chemical transport model to include (i) a semi-volatile and reactive treatment of primary organic aerosol (POA), (ii) emissions and SOA formation from IVOCs, (iii) the NO_x influence on SOA formation, and (iv) SOA parameterizations for SVOCs and IVOCs that are corrected for vapor wall loss artifacts during chamber experiments. All updates were implemented in the statistical oxidation model (SOM) that simulates the oxidation chemistry, thermodynamics, and gas/particle partitioning of organic aerosol (OA). Model treatment of POA, SVOCs, and IVOCs was based on an interpretation of a comprehensive set of source measurements available up to the year 2016 and resolved broadly by source type. The NO_x influence on SOA formation was calculated offline based on measured and modeled VOC:NO_x ratios. And finally, the SOA formation from all organic precursors (including SVOCs and IVOCs) was modeled based on recently derived parameterizations that accounted for vapor wall loss artifacts in chamber experiments. The updated model was used to simulate a two week summer episode over southern California at a model resolution of 8 km.

When combustion-related POA was treated as semi-volatile, modeled POA mass concentrations were reduced by 30-50% in the urban areas in southern California but were still too high when compared against “hydrocarbon-like organic aerosol” factor measurements made at Riverside, CA during the Study of Organic Aerosols at Riverside (SOAR-1) campaign of 2005. The use of a lower but more realistic volatility for POA from food cooking sources resulted in 20% higher POA mass concentrations or in a reduction of a 15-40% in the urban areas in southern California. Treating all POA (except that from marine sources) to be semi-volatile, similar to diesel exhaust POA, resulted in a larger reduction in POA mass concentrations and allowed for a better model-measurement comparison at Riverside, but this scenario is unlikely to be realistic since this assumes that POA from sources such as road and construction dust are semi-volatile too. Model predictions suggested that both SVOCs (evaporated POA vapors) and IVOCs did not contribute as much as other anthropogenic precursors (e.g., alkanes, aromatics) to SOA mass concentrations in the urban areas (<5% and <15% of the total SOA respectively) as the timescales for SOA production appeared to be shorter than the timescales for transport out of the urban airshed. Comparisons of modeled IVOC concentrations with measurements of anthropogenic SOA precursors in southern California seemed to imply that IVOC emissions were underpredicted in our updated model by a factor of 2. We suspect that these missing IVOCs might arise from the use of volatile chemical

Deleted: →

Deleted: significantly

products such as pesticides, coatings, cleaning agents, and personal care products. Correcting for the vapor wall loss artifact in chamber experiments enhanced SOA mass concentrations although the enhancement was precursor- as well as NO_x-dependent. Accounting for the influence of NO_x using the VOC:NO_x ratios resulted in better predictions of OA mass concentrations in rural/remote environments but still underpredicted OA mass concentrations in urban environments, potentially due to the missing urban emissions/chemical source of OA. Finally, simulations performed for the year 2035 showed that despite reductions in VOC and NO_x emissions in the future, SOA mass concentrations may be higher than in the year 2005, primarily from increased hydroxyl radical (OH) concentrations due to lower ambient NO₂ concentrations.

Formatted: Font: 12 pt

Glossary

OA - Organic aerosol
POA - Primary organic aerosol or direct emissions of organic aerosol
SOA - Secondary OA or organic aerosol formed in the atmosphere
VOC - Volatile organic compound
NMOG - Non-methane organic gas
SVOC - Semi-volatile organic compound
IVOC - Intermediate-volatility organic compound
HOA - Hydrocarbon-like organic aerosol measured by the aerosol mass spectrometer
OOA - Oxygenated organic aerosol measured by the aerosol mass spectrometer
aV-SOA - Anthropogenic SOA formed from VOC oxidation
bV-SOA - Biogenic SOA formed from VOC oxidation
aS-SOA - Anthropogenic SOA formed from SVOC oxidation
aI-SOA - Anthropogenic SOA formed from IVOC oxidation

1 Introduction

Organic aerosol (OA) is an important yet uncertain component of atmospheric aerosol (Fuzzi et al., 2015; Jimenez et al., 2009) and has large impacts on air quality, climate, and human health (Pachauri et al., 2014). Combustion sources such as motor vehicles, biomass burning, and food cooking are significant contributors to atmospheric OA from urban to regional to global scales (Bond et al., 2004). Yet, in urban environments where combustion emissions are a dominant source, atmospheric models often underpredict total OA mass concentrations (e.g., Carlton et al. (2010)). Models based on older parameterizations also predict much lower contributions of secondary organic aerosol in urban areas (e.g., Volkamer et al. (2006); Jathar et al. (2017a)), and may overemphasize the role of mobile sources (e.g., Ensberg et al. (2014)), suggesting that combustion-related OA and other urban sources may not be well represented in models. There is a need to improve the treatment of combustion-related OA in atmospheric models since these improvements will allow for better predictions of air quality that are needed to mitigate climate and health impacts from anthropogenic combustion sources, and will facilitate improved understanding of additional potentially missing sources.

Research over the past decade has made major inroads in understanding the sources and properties of combustion-related OA (Gentner et al., 2017). Combustion sources directly emit organic particles (primary organic aerosol, POA) and also emit gaseous organic compounds that are oxidized in the atmosphere to form secondary organic aerosol (SOA). A significant fraction of the combustion-related POA mass is now understood to be semi-volatile, that is material that

Deleted: majority

exists in a dynamic equilibrium between the vapor and particle phases (Grieshop et al., 2009a, 2009b; Huffman et al., 2009; Kuwayama et al., 2015; Lipsky and Robinson, 2006; May et al., 2013a, 2013b, 2013c; Robinson et al., 2007). This POA is formed as vapors in the combustion exhaust cool down to become supersaturated and condense on existing seed aerosol (Robinson et al., 2010). After emission, some of this POA evaporates with atmospheric dilution since the aerosol mass available for partitioning decreases as the POA is transported away from source regions. Further, diurnal changes in temperature leading to changes in the vapor pressure can also cycle POA between the two phases. Both vapor and particle forms of semi-volatile POA have been shown to photochemically react in the atmosphere to add or remove organic material from the particle-phase (Miracolo et al., 2010) and become more oxygenated (Kroll et al., 2009), although the vapors react much faster. In addition, all combustion processes are now believed to include emissions of an important additional class of SOA precursors: intermediate-volatility organic compounds (IVOCs) (Jathar et al., 2014). Gas-chromatography mass-spectrometry applications have suggested that they are primarily composed of high molecular weight linear, branched, and cyclic alkanes (carbon numbers greater than 12) and aromatics (Gentner et al., 2012; Zhao et al., 2014, 2017). Model IVOCs have been shown to form SOA efficiently in chamber experiments (Chan et al., 2009; Lim and Ziemann, 2009; Presto et al., 2010; Tkacik et al., 2012) and have been hypothesized to account for a large fraction of the SOA formed from the photooxidation of motor vehicle exhaust and biomass burning emissions (Jathar et al., 2014; Zhao et al., 2017). The emissions and atmospheric properties (e.g., volatility, reactivity, SOA mass yields) of POA and IVOCs are known (or very likely) to vary by source (e.g., mobile sources versus biomass burning) and hence atmospheric models need to include a source-resolved treatment to accurately predict source contributions to OA and fine particulate matter.

Deleted: ,

Deleted: to emissions of "traditional" SOA precursors such as aromatics and long alkanes,

Deleted: while the bulk of the IVOC mass cannot be typically speciated,

Deleted: aromatics (carbon numbers greater than 12) (Gentner et al., 2012; Zhao et al., 2014, 2017)

Formatted: Font color: Black

Most commonly used chemical transport models (e.g., CMAQ, CAMx, PMCAMx, WRF-Chem, GEOS-Chem) have been updated to include a semi-volatile and reactive treatment of POA and emissions and SOA formation from IVOCs (Ahmadov et al., 2012; Koo et al., 2014; Murphy and Pandis, 2009; Pye and Seinfeld, 2010). However, their representation in models has been based on limited data and there are major differences between the implementations in different models. For example, in most models, with a few exceptions (e.g., most recent research version of the OA model in CMAQ developed by Koo et al. (2014)), the gas/particle partitioning of POA was modeled based on measurements performed on a small off-road diesel engine from more than a decade ago (Robinson et al., 2007) and IVOC emissions were based on data gathered from two medium duty diesel vehicles from two decades ago (Schauer et al., 1999). Models have assumed that these data are representative of emissions from modern diesel-powered sources and the POA/IVOC properties from diesel sources are similar to those from other sources. New source data are now available to update POA and IVOC emissions estimates in chemical transport models. Further, the most common schemes to model SOA formation from POA vapors and IVOCs use a single lumped precursor to simulate SOA formation from all sources (e.g., Pye and Seinfeld (2010)) or use an *ad hoc* aging routine that continuously reduces the volatility of the precursor/oxidation products until they partition into the particle phase (Robinson et al., 2007). While some of these schemes have been validated against experimental data (Fountoukis et al., 2016; Hodzic and Jimenez, 2011; Murphy et al., 2017; Zhang et al., 2015), most have assumed that all sources have the same rate and potential to form SOA and, in some cases, ignore fragmentation reactions tied to multigenerational chemistry. *Ad hoc* aging schemes can overestimate net aerosol mass yields from an SOA precursor and can sometimes overpredict ambient SOA mass concentrations too, especially over larger regional scales (Dzepina et al., 2009, 2011; Hayes et al., 2015; Jathar et al., 2016). Recently, a host of studies have quantified the volatility of POA emissions from over 100 unique sources and measured SOA formation in more than 100 chamber experiments across six broad source classes: on- and off-road gasoline and diesel sources, wood stoves, and biomass burning (Gordon et al., 2014a, 2014b; Hennigan et al., 2011;

Deleted: very

Deleted: and often obsolete

Deleted: The continued use of these data as inputs for models assumes that not only are

Deleted:

Deleted: but also that the

Deleted:

Deleted: Most of these schemes have rarely been

Deleted: (Hodzic and Jimenez, 2011; Fountoukis et al., 2016; Murphy et al., 2017; Zhang et al., 2015)

Deleted: As an exception, Hodzic and Jimenez (2011) have used a single lumped precursor to account for all SOA precursors (VOC, IVOC, and SVOC) and the SOA formation from this precursor has been constrained and tested against measurement data.

4 May et al., 2013a, 2013b, 2013c, 2014; Tkacik et al., 2017). These data offer a comprehensive set of measurements to
5 inform and update the source-resolved semi-volatile and reactive behavior of POA and the emissions and SOA
6 formation from IVOCs in atmospheric models.

8 SOA formation is strongly influenced by the presence of NO_x (Camredon et al., 2007; Chhabra et al., 2010; Loza et al.,
9 2014; Ng et al., 2007b). For most SOA precursors, with the exception of alkanes (Loza et al., 2014) and certain
10 sesquiterpenes (Ng et al., 2007b), environmental chamber data suggest that the reaction chemistry at low NO_x, or more
11 precisely low NO, conditions (<2 ppbv) produces more SOA than at high NO_x conditions (>50 ppbv and up to ~1 ppmv)
12 (Camredon et al., 2007; Chhabra et al., 2010; Loza et al., 2014; Ng et al., 2007; Zhang et al., 2014). The consensus
13 seems to be that at low NO_x conditions such as those found in remote continental or marine regions the peroxy radical
14 (RO₂) – formed immediately after the reaction of the precursor with the oxidant – combines with the hydroperoxy radical
15 (HO₂) or RO₂ to form lower volatility hydroperoxides or organic peroxides (Kroll and Seinfeld, 2008). Low NO
16 conditions in remote regions, and in some cases in urban regions that have recently witnessed dramatic reductions in
17 NO_x concentrations, can promote autooxidation reactions to form extremely low-volatility organic compounds (Ehn et
18 al., 2014; Praske et al., 2018). At high NO_x, or more precisely high NO, conditions such as those found in urban regions
19 or biomass burning plumes, the RO₂ reaction with NO either leads to the formation of alkoxy radicals that can then
20 fragment the carbon backbone, or to the formation of organic nitrates where both reactions result in more volatile
21 products (Kroll and Seinfeld, 2008). Most atmospheric models (e.g., CMAQ, WRF-Chem, GEOS-Chem) have
22 incorporated this knowledge to account for the influence of NO_x on the magnitude, composition, and spatial distribution
23 of SOA.

4 In the mostly commonly used scheme (i.e. Henze et al. (2008)), RO₂ reacts with HO₂ to form ‘low-NO’ SOA or with
5 NO to form ‘high-NO’ SOA. The HO₂:NO ratio determines the branching ratio for RO₂ and controls the SOA formed
6 under varying NO_x levels. The SOA yields under the low and high NO_x conditions are parameterized based on chamber
7 data gathered under low and high NO_x conditions respectively. Despite being widely implemented, this scheme has one
8 key limitation that might tend to bias the NO_x-dependent predictions of SOA. This scheme relies on an accurate
9 prediction of NO and HO₂ to determine the branching ratio for the RO₂ radical. Although NO predictions can be
10 validated against routine measurements and most chemical mechanisms seem to predict NO_x (NO+NO₂) within a factor
11 of 2, there are very few ambient data to validate model predictions of HO₂. For example, as will be shown later, we find
12 that predictions of HO₂ concentrations from the use of a typical gas-phase chemical mechanism (SAPRC-11) in a 3D
13 model at Pasadena, CA were almost an order of magnitude lower when compared against measurements at the same
14 site in 2010 (Griffith et al., 2016). In this case, underpredicting HO₂ concentrations by an order of magnitude could shift
15 the scheme to produce most of the SOA via the high NO pathway. In contrast, box models that have used the regional
16 atmospheric chemistry mechanism (RACM) have shown good model-measurement comparisons for HO₂
17 concentrations in polluted regions (Griffith et al., 2016; Hofzumahaus et al., 2009). Regardless, gas-phase chemical
18 mechanisms that use the aforementioned scheme need to ensure accurate predictions of HO₂ and NO concentrations to
19 simulate the influence of NO_x on SOA formation.

2 In this work, we update the organic aerosol model in the UCD/CIT chemical transport model to include a semi-volatile
3 and reactive treatment of POA, emissions and SOA formation from IVOCs, the NO_x influence on SOA formation, and
4 SOA parameterizations for SVOCs and IVOCs that are corrected for vapor wall loss artifacts during chamber
5 experiments. All of these updates are implemented in the statistical oxidation model (SOM) that simulates the oxidation

Deleted: >

Deleted: 50

Deleted: (Camredon et al., 2007; Chhabra et al., 2010; Loza et al., 2014; Ng et al., 2007b; Zhang et al., 2014)

Deleted: e.g.

chemistry, thermodynamics, and gas/particle partitioning of OA. Model inputs for POA and IVOCs are based on an interpretation of a comprehensive set of source measurements and resolved broadly by the source type. The NO_x influence on SOA formation is calculated offline based on measured and modeled VOC:NO_x ratios and NO_x concentrations. And finally, the SOA formation from SVOCs and IVOCs is modeled based on recently derived parameterizations that account for vapor wall loss artifacts in chamber experiments. Building on our earlier work (Cappa et al., 2016; Jathar et al., 2015, 2016), these updates within the framework of the SOM have improved the representation of OA in a chemical transport model.

To help the reader, we provide a brief overview of the different sections in this manuscript (section numbers in parentheses). Section 2 discusses details of the chemical transport model (2.1), organic aerosol model (2.2), simulations performed (2.3), and measurements used for model evaluation (2.4). In Section 3, we first describe the emissions (3.1), spatial distribution (3.2), and precursor contributions to OA (3.3), followed by the influence of vapor wall losses (3.4) and NO_x (3.6) on SOA formation. In the same section, we describe results from sensitivity simulations performed on the most sensitive inputs (3.5). Next, we compare model predictions of SOA precursors (4.1), OA (4.2), POA, and SOA (4.3) mass concentrations, and OA elemental composition (4.4) against measurements in southern California. Finally, we highlight key findings from this work in the summary and discussion section (5).

Formatted: Font: Not Italic, Font color: Text 1

Formatted: Font color: Text 1

Deleted: ¶

2 Methods

2.1 Chemical Transport Model

We used the UCD/CIT regional chemical transport model (Kleeman and Cass, 2001) to simulate the emissions, transport, chemistry, and deposition of air pollutants over the state of California at a grid resolution of 24 km and over southern California (see Fig. S1) using a nested 8 km grid from 20th July to 2nd August 2005. The results and analysis were focused on model predictions over Southern California because the region, with approximately 15 million people, is home to one of the most polluted cities in the United States (Los Angeles; ALA (2017)). The time period for simulation was primarily chosen because the model has been previously evaluated for this time period (Jathar et al., 2016) and applied to examine important sources and formation pathways of OA (Cappa et al., 2016; Jathar et al., 2015, 2016, 2017b). The recent literature describes the latest version of the UCD/CIT model but we provide a very brief description of the models and inputs used in this work. Anthropogenic emissions for California were developed using the California Regional PM10/PM2.5 Air Quality Study (CRPAQS) inventory of 2000 but scaled to match conditions in 2005. Wildfire emissions were based on the model FINN (Fire Inventory for National Center for Atmospheric Research) (Wiedinmyer et al., 2011) although they were not found to significantly contribute to OA during the simulated time period (Docherty et al., 2011). Biogenic emissions were based on the model MEGAN (Model of Emissions of Gases and Aerosols from Nature) (Guenther et al., 2006). The Weather Research and Forecasting (WRF) v3.4 model (www.wrf-model.org) was used to produce hourly meteorological fields. National Center for Environmental Protection's NAM (North American Mesoscale) analysis data were used to set the initial and boundary conditions for WRF. The gas- and particle-phase initial and hourly varying boundary conditions were based on the results from the global model MOZART-4/NCEP (Emmons et al., 2010). The gas-phase chemistry was modeled using SAPRC-11 (Carter, 2010).

2.2 Organic Aerosol Model

2.2.1 Statistical Oxidation Model (SOM)

In this work, we use the Statistical Oxidation Model (SOM) developed by (Cappa and Wilson, 2012). The SOM is a

semi-explicit and parameterizable model that simulates the oxidation chemistry, thermodynamics, and gas/particle partitioning of OA and its precursors. The SOM has been used to model SOA formation in chamber (Cappa et al., 2013; Cappa and Wilson, 2012; Zhang et al., 2014) and flow reactor (Eluri et al., 2017) experiments. and was recently coupled with SAPRC-11 (gas-phase chemical mechanism) in the UCD/CIT model (Jathar et al., 2015) to investigate the role of chamber-based vapor wall losses (Cappa et al., 2016) and multigenerational aging (Jathar et al., 2016) on the ambient SOA burden. In this work, we used an updated version of the SAPRC-SOM model embedded in the UCD/CIT model that included the POA and IVOC updates described in Section 2.2.2. A detailed description of the mathematical and numerical formulation of the SOM can be found in earlier literature but a brief description of the SOM framework follows. The SOM uses a 2-dimensional carbon-oxygen grid to describe and track the evolution of the gas- and particle-phase organic carbon that is known to yield OA. Each grid cell in the SOM represents an organic species with the molecular formula: $C_XH_{2X+2-Z}O_Z$, where $X=N_C$, and $Z=N_O$. This species is expected to capture the average properties (e.g. volatility, reaction rate constants) of species with the same number of carbon (N_C) and oxygen (N_O) atoms that are formed from a given SOA precursor. Each species, in the gas and particle phases, is assumed to react with the hydroxyl radical (OH). Operationally, OH is not consumed within the SOM as the chemistry captured in the SOM overlaps with that represented in the gas-phase mechanism (i.e., SAPRC-11). Reactions with the OH radical result in functionalization or fragmentation of the organic species and the distribution of the reaction products is tracked in the carbon-oxygen grid. Six precursor-specific adjustable parameters are assigned for each SOM grid: four parameters that define the molar yields of the four functionalized, oxidized products (P_{func}), one parameter that determines the probability of functionalization or fragmentation (q_{frag}) and one parameter that describes the relationship between N_C , N_O and volatility ($ALVP$). In the model, the probability of fragmentation is modeled as a function of the O:C ratio since species with higher O:C ratios have been shown to fragment much more easily than species with lower O:C ratios (Chacon-Madrid and Donahue, 2011). All SOM species properties (e.g., OH reactivity, volatility) are described in terms of N_C and N_O .

Seven SOM grids were used to represent SOA formation from nine different precursor classes: (i) long alkanes, (ii) benzene, (iii) high-yield aromatics, (iv) low-yield aromatics, (v) isoprene, (vi) monoterpenes, (vii) sesquiterpenes, (viii) semi-volatile POA (SVOC), and (ix) IVOCs. Long alkanes as a precursor class includes linear, branched, and cyclic alkanes roughly up to a carbon number of C_{43} and represent they speciated alkanes present in existing emissions inventories. These long alkanes are distinct from the alkanes that might be present in SVOC and IVOCs. High-yield and lower-yield aromatics include all speciated aromatic compounds present in existing emissions inventories and, similar to the long alkanes precursor class, are distinct from the aromatics that might be present in SVOC and IVOCs. Classes (i) through (vii) have been included in previous applications of the SOM and we refer the reader to our earlier publications for more details (Cappa et al., 2016; Jathar et al., 2015, 2016). Classes (viii) and (ix) were included in this work for the first time. The SOA formation from monoterpenes and sesquiterpenes (classes vi and vii) was modeled in the same SOM grid since both precursors used the SOM parameter sets for α -pinene. Similarly, the SOA formation from SVOCs and IVOCs was modeled in the same SOM grid and both used the SOM parameter sets for n -dodecane; sensitivity simulations were performed using the SOM parameter set for toluene. SOM parameters were determined from fitting the observed SOA volume produced in chamber experiments, with and without accounting for losses of vapors to the chamber walls. Details about how the vapor wall losses were modeled are described in Zhang et al. (2014) and Cappa et al. (2016). Briefly, loss of vapors to the Teflon walls of the chamber was modeled reversibly where the first-order uptake to the walls was assumed to be $2.5 \times 10^{-4} \text{ s}^{-1}$ and the release of vapors from the walls was modeled using absorptive partitioning theory with the Teflon wall serving as an absorbing mass with an effective mass concentration of 10 mg m^{-3} . Recent work has argued that vapor wall loss rates in Teflon chambers are much higher

Formatted: Font: Italic

Formatted: Font: Italic, Subscript

Formatted: Font: Not Bold

Formatted: Subscript

Formatted: Superscript

Formatted: Superscript

Formatted: Superscript

(larger than a factor of 5) than those used by Cappa et al. (2016) to derive the SOM parameterizations (Huang et al., 2018; Krechmer et al., 2016; Sunol et al., 2018). The use of a higher wall loss rate will tend to increase SOA aerosol mass yields further. This new understanding will need to be considered in the future.

We used low and high NO_x-specific parameter sets to simulate SOA formation separately under low and high NO_x conditions respectively since the current version of the SOM cannot account for continuous variation in NO_x. The SOM parameters used for the nine different classes and seven different grids are listed in Table 1. Parameters for all species except for isoprene were from Cappa et al. (2016). The parameters for isoprene were from Hodzic et al. (2016) that included updates for the reactions rate constants for the first generation products from isoprene photooxidation. Jathar et al. (2016) investigated the influence of oligomerization reactions by allowing irreversible conversion of particle-phase SOM species into a single non-volatile species and found that the oligomerization pathway (as simulated) did not substantially affect the OA mass concentration in Southern California. Hence, the oligomerization pathway was not considered in this work. We also did not include the formation of extremely low-volatility organic compounds from oxidation of SOA precursors such as α -pinene (Ehn et al., 2014) and alkanes (Praske et al., 2018) through autooxidation pathways, which will very likely be addressed in future versions of the SOM.

Table 1: SOA precursors and SOM parameters used in this work. VWL=Vapor Wall Loss Corrected, ΔLVP = change in vapor pressure linked to addition of one oxygen atom, P_{func} = molar yields of species that add 1 to 4 oxygens per reaction (Pf_1 through Pf_4), m_{frag} = exponent influencing the probability of fragmentation.

SOA Precursors	SAPRC Species /SOM Grid	SOM Surrogate	VWL	NO _x	ΔLVP	P_{func}				m_{frag}	Reference
						Pf_1	Pf_2	Pf_3	Pf_4		
SVOC/IVOC	POA+IVOC	<i>n</i> -dodecane/toluene	No	Low	1.54	0.717	0.278	0.0028	0.0022	0.122	Loza et al. (2014)
				High	1.39	0.927	0.0101	0.018	0.0445	0.098	
Alkanes	ALK		Yes	Low	1.83	0.999	0.001	0.001	0.001	2	
				High	1.47	0.965	0.001	0.002	0.032	0.266	
Benzene	BENZ	benzene	No	Low	2.01	0.769	0.001	0.0505	0.180	2.010	Ng et al. (2007a)
				High	1.7	0.079	0.001	0.919	0.001	0.535	
			Yes	Low	1.97	0.637	0.001	0.002	0.360	0.0807	
				High	1.53	0.008	0.001	0.991	0.001	0.824	
High-yield aromatics	ARO1	toluene	No	Low	1.84	0.561	0.001	0.001	0.438	0.010	Zhang et al. (2014)
				High	1.24	0.003	0.001	0.001	1.010	0.222	
			Yes	Low	1.77	0.185	0.001	0.002	0.812	1.31	
				High	1.42	0.856	0.001	0.002	0.141	4.61	
Low-yield aromatics	ARO2	<i>m</i> -xylene	No	Low	1.76	0.735	0.001	0.002	0.262	0.010	Ng et al. (2007a)
				High	1.68	0.936	0.001	0.002	0.061	0.010	
			Yes	Low	2.05	0.102	0.001	0.878	0.019	1.08	
				High	1.46	0.001	0.001	0.942	0.056	0.0671	
Isoprene	ISOP	isoprene	No	Low	2.26	0.973	0.001	0.001	0.026	0.010	Chhabra et al. (2011); Hodzic et al. (2016)
				High	1.94	0.952	0.001	0.030	0.016	0.063	
			Yes	Low	2.25	0.1646	0.5164	0.3012	0.0179	0.0244	
				High	1.93	0.988	0.0002	0.0116	0.0009	0.51	
Monoterpenes /Sesquiterpenes	TRP	α -pinene	No	Low	1.87	0.001	0.869	0.078	0.053	0.010	Chhabra et al. (2011)
				High	1.62	0.068	0.633	0.275	0.024	0.035	
			Yes	Low	1.97	0.419	0.426	0.140	0.014	0.305	
				High	1.91	0.500	0.422	0.070	0.008	0.16	

Deleted:

Formatted: Subscript

Formatted: Subscript

Formatted: Subscript

Formatted: Border: Top: (No border), Bottom: (No border), Left: (No border), Right: (No border), Between : (No border)

Deleted: ¶

2.2.2 Model Inputs

Semi-Volatile and Reactive POA (SVOC). POA from gasoline, diesel, biomass burning, and food cooking sources was treated as semi-volatile and reactive. POA from all other sources (e.g., marine, dust) was assumed to be non-volatile in all simulations except one where we explored the sensitivity in model predictions to this assumption (see Section 2.3 for more details). Semi-volatile POA was modeled by distributing POA emissions from the emissions inventory in the SOM grid as hydrocarbon species modeled as linear alkanes, i.e. as species with no oxygen (i.e., C_nH_{2n+2}). The hydrocarbon/linear alkane distribution in the SOM grid was determined by refitting the volatility distributions published by May and coworkers (May et al., 2013a, 2013b, 2013c) such that the hydrocarbon distribution reproduced the observed gas/particle partitioning behavior; the hydrocarbon distributions are listed in Table S1. We assumed all on- and off-road gasoline exhaust POA to have the same hydrocarbon/linear alkane distribution as the volatility distribution determined by May et al. (2013a) from data for 51 light-duty gasoline vehicles. Almost three-quarters of the light-duty gasoline vehicles used in May et al. (2013a) were manufactured in or prior to 2005 (the year modeled in this work) and they did not find the POA volatility distribution data to be sensitive to the model year of the vehicle. Hence, the volatility distribution used in this work should still be representative of the vehicle fleet in 2005. Based on tests performed on eight light-duty gasoline vehicles, Kuwayama et al. (2015) found that the POA volatility for their vehicles was consistent with that determined by (May et al., 2013a) for about half the vehicles but substantially lower for the other half. They hypothesized that the lower POA volatility could be attributed to fuel oxidation products. The findings of Kuwayama et al. (2015) suggest that the volatility distribution used in this work may overestimate the evaporation of POA with dilution. We assumed all on- and off-road diesel exhaust POA to have the same hydrocarbon/linear alkane distribution as the volatility distribution determined by May et al. (2013b) from data for two medium-duty diesel trucks, three heavy-duty diesel trucks, and a single off-road diesel engine. May et al. (2013b) did not report on differences in the POA volatility distribution between vehicles that did or did not use a modern emissions control system (diesel particulate filter (DPF) and/or diesel oxidation catalyst (DOC)). Hence, we assumed that the volatility distribution used here was still representative of the mostly non-DPF and non-DOC vehicle fleet in 2005. We assumed residential wood combustion and wildfires to have the same hydrocarbon/linear alkane distribution as the volatility distribution determined by May et al. (2013c) from a selection of fifteen different fuels. We assumed food cooking to have the same hydrocarbon/linear alkane distribution as that for wildfires. Recent work suggests that food cooking OA may be significantly less volatile than wildfire OA (Louvaris et al., 2017; Woody et al., 2016). To examine the influence of this finding, we performed sensitivity simulations to model the POA from food cooking sources using the volatility distribution of Louvaris et al. (2017). This work, similar to the most recent implementation in the Community Multiscale Air Quality (CMAQ) model (Koo et al., 2014; Woody et al., 2016), included a source-resolved treatment of semi-volatile POA that was tied to a comprehensive set of source measurements.

The reactive behavior of POA was modeled by assuming that the POA vapors (i.e. SVOCs) (represented as a hydrocarbon distribution) and their products participated in gas-phase oxidation and formed SOA similar to linear alkanes and utilized the SOM parameter set for *n*-dodecane. The surrogate, in this case *n*-dodecane, only informs the multi-generational oxidation chemistry of the precursor and the actual compound of interest (e.g., a C_{15} linear alkane) can have a different SOA mass yield than that of *n*-dodecane. The reaction rate constants with OH for the parent hydrocarbons were assumed to be similar to the carbon-equivalent linear alkane. We should note that the presence of branched/cyclic alkane and aromatic compounds in the SVOCs would require the use of a higher reaction rate constant with OH as these compounds are more reactive with OH than carbon-equivalent linear alkanes. The equivalence to linear alkanes while not perfect was probably a good assumption for gasoline and diesel sources since alkanes account

Deleted: e

Deleted: 67

Deleted: although re

Deleted: significantly

Field Code Changed

Deleted: Hence, model predictions in this work probably underestimate the POA mass concentrations and overestimate the SVOC emissions from food cooking sources....

Deleted:

for a substantial fraction of gasoline and diesel fuel (Gentner et al., 2012) and lubricating oil (Caravaggio et al., 2007) and are a dominant organic class in both gas- and particle-phase emissions from mobile sources (Brandenberger et al., 2005; Hays et al., 2017; Schauer et al., 1999, 2002b)(Worton et al., 2014). However, alkanes do not make up a significant fraction of the gas- and particle-phase emissions from biomass burning (Hatch et al., 2015; Schauer et al., 2001; Stockwell et al., 2015) or food cooking (Schauer et al., 2002a) and hence it is unlikely that linear alkanes are good surrogates to model the oxidation of SVOCs from these sources. To test the sensitivity of the model predictions to the surrogate used to model SOA formation from SVOCs, we ran sensitivity simulations where we modeled the SVOCs as a mixture of aromatic compounds using the SOM parameter set for toluene (see rationale in Section 2.4).

Deleted: unclear whether

Deleted:

Intermediate-Volatility Organic Compounds. We included IVOC emissions from gasoline, diesel, and biomass burning. We assumed none of the other sources emitted IVOCs for all simulations except one where we explored the sensitivity in model predictions to this assumption (see Section 2.4 for more details). The IVOC emissions estimates and their potential to form SOA was based on the work of Jathar et al. (2014). In Jathar et al. (2014), IVOC emissions, defined as the sum of all unspciated compounds, were determined as a mass fraction of the total non-methane organic gas (NMOG) emissions for three different source categories: gasoline vehicles, diesel vehicles, and biomass burning. Here, the IVOCs, as unspciated organic compounds, are new SOA precursors added to the emissions inventory and regardless of their chemical makeup are distinct from the speciated precursors such as long alkanes and aromatics already present in existing emissions inventories. IVOCs were assumed to be 25% of the NMOG emissions for on- and off-road gasoline exhaust, 20% of the NMOG emissions for on- and off-road diesel exhaust, and 7% of the NMOG emissions for residential wood combustion and wildfires. The IVOC:NMOG fractions did not appear to be statistically different for the gasoline and diesel sources manufactured before or after 2005 and hence those fractions were assumed to be representative of the source fleet in 2005. No IVOCs were considered for the food cooking source but recent work suggests that they might play a role in influencing the OA evolution from a multitude of food cooking sources (Kaltsonoudis et al., 2017; Liu et al., 2017). We assumed that the NMOG emissions in the emissions inventory accounted for most of the gas-phase organic compound mass that included the IVOCs and hence the addition of IVOC emissions meant that the non-IVOC emissions had to be reduced to conserve total NMOG mass. Recent literature suggests that IVOCs could be lost to walls of the sampling hardware (e.g., tubing, bags) (Pagonis et al., 2017) and therefore would be excluded in the NMOG measurement. Our assumption should result in conservative estimates for the influence of IVOC emissions on SOA formation.

Deleted: Based on that work,

Deleted:

Deleted: to account

Following Jathar et al. (2014), the IVOCs were modeled as a C₁₃ hydrocarbon for those from on- and off-road gasoline sources and as a C₁₅ hydrocarbon for those from on- and off-road diesel sources and biomass burning. The oxidation of the IVOC hydrocarbons and their reaction products and the subsequent SOA formation was modeled assuming equivalence to a linear alkane and used the SOM parameter set for *n*-dodecane. As mentioned earlier, *n*-dodecane only informs the multi-generational oxidation chemistry of the precursor and the actual compound of interest (e.g., a C₁₃ or C₁₅ linear alkane) can have a different SOA mass yield than that of *n*-dodecane. The equivalent linear alkane to model SOA formation from IVOCs in Jathar et al. (2014) was based on fitting the SOA formation observed in chamber experiments (Gordon et al., 2014a, 2014b; Hennigan et al., 2011) and hence the choice of the hydrocarbon in this work was experimentally constrained. Jathar et al. (2014) used linear alkanes as a surrogate as the SOA formation from linear alkanes was well studied when they developed the parameterization and the SOA mass yields increased predictably with the carbon number of the precursor. Recent application of gas-chromatography mass-spectrometry to combustion emissions has found that IVOCs are mostly composed of branched/cyclic alkane and aromatic compounds (Gentner et

Formatted: Subscript

Deleted: (Gordon et al., 2014a; Gordon et al., 2014b; Hennigan et al., 2011)

al., 2012; Koss et al., 2018; Zhao et al., 2016, 2017). So while it would have been more appropriate to model the IVOCs as an alkane-aromatic mixture, this choice would not have substantially changed the model predictions in the work as the SOA formation from this alkane-aromatic mixture would still be constrained to the same chamber experiments. We will consider the recent detailed speciation work surrounding IVOCs in future applications of this model. In this work, we also investigated the sensitivity in model predictions to the use of an aromatic compound (i.e., toluene) as a surrogate instead of an alkane (i.e., *n*-dodecane) to model SOA formation from IVOCs (see rationale in Section 2.4).

Recently, Zhao and coworkers (Zhao et al., 2015, 2016) used thermal desorption gas-chromatography mass spectrometry (TD-GC-MS) to measure IVOC emissions in gasoline and diesel exhaust and speciated/classified the IVOCs as a mixture of linear, branched, and cyclic compounds resolved by carbon number. We should note that Zhao et al. (2015, 2016) defined IVOCs as the sum of speciated and unspeciated hydrocarbons roughly larger than a C₁₂ alkane, which was different from the definition adopted by Jathar et al. (2014). In their first paper, Zhao et al. (2015) found IVOCs to be about 60% of the NMOG mass emissions for tailpipe exhaust from older diesel vehicles/engines (ones without particle filters or oxidation/reduction catalysts). In this work we used an IVOC:NMOG ratio of 0.2 and likely underestimated IVOC emissions from diesel sources by a factor of 2.5. Zhao et al. (2015) concluded that the effective IVOC yield based on their speciation was comparable to the yield of the C₁₅ linear alkane used in this work but the application of that yield over-predicted the chamber SOA data from Gordon et al. (2014a) by a factor of 1.8; virtually all of the SOA predicted by Zhao et al. (2016) was from the oxidation of IVOCs. If one assumed that the effects from lower IVOC emissions (factor of 2.5) were roughly balanced by the use of higher SOA yields (factor of 1.8), then the SOA formation from diesel sources was probably well represented in our work.

In their second paper, Zhao et al. (2016) found the IVOCs to be only about 4% of the NMOG mass emissions in gasoline exhaust but we used an IVOC:NMOG ratio of 0.25 in this work. This suggests that we may be overestimating the gasoline exhaust IVOC emissions by approximately a factor of six in this work. Based on the speciation performed, Zhao et al. (2016) estimated that the IVOCs collectively had an SOA yield between 19 and 24% at an OA mass concentration of 9 µg m⁻³ (9 µg m⁻³ was the average end-of-experiment concentration in the chamber experiments of Gordon et al. (2014a)), which was slightly more than twice the SOA yield for a C₁₃ linear alkane (7-12%) – used to model gasoline IVOCs in this work – at the same OA mass concentration. However, application of the Zhao et al. (2016) SOA yields for IVOCs underpredicted the observed chamber SOA formation for newer gasoline vehicles by a factor of ~2. Since IVOC oxidation accounted for slightly less than half of the SOA formed (with the other half coming from single-ring aromatics), the IVOC SOA yields in Zhao et al. (2016) would need to be tripled to explain the chamber SOA measurements. If we assumed that the effects from higher IVOC emissions (factor of 6) were approximately balanced by the use of lower SOA yields (factor of 2×3=6), then the SOA formation from gasoline sources in this work was probably well represented in our work. To summarize, the IVOC emissions estimates and the surrogates used to model SOA formation from IVOCs from gasoline and diesel sources in this work, while different from those suggested in Zhao et al. (2015, 2016), are still consistent with the SOA measurements made by Gordon et al. (2014a, 2014b).

2.2.3 Modeling the NO_x Dependence on SOA Formation

Previous applications of the SOM have simulated SOA under low and high NO_x conditions separately since the SOM, in its current form, cannot model the continuous evolution of SOA under varying NO_x conditions using the local NO/HO₂. Predictions from either of these simulations (Jathar et al., 2016) or the average of these simulations (Cappa et al., 2016) likely do not accurately characterize the evolution or spatial distribution of SOA since NO_x concentrations

Deleted: (Gentner et al., 2012; Zhao et al., 2016; Zhao et al., 2017; Koss et al., 2018)

Formatted: Font color: Text 1

Formatted: Font: Not Italic, Font color: Text 1

Formatted: Font color: Text 1

Deleted:

Deleted: W

Deleted: ¶

Deleted: ¶

exhibit strong spatial variability with higher concentrations in urban (e.g., traffic) and source (e.g., wildfires) regions. For example, since most precursors have higher SOA yields under low NO_x conditions than under high NO_x conditions, the use of an average is expected to overestimate SOA in high-NO_x urban areas and underestimate SOA in low-NO_x rural/remote continental areas.

In this work, we used two different offline techniques to account for the influence of NO_x on SOA formation. For both methods, we assumed that the 3D model predictions based on the low and high NO_x SOA parameterizations bounded the minimum and maximum ambient SOA mass concentrations. Xu et al. (2015) found that the SOA formation from isoprene photooxidation was maximized at intermediate NO_x levels with lower values at the extreme NO_x levels, suggesting that our bounding assumption may not necessarily hold for all precursor species. Presto and Donahue (2006) found that the SOA from α -pinene ozonolysis under varying NO_x conditions could be estimated by interpolating the SOA formed between the low and high NO_x conditions using the VOC:NO_x ratio. Hence, in the first method, we used the VOC:NO_x ratios from the low and high NO_x chamber experiments as our bounds and used the 3D model predicted VOC:NO_x ratio to interpolate between the minimum and maximum SOA mass concentrations predicted from the low and high NO_x simulations. Previous work (e.g., Camredon et al. (2007), Xu et al. (2015)) has also found SOA formation to vary along a NO_x scale and hence, in the second method, we used NO_x concentrations from the low and high NO_x chamber experiments and the 3D model predictions to perform the interpolation. For each method, we performed the interpolation on the SOA mass concentrations assuming a linear or logarithmic dependence on the VOC:NO_x ratios and NO_x concentrations. The linear dependency was chosen for simplicity while the logarithmic dependency was chosen to mimic the visual trends in SOA and VOC:NO_x or NO_x reported in previous work and also to produce the highest response in the SOA formation with NO_x. The VOC:NO_x ratio and the NO_x concentration served as an approximate surrogate for the HO₂:NO ratio used in most atmospheric models to simulate the NO_x-dependent SOA formation. The NO_x-adjusted SOA concentrations (SOA_{eff}) from each precursor at each grid cell were calculated from model predictions from the low and high NO_x simulations using the following equations:

$$SOA_{eff} = SOA_{high\ NO_x} + \frac{SOA_{low\ NO_x} - SOA_{high\ NO_x}}{(VOC:NO_x)_{low\ NO_x} - (VOC:NO_x)_{high\ NO_x}} \times ((VOC:NO_x)_{model} - (VOC:NO_x)_{high\ NO_x}) - (1)$$

$$SOA_{eff} = SOA_{high\ NO_x} + \frac{SOA_{low\ NO_x} - SOA_{high\ NO_x}}{\log(VOC:NO_x)_{low\ NO_x} - \log(VOC:NO_x)_{high\ NO_x}} \times (\log(VOC:NO_x)_{model} - \log(VOC:NO_x)_{high\ NO_x}) - (2)$$

$$SOA_{eff} = SOA_{low\ NO_x} - \frac{SOA_{low\ NO_x} - SOA_{high\ NO_x}}{(NO_x)_{high\ NO_x} - (NO_x)_{low\ NO_x}} \times ((NO_x)_{model} - (NO_x)_{low\ NO_x}) - (3)$$

$$SOA_{eff} = SOA_{low\ NO_x} - \frac{SOA_{low\ NO_x} - SOA_{high\ NO_x}}{\log(NO_x)_{high\ NO_x} - \log(NO_x)_{low\ NO_x}} \times (\log(NO_x)_{model} - \log(NO_x)_{low\ NO_x}) - (4)$$

where $SOA_{low\ NO_x}$ and $SOA_{high\ NO_x}$ are model predictions of SOA from using the low and high NO_x parameterizations respectively, $(VOC:NO_x)_{low\ NO_x}$ and $(VOC:NO_x)_{high\ NO_x}$ are the initial VOC:NO_x ratios from the chamber experiments used to develop the low and high NO_x SOA parameterizations, $(VOC:NO_x)_{model}$ is the model predicted VOC:NO_x ratio in the model grid cell, $(NO_x)_{low\ NO_x}$ and $(NO_x)_{high\ NO_x}$ are the NO_x concentrations from the chamber experiments used to develop the low and high NO_x parameterizations, and $(NO_x)_{model}$ is the model predicted NO_x concentration in the model grid cell. Equations (1) and (3) assume linear dependence while equations (2) and (4) assume logarithmic dependence. For the $(VOC:NO_x)_{model}$ ratio, the VOC is the sum of all organic species tracked in the SAPRC-11 gas-phase chemical mechanism, including all IVOCs and gas-phase SVOCs. NO_x is the sum of NO and

Deleted: (Xu et al., 2015)

Field Code Changed

Deleted: Presto et al. (2006)

Deleted: I

Deleted: (e.g., Camredon et al. (2007), Xu et al. (2015))

Formatted: Subscript

Deleted: I

Formatted: Subscript

Formatted: Subscript

Formatted: Subscript

Formatted: Font color: Black

NO₂. The (VOC:NO_x) ratios and the NO_x concentrations from the chamber experiments used in the equations were gathered directly from the primary references and are listed in Table 2. When the (VOC:NO_x)_{model} or (NO_x)_{model} values were lower or higher than the chamber values in Table 2, the SOA formation was set to model predictions from the bounding simulations.

Table 2: Low and high VOC:NO_x ratios in ppb ppb⁻¹ from chamber experiments used to model the influence of NO_x on SOA formation.

SOM surrogate	(VOC:NO _x) _{low NO_x}	(NO _x) _{low NO_x}	(VOC:NO _x) _{high NO_x}	(NO _x) _{high NO_x}	Reference
<i>n</i> -dodecane	17.0 ^Δ	<2 ppbv	0.09	343	Loza et al. (2014)
benzene	207 ^Δ	<2 ppbv	1.98	169	Ng et al. (2007a)
toluene	46.3 ^{Δ*}	<0.8 ppbv	0.76 [*]	50	Zhang et al. (2014)
<i>m</i> -xylene	12.1 ^{Δ#}	<2 ppbv	0.10	943	Ng et al. (2007a)
isoprene	24.5 ^Δ	<2 ppbv	0.29	937	Chhabra et al. (2010)
α -pinene	33.1 ^Δ	<2 ppbv	0.05	844	Chhabra et al. (2010)

^Δ minimum VOC:NO_x ratios since these assume a NO_x concentration of 0.8 ppbv in the chamber

^{*} average of six experiments performed by Zhang et al. (2014)

[#] average of two experiments performed by Ng et al. (2007a)

We acknowledge that this approach to modeling the NO_x influence on SOA formation is limited and is sensitive to the following assumptions: (i) the VOC:NO_x ratio plus NO_x concentration is a good proxy to model the HO₂:NO ratio and the branching between low and high NO_x SOA formation, (ii) the low and high NO_x chamber experiments for a particular precursor bound the minimum and maximum SOA formed, (iii) the SOA response between the low and high NO_x levels varies linearly or logarithmically with VOC:NO_x ratios/NO_x concentrations, and (iv) the model predicted VOC concentrations at each grid cell, summed across a mixture of organic compounds, are analogous to the initial VOC concentrations from the chamber experiment to calculate VOC:NO_x ratios. There are few experimental data to test these assumptions and these need to be investigated in future work. In addition to modeling the influence of NO_x on ambient SOA concentrations, this approach allowed us to explore the influence of reductions in NO_x emissions and concentrations on ambient OA concentrations in the future.

2.3 Simulations

Table 3: Names and descriptions of the simulations performed in this work

No.	Name	Semi-volatile & Reactive POA (SVOC)	IVOC	Vapor Wall Losses for SVOC, IVOC, and VOC	Additional Details
1	Traditional	No	No	No	Same as model of Cappa et al. (2016)
2	SVOC	Yes ^Δ	No	No	-
3	IVOC	Yes ^Δ	Yes	No	-
4	Base	Yes ^Δ			Base case model used in this work
5	SVOC _{max} ¹				SVOCs modeled as per diesel parameterization
6	IVOC _{max} ¹				IVOCs modeled as per diesel parameterization
7	No-Aging ¹				No multi-generational aging
8	VOC _{spec} ¹		Yes	Yes	VOC speciation from May et al. (2014)
9	Aromatic ¹				S/IVOCs modeled using the toluene parameterization
10	SVOC _{cooking} ¹	Yes ^Δ			SVOCs from food cooking modeled using the volatility distribution of Louvaris et al. (2017).

Formatted: Superscript

Deleted: and

Deleted:

Formatted: Superscript

Deleted: *

Deleted: *

Deleted: *

Deleted: *

Deleted: *

Deleted: *

Formatted: Subscript

Formatted: Superscript

¹Same as the Base simulation but with differences noted in the 'Additional Details' section. ²Assumes volatility of food cooking POA to be similar to volatility of biomass burning. ³Uses measured volatility of food cooking POA.

Deleted: *

The Base simulation – representing our most comprehensive simulation – included the updates described in Section 2.2.2; a source-resolved semi-volatile and reactive treatment of POA, source-resolved SOA formation from SVOCs and IVOCs, and correction of the subsequent SOA formation for vapor wall losses in chambers. The Base simulation included sub-simulations at two resolutions (24 km and 8 km) with two NO_x parameterizations (low and high NO_x).

Additional simulations were designed and performed with two objectives in mind: (i) to examine the influence of each update included in this work and (ii) to test the sensitivity in model predictions to uncertainties inherent in the updates and other model inputs. A set of four simulations were performed to systematically study the influence of model updates. These included the following simulations where only one update (as underlined) was made over the previous configuration: (1) Traditional – Non-volatile POA, no IVOCs, SOA from VOCs, and no correction for chamber vapor wall losses, (2) SVOC – Semi-volatile POA, no IVOCs, SOA from SVOCs and VOCs, and no correction for chamber vapor wall losses, (3) IVOC – Semi-volatile POA, IVOCs, SOA from SVOCs, IVOCs, and VOCs, and no correction for chamber vapor wall losses, and (4) Base – Semi-volatile POA, IVOCs, SOA from SVOCs, IVOCs, and VOCs, and correction for chamber vapor wall losses. Successive differences in model predictions between the Traditional, SVOC, IVOC, and Base simulations were used to systematically examine the influence of the semi-volatile and reactive POA, IVOCs, and chamber vapor wall losses respectively.

A set of six simulations were performed to study uncertainties in model inputs. The SVOC_{max} simulation (5) assumed that POA from all sources (all POA except marine POA) was semi-volatile and modeled using the volatility distribution for diesel exhaust POA. Diesel POA was chosen since it was the most volatile of the volatility distributions used in this work. This simulation bounded the maximum loss in POA mass to evaporation. The IVOC_{max} (6) simulation assumed that all sources (combustion and non-combustion except biogenic sources) emitted IVOCs, which were estimated using an IVOC:NMOG ratio of 0.2 and allowed to form SOA equivalent to a C₁₅ alkane. This simulation provided an upper bound estimate to the contribution of IVOCs to ambient SOA although the IVOC emissions and their potential to form SOA could be even higher than that assumed here. The No-Aging (7) simulation assumed no multi-generational aging or in other words, the emitted precursor was allowed to react with OH and form four functionalized products with no further oxidation. This simulation investigated the influence of multi-generational aging on ambient SOA. The VOC_{spec} (8) simulation updated the VOC speciation for on- and off-road gasoline and diesel vehicles based on a comprehensive set of measurements performed on an in-use fleet (May et al., 2013a, 2013b). This simulation examined the influence of updated emissions profiles on the non-IVOC contribution to SOA. The Aromatic (9) simulation assumed that the oxidation of SVOCs and IVOCs to form SOA was modeled using toluene. There were two reasons for choosing toluene. First, both mono- and poly-cyclic aromatic compounds are found in gasoline and diesel fuel (Gentner et al., 2012) and in tailpipe emissions from mobile sources (Zhao et al., 2015, 2016), and oxygenated aromatic compounds such as phenols, guaiacols, and syringols are found in biomass burning emissions (Schauer et al., 2001; Stockwell et al., 2015). Second, aromatic compounds, similar to alkanes, have been studied in detail for their potential to form SOA and are recognized to form more SOA than linear alkanes for the same carbon number. This simulation provided an upper bound estimate for SOA formation from the oxidation of SVOCs and IVOCs. Finally, the SVOC_{cooking} (10) simulation used a hydrocarbon/linear alkane distribution based on the measured volatility distribution of Louvaris et al. (2017) to represent POA from food cooking sources. This simulation examined the effect a more realistic volatility distribution for food

Deleted: five

Deleted: Finally, the

Formatted: Subscript

[cooking POA on mass concentrations of POA and SOA from SVOCs.](#)

The UCD/CIT model was run on the High Performance Computing cluster run by Engineering Network Services at Colorado State University. Although the number of cores varied based on availability, on average each simulation used 96 cores and required 5 days to execute 19 simulated days. Since each set included four sub-simulations, each simulation required ~5 days and all simulations in this work required ~180 days of computational time.

2.4 Measurements for Model Evaluation

Model predictions were evaluated against gas-phase measurements of SOA precursors and particle-phase measurements of OA mass concentrations and composition. Here, we briefly describe the primary measurement data and any post-processing of the data we performed prior to undertaking the model evaluation.

Gas-phase measurements of SOA precursors were from two different sources. The first source was routine daily-averaged measurements of single-ring aromatics made by the South Coast Air Quality Management District (SCAQMD, 2017) in southern California at three different sites: North Los Angeles, Riverside, and Long Beach. While measurement data were available at three other sites, data were not available for 2005, our modeled year and hence not included. These gas-chromatography-based measurements were available every twelfth day and included the following aromatic species: benzene, toluene, *o/m/p*-xylene, ethyl-benzene, and styrene. Since there was little overlap between the modeled episode (14 day period over July-August) and available aromatic data, the measurement data were averaged over a three month period in the summer (May 15th to September 15th) and then compared to the episode-averaged model predictions. The second source was gas-chromatography mass-spectrometry measurements of single-ring aromatics (Borbon et al., 2013) and IVOCs (Zhao et al., 2014) made at the Pasadena ground site in the months of May and June of 2010 as part of the CalNex campaign. The single-ring aromatics were measured every hour and included the following species: benzene, toluene, *o/m/p*-xylene, ethyl-benzene, and styrene. The IVOCs were measured every three hours and included most of the reduced and oxidized organic species with a carbon number larger than 12. Since these measurements were from a different time period, we compared campaign-averaged measurements against episode-averaged model predictions.

Particle-phase measurements were from two different sources as well. The first source was routine daily-integrated measurements of organic carbon (OC) in southern California from four sites in the Chemical Speciation Network (CSN; Central Los Angeles, Riverside, Simi Valley, and Escondido) and six sites in the Interagency Monitoring of Protected Visual Environments (IMPROVE) network (San Rafael, Rubidoux-Riverside, San Geronio Wilderness, Joshua Tree NP, Agua Tibia, and San Gabriel). The CSN is a network of ~50 urban measurement sites across the United States where pollutant concentrations are typically higher, more variable, and representative of local sources and measurements are made once every three days. The IMPROVE is a network of ~200 rural/remote continental sites typically located in national parks across the United States where pollutant concentrations are lower, less variable, and representative of regional influences and measurements are made once every three days. Over the 14 day episode modeled in this work, three measurements from the CSN and five measurements from the IMPROVE network were available for comparison. We used an organic aerosol to organic carbon ratio (OA:OC) of 1.6 to calculate OA at the CSN sites (Docherty et al. (2011) measured an OA:OC ratio of 1.77 during the SOAR-1 campaign, after correction with the updated calibration of Canagaratna et al. (2015)) and a ratio of 2.1 to calculate OA at the IMPROVE sites (Turpin and Lim, 2001). The CSN data are artifact corrected but we subtracted $0.5 \mu\text{g m}^{-3}$ from the calculated OA mass concentrations to blank correct the

data (Subramanian et al., 2004). The IMPROVE data are both blank and artifact corrected. We note that a negative evaporation artifact has been reported for at IMPROVE sites in the southeast US (Kim et al., 2015) but it is not known whether such an artifact may be present in this region and no correction has been made. The second source was particle measurements made at the ground site in Riverside as part of the SOAR-1 campaign during the summer of 2005 (Docherty et al., 2008, 2011). These measurements included hourly-averaged mass concentrations and elemental ratios of H:C and O:C for OA, and estimates of the POA-SOA split based on results from a positive matrix factorization analysis.

3 Results

3.1 POA and SOA Precursor Emissions

Gas- and particle-phase emissions of organic compounds in the 8 km southern California domain, averaged over the 14-day episode, are shown in Figure 1. The 8 km domain, shown in Figure S1, includes the entire Los Angeles metropolitan statistical area, parts of the Pacific Ocean, and forested areas surrounding the urban area. The emissions are color-coded by source type and include all species that contribute to direct emissions and atmospheric formation of OA. These do not include emissions of marine POA since those were calculated inline in the UCD/CIT model. Since the POA repartitioned between the gas and particle phases after emission, POA was split into POA and SVOC that represented the particle and gas portions of POA partitioned at an urban OA mass concentration of $9 \mu\text{g m}^{-3}$. We chose $9 \mu\text{g m}^{-3}$ to partition POA because the campaign-averaged OA mass concentration at Riverside during SOAR-1 was $9 \mu\text{g m}^{-3}$. If one discounts the POA emissions in the ‘Other’ category (which is mostly made of road, agricultural, and construction dust), the re-partitioning resulted in about 60% of the POA emitted to evaporate as SVOC vapors; these vapors will oxidize in the atmosphere to form SOA. As noted earlier, a relatively more volatile treatment compared to that described in the recent literature suggests that we may have overestimated the POA evaporation from food cooking sources. Mobile sources accounted for 20% of the POA and 35% of the SVOC vapors and competed with food cooking as an important source of primary emissions and one which accounted for 15% of the POA and 44% of the SVOC vapors. IVOC, long alkane, and aromatic emissions were roughly on the same order of magnitude but taken together were approximately an order of magnitude larger than the POA emissions. This suggests that even at low SOA mass yields (say <10%), the OA formed from the oxidation of these precursors could quickly exceed direct emissions of POA.

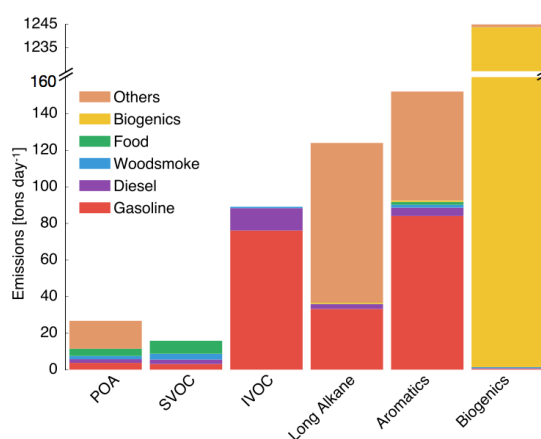
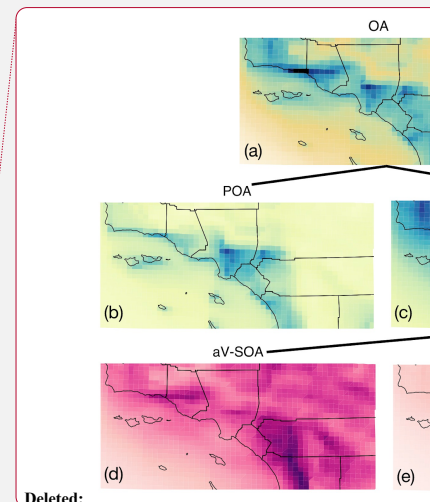


Figure 1: Episode-averaged gas- and particle-phase organic emissions in tons per day over the 8 km southern California domain resolved by source. POA and SVOC represent the particle- and gas-phase emissions partitioned to an OA mass concentration of $9 \mu\text{g m}^{-3}$. SVOC, IVOC, long alkanes, aromatics, and biogenics represent gas-phase emissions of precursor species that are modeled to form SOA. *We note that recent measurements suggest that POA from food cooking sources is less volatile than assumed in these results.*

Emissions of total IVOCs were slightly lower than those for long alkanes (by ~30%) and aromatics (by ~40%) but a factor of 2 higher than the sum of POA and SVOCs. Previously, IVOC emissions have been estimated by scaling POA emissions by a factor of 1.5 to 4 derived from gas/particle partitioning calculations (Dzepina et al., 2009; Shrivastava et al., 2008) and from atmospheric measurements (Ma et al., 2017). While our estimate for IVOC emissions are within the previously used range, our estimates were informed by a broader suite of source measurements, which will help reduce the uncertainty in IVOC emissions and related SOA formation in atmospheric models. IVOC emissions from mobile sources were similar to aromatic emissions but twice the long alkane emissions. Hence, we anticipated IVOCs to contribute meaningfully to the anthropogenic SOA burden. We note that in this work we only considered IVOC emissions from combustion sources but recent work suggests that volatile chemical products present in sources such as pesticides, coatings, cleaning agents, and personal care products may be a large source of SVOCs and IVOCs in urban environments (McDonald et al., 2018).

Mobile sources – dominated by gasoline use – accounted for a much larger fraction of the anthropogenic SOA precursors (85% of IVOCs, 27% of long alkanes, and 55% of aromatics) in this study. Hence, mobile source regulation on precursor emissions from gasoline vehicles (e.g., limits on emissions of unburned hydrocarbons) has and could have a much larger influence on controlling ambient OA than regulating direct emissions of POA, although this ultimately depends on the extent of conversion of these species to SOA. Finally, biogenic precursor emissions of isoprene, monoterpenes, and sesquiterpenes were about a factor of three higher than the combined emissions of SVOCs, IVOCs, long alkanes, and aromatics and will continue to be an important source of SOA in southern California. However, their impact on urban OA/SOA will be smaller since these emissions are primarily limited to regions outside the urban areas.



Deleted:

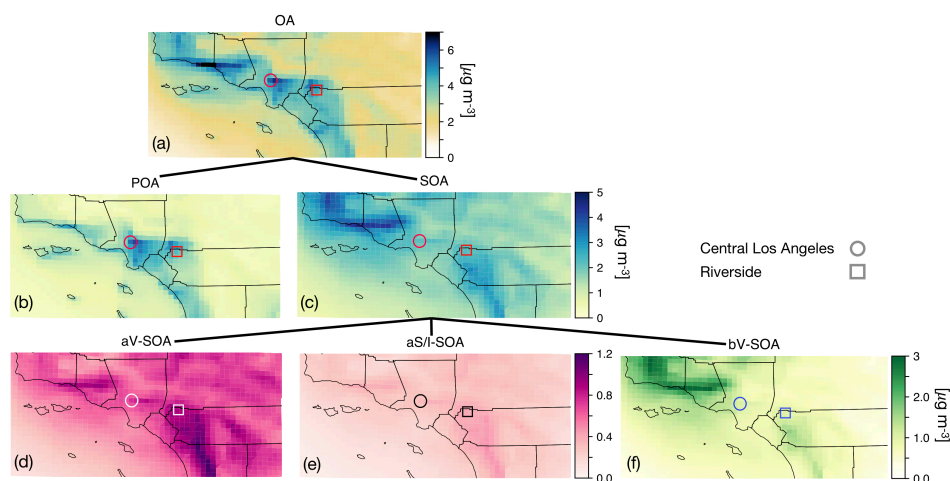


Figure 2: 14-day averaged model predictions of mass concentrations for OA, POA, SOA, aV-SOA, aS/I-SOA, and bV-SOA in $\mu\text{g m}^{-3}$ over the southern California domain from the Base simulation. *We note that recent measurements suggest that POA from food cooking sources is less volatile than assumed in these results.*

3.2 Spatial Distribution of OA Concentrations and Bulk Composition

In Figure 2 we plot predictions of the 14-day averaged mass concentrations for OA, POA, SOA, and contributions from three lumped SOA precursors (long alkanes and aromatics, SVOC and IVOCs, and biogenic VOCs) from the Base case simulation. We used the terminology developed by Murphy et al. (2014) to describe the SOA from the different sources. To reiterate, the Base case simulation included a semi-volatile treatment of POA, SOA formation from oxidation of SVOCs, IVOCs, and VOCs, multi-generational aging, and SOA parameterizations that accounted for the influence of chamber vapor wall losses. The mass concentrations in Figure 2 account for SOA formation under varying NO_x levels as per equation 2 (logarithmic dependence on the $\text{VOC}:\text{NO}_x$ ratio). We chose equation 2 because it produced the highest SOA mass concentrations and presented an upper bound on SOA formation.

The highest OA mass concentrations were found in three general regions: the densely-populated Los Angeles-Orange-Riverside County region likely attributed to heavy transportation emissions, along the coast as a result of sea spray emissions, and in biogenic VOC dominated areas. In central Los Angeles (*grid cell containing the CSN site*), OA accounted for 38% of the modeled non-refractory $\text{PM}_{2.5}$ mass concentration with 20, 25, and 18% contributions from sulfate, nitrate, and ammonium aerosol. A sensitivity simulation that turned emissions of marine POA off suggested that the marine POA mass concentrations in central Los Angeles were $\sim 0.9 \mu\text{g m}^{-3}$, which were considerably higher than the coastal measurements made during CalNex in 2010 (Hayes et al., 2013). Measured mass concentrations of POA over the open ocean west of California were $\sim 0.2 \mu\text{g m}^{-3}$ during CalNex in 2010 and it was expected that these mass concentrations would be substantially lower by the time they were transported to central Los Angeles (Hayes et al., 2013). Sea spray emissions in the UCD/CIT model are based on the parameterization of Gong et al. (2003) and may need to be revisited in the future.

2 The broader spatial trends of OA, POA, and SOA were in line with results from earlier chemical transport model
3 studies that have treated POA as semi-volatile and modeled SOA formation from SVOCs and IVOCs (Ahmadov et
4 al., 2012; Jathar et al., 2017a; Koo et al., 2014; Robinson et al., 2007; Tsimpidi et al., 2010). POA mass
5 concentrations were highest in upwind (e.g., 3.4 $\mu\text{g m}^{-3}$ in central Los Angeles) and lower in downwind (e.g., 2.7 μg
6 m^{-3} in Riverside) locations as the POA emissions that were transported away from the source region evaporated with
7 dilution. SOA mass concentrations, in contrast to POA, had a more regional presence with lesser differences between
8 the upwind and downwind regions (e.g., 2.4 $\mu\text{g m}^{-3}$ in Riverside versus 2.2 $\mu\text{g m}^{-3}$ in central Los Angeles) or in
9 regions with high emissions of biogenic VOCs (e.g., 2.5 $\mu\text{g m}^{-3}$ inside the Los Padres National Forest). To assess the
10 relative contribution of POA and SOA to total OA, we plot the POA:SOA ratio in Figure S2, which suggests a
11 POA:SOA ratio of ~ 1.6 in near-source regions and lower elsewhere, e.g., ~ 0.4 , 0.8, and 1.2 in representative marine,
12 biogenic-dominated, and urban downwind regions. These POA:SOA splits qualitatively aligned with the hydrocarbon-
13 like and oxygenated organic aerosol (HOA and OOA) splits estimated in aerosol mass spectrometer datasets in urban
14 locations worldwide (Jimenez et al., 2009; Zhang et al., 2007). However, we predict POA:SOA ~ 1 for Riverside
15 during SOAR-1, compared to a measured ratio of ~ 0.25 (Docherty et al., 2008), which indicates that SOA may still be
16 underestimated in the model. A comparison of the OA composition predictions with the aerosol mass spectrometer
17 measurements is described in Section 4.

9 Panels (d) through (f) show contributions of three distinct SOA precursor classes to total SOA. Alkane and aromatic
10 VOCs – included as SOA precursors in most atmospheric models – appeared to contribute a maximum of 1.2 $\mu\text{g m}^{-3}$
11 of what we refer to as aV-SOA downwind of the source region. The majority of this aV-SOA (75%) originated from
12 aromatic precursors implying that alkane VOCs are unlikely to contribute much to the anthropogenic SOA or total OA
13 burden in urban areas, consistent with our earlier work (Cappa et al., 2016; Jathar et al., 2016). We note that emissions
14 inventories typically only include alkane species with carbon numbers less than 12 (Pye and Pouliot, 2012) and longer
15 alkanes with carbon numbers larger than 12 are included as part of the POA, SVOC, and IVOC emissions. Together
16 aS-SOA and al-SOA mass concentrations exhibited a similar spatial pattern over the domain but were substantially
17 lower than the aV-SOA mass concentrations – reaching a maximum of only 0.5 $\mu\text{g m}^{-3}$. The lower aS-SOA and al-
18 SOA mass concentrations were somewhat contrary to earlier work that has argued that SVOCs and IVOCs are an
19 equal or dominant precursor of anthropogenic SOA when compared to aV-SOA, especially in urban areas (Jathar et
20 al., 2014, 2017a; Woody et al., 2016). The reason for these lower concentrations can be partially attributed to the
21 precursor-dependent influence of accounting for vapor wall losses in chamber experiments (probed in greater detail in
22 Section 3.4). Biogenic SOA or bV-SOA mass concentrations exceeded 3.2 $\mu\text{g m}^{-3}$ in regions with high biogenic
23 emissions but were slightly less than 1 $\mu\text{g m}^{-3}$ in urban regions where the POA mass concentrations were the highest.
24 Previous work has suggested that the bV-SOA in urban regions is formed outside but later transported to the urban
25 region (Hayes et al., 2015; Heo et al., 2015). Overall, the averaged results over the urban areas appeared to be split
26 evenly between POA, anthropogenic SOA (aV-SOA+aS-POA+al-SOA), and biogenic SOA (bV-SOA).

3.3 Precursor Contributions to OA and SOA

9 We examined the absolute OA mass concentrations and precursor contributions to SOA in central Los Angeles across
10 four different simulations to better understand the effect of successive updates: semi-volatile and reactive POA,
11 IVOCs, and accounting for vapor wall losses. We chose central Los Angeles (grid cell containing the CSN site) as our
12 study area as it is representative of an urban location with a large population density and suffers from some of the
13 poorest air quality in the United States (ALA, 2017); results from the sensitivity simulations in Section 3.5 are also

Deleted: compared

Deleted: higher concentrations either downwind of the source regions ...

Deleted: to

Deleted: -

Deleted: -

Deleted: /

1 discussed at this specific site. Results at other urban locations (e.g., Riverside, Simi Valley) had similar SOA
2 precursor fractional contributions although the absolute concentrations did vary a little (see Figure S3). In Figure 3,
3 we plot the 14-day averaged, precursor-resolved OA mass concentrations and precursor contributions to SOA in Los
4 Angeles from two pairs of four different simulations. The two pairs represent model predictions based on the low and
5 high NO_x parameterizations.

6
7 *Semi-volatile and Reactive POA.* Differences in the Traditional and SVOC simulations were used to highlight the
8 influence of including a semi-volatile and reactive treatment of POA. The semi-volatile POA treatment resulted in
9 evaporation of the primary POA emissions from combustion sources (on- and non-road gasoline and diesel,
0 woodsmoke, biomass burning, and food cooking) and reduced POA mass concentrations by 35% in central Los
1 Angeles. A ratio of the POA mass concentrations from the SVOC simulation to those from the Traditional simulation
2 suggested that the POA mass was reduced by approximately 30 to 50% in the urban environment around the central
3 Los Angeles site (Figure S4). Overall, the POA reductions appeared to be smaller than those implied by the volatility
4 distributions of May and coworkers (May et al., 2013a, 2013b, 2013c) and those simulated in other atmospheric
5 models (Robinson et al., 2007). For gasoline, diesel, and biomass burning, May and coworkers (May et al., 2013a,
6 2013b, 2013c) proposed a 45 to 80% reduction in POA mass concentrations at ambient OA mass concentrations
7 between 1 and 10 µg m⁻³. This difference was mainly because we only modeled certain combustion-related POA to be
8 semi-volatile (i.e., gasoline, diesel, biomass burning, and food cooking sources) while earlier modeling work has
9 considered POA from all sources to be semi-volatile (e.g., marine, dust). The use of a less volatile **and more realistic**
0 food cooking POA than that used in this work (informed by the works of Woody et al. (2016) and Louvaris et al.
1 (2017)) would tend to further increase the discrepancy between our work and the findings of May and coworkers. Hu
2 et al. (2014) found that the combustion sources considered to be semi-volatile in this work accounted for about half of
3 PM_{2.5} mass concentrations in Los Angeles. **The POA mass reductions shown here are conservative, and might have**
4 **been larger if there was evidence that sources other than those considered here (e.g., marine, dust) produced POA that**
5 **was semi-volatile too, although this scenario seems unlikely.**

Deleted: While conservative, our

Deleted: are more realistic

Deleted: until

Deleted: i

Deleted: emissions

Deleted: are

Deleted: .

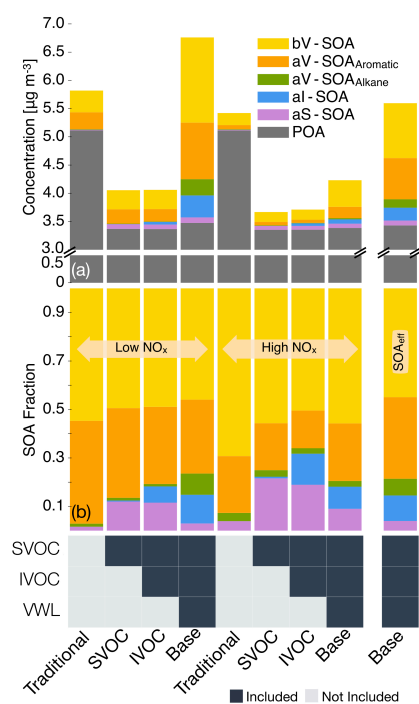
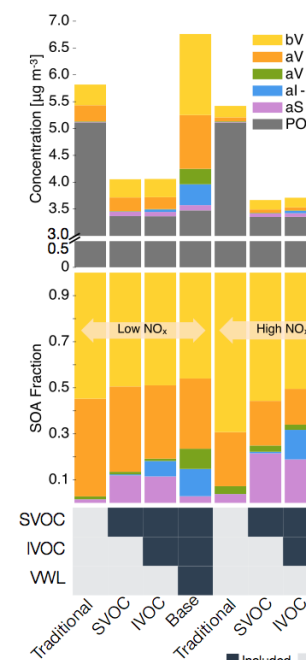


Figure 3: 14-day averaged model predictions of POA and SOA mass concentrations and precursor contributions at the central Los Angeles site from the sensitivity simulations that examined the influence of updates made in this work. Panel (a) shows absolute concentrations and panel (b) shows precursor contributions. The legend at the bottom tracks how the different pathways (i.e., SOA formation from SVOCs, SOA formation from IVOCs, and correction for chamber vapor wall losses (VWL)) were turned on for the different simulations. Model predictions from the low and high NO_x simulations are shown separately. Model predictions to the extreme right are from accounting for the influence of NO_x on SOA formation using equation 2. *We note that recent measurements suggest that POA from food cooking sources is less volatile than assumed in these results.*

Allowing the POA vapors or SVOCs to react resulted in only a small fraction of their oxidation products to condense back as aS-SOA. For example, of the $1.75 \mu\text{g m}^{-3}$ of POA lost at the central Los Angeles site, only $0.082 \mu\text{g m}^{-3}$ for the low NO_x and $0.068 \mu\text{g m}^{-3}$ for the high NO_x simulations was regained as aS-SOA from oxidation reactions. This implied a very low chemical conversion efficiency ($\sim 4\%$) for the POA-to-SVOC-to-aS-SOA pump within the urban area (Miracolo et al., 2010). The SVOCs, at an ambient concentration of $9 \mu\text{g m}^{-3}$, from gasoline exhaust, diesel exhaust, and biomass burning emissions had an average carbon number between 18 and 20. Calculations with a box model version of the SOM suggested that the SOA mass yields for C_{18} and C_{20} alkanes were between 33 and 86% where the range includes yields for low NO_x and high NO_x parameterizations. One possible explanation for the difference between the chemical conversion efficiency in the 3D model and box model yields was that only a small fraction of the SVOCs had the opportunity to react with OH and form SOA before they were transported out of the urban area. *If we assume that most of the sS-SOA in the grid cell that contains the Los Angeles site was from the oxidation of SVOCs released in that grid cell and from grid cells that are up to two grid cells away, our results do not*



Deleted:

Deleted:

Deleted: This

Deleted: es

appear unrealistic. For example, for an SOA precursor with an OH reaction rate constant of $2.4 \times 10^{-11} \text{ cm}^3 \text{ molecules}^{-1} \text{ s}^{-1}$ (average value from a C_{18} and C_{20} linear alkane) and an SOA mass yield of 60% (average from the SOA mass yield range described earlier for a C_{18} and C_{20} linear alkane), the chemical conversion efficiency would be 3.5-15% with a daily-averaged OH concentration of $1.5 \times 10^6 \text{ molecules cm}^{-3}$ and a reaction time of 0.5-2.3 hours. A reaction time of 0.5 to 2.3 hours corresponds to a transport of 2.5 (half a grid cell) and 12.5 (2.5 grid cells) miles at an average wind speed of 5.4 miles per hour (Weather Spark).

The low and high NO_x parameterizations had little effect on the aS-SOA mass concentrations presumably because the *n*-dodecane based parameterization used for semi-volatile POA exhibited marginal differences in SOA production under low and high NO_x environments (Loza et al., 2014). Finally, SOA parameterizations based on including the vapor wall loss effect only marginally increased the aS-SOA mass concentrations, especially when viewed in light of the SOA increases from other precursors. We examine the precursor-resolved vapor wall loss effect in more detail in Section 3.4. For the Base simulations, the aS-SOA mass concentrations were a factor of 10 and 2 lower than the aV-SOA mass concentrations for the low and high NO_x parameterizations respectively.

IVOC. Differences in the SVOC and IVOC simulations were used to determine the influence of including SOA formation from IVOCs. For both the low and high NO_x simulations, IVOCs contributed marginally to the aI-SOA mass concentrations in Los Angeles ($\sim 0.045 \text{ } \mu\text{g m}^{-3}$) and elsewhere too (see Figures S3 and S4). The aI-SOA mass concentrations were about half of the aS-SOA mass concentrations for both the low and high NO_x simulations. When compared to the aV-SOA mass concentrations, the aI-SOA mass concentrations were slightly lower for the high NO_x simulations ($\sim 40\%$) but about a factor of five lower for the low NO_x simulations. The inclusion of vapor wall losses seemed to make aI-SOA as or more important than aS-SOA but still less important than aV-SOA; the aI-SOA mass concentrations were a factor of 3.3 and 2.9 lower than the aV-SOA mass concentrations for the Base simulations for the low and high NO_x simulations respectively. Our simulations imply that IVOCs might be as influential as SVOCs as a bulk class of SOA precursors but they were still less important than the traditional SOA precursors (that included long alkanes and aromatics) in contributing to ambient SOA levels. In this work, the IVOC contribution to SOA was smaller compared to that from traditional SOA precursors mostly because IVOC emissions were only about a third of the traditional SOA precursors (see Section 3.1 for details on emissions). So although IVOCs have higher SOA yields than most of the traditional SOA precursors, the significantly lower IVOC emissions more than offset the increased SOA formation from higher yields. While there are exceptions (e.g., Tsimpidi et al. (2010); Jathar et al. (2017a)), our results did not align with previous box (e.g., Dzepina et al. (2009); Hayes et al. (2015); Ma et al. (2017)) and 3D (e.g., Bergstrom et al. (2012); Zhang et al. (2013)) modeling literature that has found IVOCs to be similar or more important than traditional SOA precursors in contributing to ambient SOA levels. Below we discuss three main reasons for this inconsistency.

First, some previous estimates of IVOC emissions are likely to be less representative of the in-use gasoline- and diesel-powered sources and unconstrained for biomass burning sources. IVOC emissions in most atmospheric models have previously been determined by scaling emissions of POA or by calculating partitioning with the measured POA, with scaling factors typically on the order of 1.5 (e.g., Shrivastava et al. (2008)) but as large as 3 (e.g., Dzepina et al. (2009)). These factors have been calculated from emissions data from two medium-duty gasoline vehicles built more than two decades ago and a POA volatility distribution from a small off-road diesel engine (Robinson et al., 2007). Additionally, since POA is semi-volatile the POA mass in the particle phase will change with OA loading, which can

Deleted: For example, for an SOA precursor with an OH reaction rate constant of $2 \times 10^{-11} \text{ cm}^3 \text{ molecules}^{-1} \text{ s}^{-1}$ and an SOA mass yield of 20%, the chemical conversion efficiency would be $\sim 7\%$ with a daily-averaged OH concentration of $1.5 \times 10^6 \text{ molecules cm}^{-3}$ and a reaction time of 4 hours; 4 hours would correspond to a transport of 20 miles at an average wind speed of 5 miles per hour. The central Los Angeles site is only slightly more than 10 miles from the coast....

Deleted: as a bulk class of SOA precursors may not contribute substantially to ambient SOA levels. While they were ...

Deleted: in forming SOA

Deleted: .

Deleted: very likely to be un

Deleted: unrepresentative sources:

complicate the use of a scaling based on POA (but this is addressed by the partitioning method used in some studies). Zhao et al. (2015) provided some evidence for this where they found that the POA-based scaling did not work that well for modern diesel vehicles and instead recommended the use of an NMOG-based scaling. We note that Ma et al. (2017) used the IVOC estimates of Zhao et al. (2015) and still found IVOCs to be comparable to VOCs in terms of SOA production in the Los Angeles area. Second, the SOA formation from IVOCs in most models to date has not been experimentally constrained. Most schemes to model SOA formation from IVOCs have relied on an *ad hoc* aging scheme where IVOCs and their oxidation products react with the OH radical to form lower volatility products with ultimate SOA yields of 100% (Robinson et al., 2007). These schemes do not account for fragmentation reactions and have not been comprehensively validated against experimental data. Jathar et al. (2016) showed that such schemes may significantly overestimate the net aerosol production from SOA precursors. And finally, most models do not use SOA parameters that yet account for the effect of vapor wall losses in chamber experiments. This effect and its particular influence on the IVOC contribution to SOA is discussed in Section 3.4. In this work, we (i) rely on a comprehensive set of IVOC emissions estimates made from measurements performed on more representative sources, (ii) model fragmentation reactions during IVOC oxidation, (iii) to some degree constrain SOA formation from IVOCs with chamber experiments, (iv) to some degree account for the influence of vapor wall losses in chamber experiments, and (v) include all of the previously mentioned updates in a chemical transport model. Hence, we argue that our findings on the IVOC contribution to SOA might be more robust than those modeled in earlier studies.

Traditional VOCs. For the Base simulations in Los Angeles, aromatics accounted for 33% of the total SOA in Los Angeles and were the most important anthropogenic precursor of SOA. Alkane contributions to SOA were less than 10% for both the low and high NO_x simulations. Biogenic VOCs accounted for 46% and 55% of the total SOA for the low and high NO_x simulations respectively and were clearly the most important precursor of SOA at the central Los Angeles site. After accounting for the influence of NO_x based on equation (2), the isoprene, monoterpene, and sesquiterpene contributions to bV-SOA were 23%, 68%, and 9% respectively, suggesting a strong monoterpene contribution to SOA in southern California. As biogenic VOCs react very quickly with OH and O₃ (chemical lifetimes of a few hours), most of the biogenic SOA at this site was likely formed outside the urban airshed and transported to this location, as suggested by Kleeman et al. (2007), Hayes et al. (2015) and Heo et al. (2015).

3.4 Influence of Vapor Wall Losses

SOA parameterizations that accounted for the influence of vapor wall losses in chambers seemed to have had a large effect on the absolute mass concentrations of SOA. This can be seen by comparing model results between the IVOC and Base simulations in Figure 3. The SOA mass concentrations were enhanced by a factor of 10.1 and 2.6 for the low and high NO_x simulations respectively and consistent with previous 3D simulations (Cappa et al., 2016). However, they were slightly higher than the range of enhancements reported by Zhang et al. (2014) and estimated by Krechmer et al. (2016) based on analyses of chamber data. The SOA enhancements resulted in an OA enhancement of 1.66 and 1.14 in the low and high NO_x simulations, which were lower than the SOA enhancements since SOA only accounted for a fraction of the OA mass. Differences in enhancements in the low and high NO_x simulations suggest that the vapor wall loss effect was modified by the NO_x level where the enhancement may be lower in urban/source regions with higher NO_x but higher in rural/remote continental regions with lower NO_x. Since urban SOA mass concentrations are usually higher than those in rural/remote continental regions, an implication of this NO_x-modified enhancement is that accounting for vapor wall loss artifacts will tend to reduce gradients in SOA mass concentrations between urban and rural/remote continental regions and make SOA more of a regional pollutant similar to ozone (O₃).

Deleted: to

Deleted: and

Deleted: .

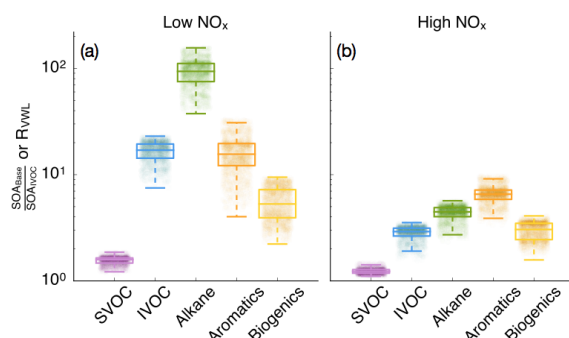


Figure 4: Ratio of model predictions from the Base simulation that accounts for the influence of vapor wall losses to model predictions from the IVOC simulation that does not account for the influence of vapor wall losses. Ratios are calculated from the 14-day averaged results for the whole domain and are resolved by precursor. Panels (a) and (b) show results from the low and high NO_x simulations respectively.

Different precursors contributed in varying degrees to the SOA enhancement. The precursor-resolved enhancements are visualized in Figure 4 where we plot the ratio of the 14-day averaged model predictions of the SOA mass concentrations from the Base simulation to those from the IVOC simulation for each grid cell in the southern California domain (dots) and overlay box-whisker plots based on those data. For all precursors the enhancements were higher for the low NO_x simulations compared to the high NO_x simulations. SVOCs showed the smallest enhancement at both the low and high NO_x levels (median of 1.6 and 1.2) and hence their fractional contribution to total SOA was reduced in the Base simulation when compared to the IVOC simulation. Alkanes showed the largest enhancement in the low NO_x simulations (median of 94) and the second largest enhancement in the high NO_x simulations (median of 4.5). Despite the large enhancements, alkanes still contributed marginally to total SOA in the Base simulations because the baseline contribution of alkanes to SOA was small in the IVOC simulations (<3%). IVOCs exhibited a larger enhancement (median of 17 and 2.9) compared to SVOCs and a smaller enhancement compared to alkanes in both simulations, despite using the same surrogate (i.e., *n*-dodecane) to model SOA formation. The reason for varying enhancements in SVOC, IVOCs, and alkanes, despite using the same surrogate (i.e., *n*-dodecane), was that the vapor wall loss-related enhancement was inversely related to the carbon number where larger carbon number precursors (e.g., SVOC that had an average carbon number of 18 to 20) showed smaller enhancements and smaller carbon number precursors (e.g., alkanes that included species between carbon numbers of 6 and 12) showed larger enhancements. The simplest explanation for this inverse relationship is that larger precursors and their oxidation products, relatively speaking, have shorter chemical lifetimes and undergo fewer chemical reactions before condensing, which make them less susceptible to being lost to the walls (see Figure S5 where we plot the vapor wall loss-related enhancement in SOA yields as a function of the carbon number at an OA mass concentration of $9 \mu\text{g m}^{-3}$). Of the two other important precursors, aromatics displayed the largest enhancement in the high NO_x simulations (median of 6.6) and were tied with IVOCs for the second largest enhancement in the low NO_x simulations (median of 16) while biogenic VOCs showed the lowest enhancement after SVOC in both the low NO_x and high NO_x simulations. Accounting for vapor wall loss artifacts is expected to result in an increase in the aromatic contribution to SOA when compared against biogenic VOCs. Vapor wall loss rates in Teflon chambers might be much higher (~factor of 5) than those used in this work to develop the SOM

Deleted:
Recent work has argued that v
Deleted: are much

parameterizations (Huang et al., 2018; Krechmer et al., 2016; Sunol et al., 2018), the use of which will be will tend to increase SOA mass concentrations even further. This new understanding will need to be considered in the future.

Deleted: (larger than a factor of 5) than by Cappa et al. (2016) and in this work to derive the SOM parameterizations

Deleted: . T

Deleted: of a higher wall loss rate

3.5 Sensitivity Analysis

Results from the sensitivity simulations that examined uncertainties in select model inputs are shown in Figure 5 where we plot the 14-day averaged model predictions from these simulations at the central Los Angeles site. We also plot model predictions from the Base simulations as all the sensitivity simulations have been performed using the Base simulation as the reference (see Table 3 for details about the simulations). Model predictions from the low and high NO_x simulations are shown separately. The No Aging simulations decreased the SOA mass concentrations by almost an order of magnitude demonstrating the importance of modeling multi-generational aging in the SOM. The inclusion of oligomerization reactions that may enhance the partitioning of semi-volatile species may alter this finding. The No-Aging simulations produced a very different precursor contribution to total SOA compared to the Base simulations and the changes in the precursor contribution were also different between the low and high NO_x simulations. For instance, the aV-SOA contributions to total SOA increased from 39% to 41% for the low NO_x simulations but decreased from 26% to less than 5% in the high NO_x simulations. This implied that the treatment of multi-generational aging in the SOM did not proportionately enhance the SOA mass concentrations from the different precursors but rather produced varying levels of enhancement for the different precursors that was further modified by the NO_x levels. This finding is of note because CTMs that have employed schemes such as the volatility basis set (VBS) have typically assumed that multi-generational aging has an approximately similar effect on SOA mass concentrations from different precursors, regardless of the NO_x levels, and one which does not significantly change the precursor contribution to SOA. With the VBS, one may observe some differences with multi-generational aging from the use of different starting VBS distributions for SOA from different precursors.

The SVOC_{max} simulations that assumed all POA (except marine POA) to be semi-volatile saw POA mass concentrations decrease by 36% compared to the Base simulations and by 56% compared to the Traditional simulations (not shown here but inferred from results in Figure 3). The increase in SVOCs from the additional evaporation of POA mass resulted in about a three-fold increase in the aS-SOA mass concentrations and a proportionate increase in the SVOC contribution to total SOA. Similar to the findings discussed in Section 3.3, only a fraction of the evaporated POA mass lost was regained as aS-SOA mass concentrations. For instance, when compared to the Traditional simulations, of the 2.9/3.3 μg m⁻³ of POA mass lost 0.32/0.22 μg m⁻³ was regained as aS-SOA reflecting a chemical conversion efficiency of 11/7% for the low/high NO_x simulations. These simulations predicted the maximum decrease in POA mass concentrations from treating all POA as semi-volatile and reactive but the results still found POA to be 40% and 69% of the total OA in the low and high NO_x simulations respectively. Direct emissions of POA were still a sizeable fraction of the ambient OA and PM burden using the current state-of-the-science treatment.

Deleted: predicted

Deleted: This indicated that d

Deleted: .

Estimating IVOCs to be 20% of the NMOG emissions for all combustion sources and modeling the SOA formation from IVOCs using a C₁₅ linear alkane – as modeled in the IVOC_{max} simulations – resulted in an approximately four-fold increase in the aI-SOA mass concentrations over the Base simulations. The increases were partly attributed to additional IVOC emissions from sources other than mobile and biomass burning (factor of 2.8 compared to IVOC emissions from the Base simulations) and partly to using a larger alkane (C₁₅ linear alkane) with a higher SOA mass yield to model SOA formation from IVOCs emitted by gasoline sources. Simulating SOA formation from IVOCs using an aromatic surrogate in the S-IVOC_{aromatic} simulations had the same effect as the IVOC_{max} simulations and increased aI-SOA mass

concentrations by a factor of 2.6/6.3 for the low/high NO_x simulations. The al-SOA mass concentrations were higher because aromatics for the same carbon number have a higher SOA mass yield than alkanes. The IVOC_{max} and $\text{S-IVOC}_{\text{aromatic}}$ simulations potentially present an upper bound contribution of IVOCs to SOA formation and in both these simulations were $\sim 30\%$ of the total SOA and a factor of ~ 1.5 -2 larger than the aromatic VOC contribution. While the IVOC_{max} and $\text{S-IVOC}_{\text{aromatic}}$ simulations dramatically increased the al-SOA mass concentrations, these simulations only modestly increased the total OA mass concentrations over the low and high NO_x simulations (average increase of 10%). Over the urban area, the OA mass concentrations in the IVOC_{max} and $\text{S-IVOC}_{\text{aromatic}}$ simulations were on average 10-12% higher compared to the Base simulations (see Figure S6). Updating the emissions profiles based on the work of May et al. (2014) had a negligible effect on the SOA mass concentrations and its precursor contribution implying that the emissions profiles from more than a decade and a half ago may be sufficient to model the modern mobile source fleet. Finally, a lower volatility (i.e., more realistic) POA in the $\text{SVOC}_{\text{cooking}}$ simulations, informed by the measurements of Louvaris et al. (2017), resulted in a 20% increase in POA mass concentrations when compared to both the low and high NO_x Base simulations. POA mass concentrations in these low and high NO_x simulations accounted for approximately 55 and 85% of the OA respectively. The SOA mass concentrations between the $\text{SVOC}_{\text{cooking}}$ and Base simulations remained the same.

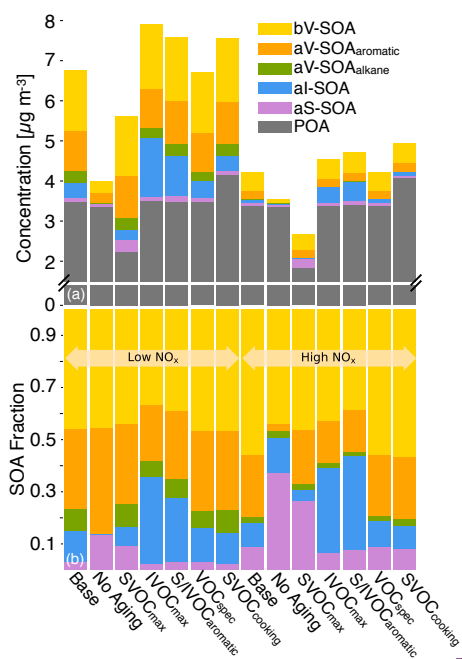
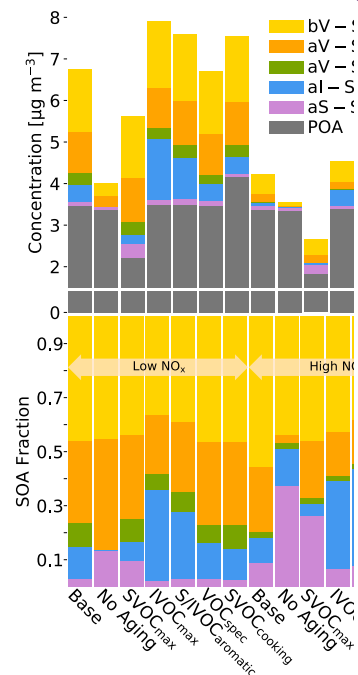
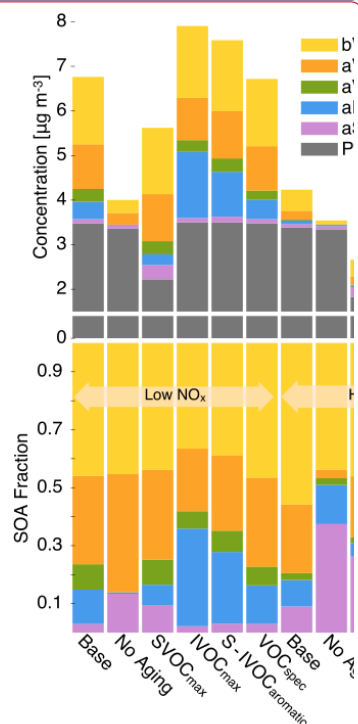


Figure 5: 14-day averaged model predictions of POA and SOA mass concentrations and precursor contributions from the sensitivity simulations. Panel (a) shows absolute concentrations and panel (b) shows precursor contributions. Model predictions from the low and high NO_x simulations are shown separately. Simulation legend: Base = Base case, No Aging = only models first generation chemistry in the SOM, SVOC_{max} = all POA treated as semi-volatile, IVOC_{max} = all combustion sources assumed to have 20% IVOC emissions and a C_{15} SOA yield, $\text{S-IVOC}_{\text{aromatic}}$ = SVOCs and IVOCs modeled as high-yield aromatic compounds, VOC_{spec} = mobile source emissions profiles based on

Deleted: Finally, u
Formatted: Subscript
Deleted: Louvaris et al. (2017),
Formatted
... [1]
Formatted: Font color: Black



Deleted:



Deleted:

May et al. (2014). $SVOC_{\text{cooking}} = \text{POA volatility distribution for food cooking sources based on the measurements of Louvaris et al. (2017)}$. All simulations besides $SVOC_{\text{cooking}}$ assumed food cooking POA to have the same volatility as biomass burning POA. More details about these simulation inputs can be found in Section 2.3.

Field Code Changed

Formatted: Subscript

Formatted: Subscript

3.6 NO_x-Adjusted SOA Formation

The SOM currently does not model the continuous evolution of SOA under varying NO_x concentrations. One of the challenges in modeling the NO_x influence on SOA formation has been in quantifying the branching of the VOC oxidation under low and high NO_x conditions. Most commonly used schemes in atmospheric models use the NO:HO₂ ratio to determine the initial branching of the precursor to form SOA via the low or the high NO_x pathway. However, this scheme depends on an accurate prediction of NO and HO₂. To assess, at least qualitatively, the ability of the model to capture NO and HO₂ concentrations, we compare 14-day averaged diurnal profiles from this work to those measured in Pasadena in 2010 during the CalNex campaign in Figure S7. We found that the model predictions were within a factor of two for NO concentrations but were about a factor of 10 lower than the measured HO₂^{*} concentrations. We should note that the HO₂^{*} measurements included HO₂ and a fraction of RO₂ radicals, where RO₂ radicals contributed to ~30% of the HO₂^{*} measurements (Griffith et al., 2016). The inclusion of RO₂ should not change the findings reported here. If the results from our modeling are representative of results from other atmospheric models that use SAPRC or other gas-phase chemical mechanisms, underestimating the HO₂ concentrations may lead NO:HO₂ ratio-based schemes to overestimate the SOA formed via the high NO_x pathway. Given this limitation and the fact that the SOM does not model the model the continuous evolution of SOA under varying NO_x concentrations, we attempted to model the NO_x-dependent SOA formation using VOC:NO_x ratios and NO_x concentrations.

Four different methods – described in equations (1) through (4) – were used to adjust the SOA mass concentrations from each individual precursor to account for the influence of NO_x. To remind the reader, equations (1) and (2) assume a linear and logarithmic dependence respectively between the SOA mass concentration and the VOC:NO_x ratio. Equations (3) and (4) assume a linear and logarithmic dependence respectively between the SOA mass concentration and the NO_x concentration. The adjusted SOA mass concentrations, referred to as SOA_{eff}, were summed to calculate the total SOA mass concentrations. Equation (2) produced the highest SOA mass concentrations while equation (3) produced the lowest SOA mass concentrations amongst the four equations. Scatter plots comparing the SOA mass concentrations calculated using equation (2) to those calculated using other equations, in Figure S8, show that the SOA mass concentrations based on equation (2) were, on average, a factor of 1.27, 3.19, and 1.92 higher than those with equations (1), (3), and (4) respectively. This meant that a calculation based on the VOC:NO_x ratio produced a stronger response of NO_x on SOA mass concentrations than the NO_x concentrations themselves. In the subsequent sections, where we evaluate the model predictions (Section 4) and predicted future changes in the OA burden (Section 5), we used the SOA_{eff} calculations based on equation 2 since they represented an upper bound estimate of the NO_x effect on SOA mass concentrations. The validity of equation 2 needs to be examined in future work.

Formatted: Subscript

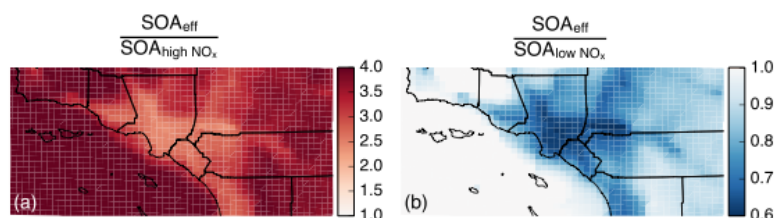


Figure 6: 14-day averaged ratio of the SOA_{eff} mass concentration to the SOA mass concentration from the (a) high NO_x and (b) low NO_x Base simulations.

In Figure 6, we plot the ratio of the total SOA_{eff} mass concentrations based on equation (2) to the total SOA mass concentrations from the (a) high NO_x and (b) low NO_x Base simulations. The SOA_{eff} mass concentrations were higher than the SOA mass concentrations predicted using the high NO_x parameterizations, with an average factor of two increase in urban areas and a maximum factor of four increase in non-urban areas. This was because the model predicted $VOC:NO_x$ ratios in the urban areas were higher than the $VOC:NO_x$ ratios produced in the high NO_x chamber experiments and based on equation (2) the SOA mass concentrations were adjusted upwards to include the SOA predicted using the low NO_x parameterizations. The adjustments increased the SOA mass concentrations because the SOA mass concentrations from each precursor were universally higher with the use of the low NO_x parameterizations compared to the high NO_x parameterizations. The SOA_{eff} mass concentrations were 30-40% lower than the SOA mass concentrations predicted using the low NO_x parameterizations in urban areas, suggesting that the SOA_{eff} mass concentrations were approximately midway between the SOA predictions using the high and low NO_x parameterizations. In contrast, the SOA_{eff} mass concentrations were only marginally lower (10-20%) in the non-urban areas implying that the $VOC:NO_x$ ratios in these regions were very similar to the $VOC:NO_x$ ratios produced in the low NO_x chamber experiments. In summary, a modest fraction of the SOA mass may be formed through the ‘low- NO_x ’ pathway in high NO_x urban areas, which may result in substantial increases in the predicted SOA mass concentration when compared against predictions purely based on the use of high NO_x parameterizations. This low- NO_x SOA will continue to increase in the future as NO_x concentrations are reduced in urban areas through controls on mobile sources. In contrast, only a small fraction of the SOA mass may be formed through the ‘high- NO_x ’ pathway in low NO_x non-urban areas and the use of a low NO_x parameterization in these regions will only marginally bias model predictions of SOA mass concentrations.

4 Model Evaluation

Model predictions from the Base simulation were evaluated against gas-phase measurements of SOA precursors and particle-phase measurements of OA mass concentrations and composition. For the particle-phase measurements, we focused the model evaluation on predictions adjusted for the NO_x influence on SOA formation using equation 2 (logarithmic dependence on $VOC:NO_x$ ratio).

4.1 SOA Precursors

In Figure 7(a), we compare 14-day averaged model predictions of aromatic concentrations for our 2005 episode against measured temporal trends in summer-averaged single-ring aromatic concentrations at three different sites in Southern California (Los Angeles-North Main Street, Riverside-Rubidoux, and Long Beach) (SCAQMD, 2017); model

predictions of aromatic concentrations are a sum of the benzene, ARO1, and ARO2 concentrations. On the same figure, we also plot model predictions of aromatic concentrations at Pasadena for our 2005 episode and measured single-ring aromatic concentrations made at the Pasadena ground site in 2010 as part of the CalNex campaign (Zhao et al., 2014). The summertime single-ring aromatic concentrations in southern California have decreased by a factor of 2 to 3 between 2000 and 2011 presumably from regulations that have targeted emissions from mobile sources. These reductions agreed well with reported temporal trends in carbon monoxide, nitrogen oxides, and non-methane organic compounds for Los Angeles over the same time period (Warneke et al. (2012); MacDonald et al. (2013)). Aromatic measurements at Pasadena in 2010 compared well with the 2010 measurements made ~12 km southwest of Pasadena at the Los Angeles-North Main Street location suggesting that the summer/campaign-averaged aromatic concentrations were spatially homogeneous over urban Los Angeles and findings from the model-measurement comparison at a particular site could be generalized for the larger modeled domain. The model-measurement comparison for aromatics in 2005 was mixed. Concentrations were overpredicted by a factor of ~1.5 at the Los Angeles-North Main Street and Long Beach sites but agreed well with measurements at Riverside-Rubidoux. The predictions might have been overestimated because we were using an older emissions inventory developed for the year 2000 but adapted for use for the year 2005 based on activity data (Hu et al., 2015). Another possibility for the over prediction was that the lumped model species ARO1 and ARO2 in SAPRC-11 also included emissions from oxygenated aromatic (e.g., phenols) and aromatic-like compounds (e.g., furans) while the measurements were limited to a handful of single-ring reduced aromatic compounds. Despite differences in the absolute concentrations, the model seemed to capture the measured spatial differences between the three sites, i.e. Los Angeles-North Main Street > Riverside-Rubidoux > Long Beach.

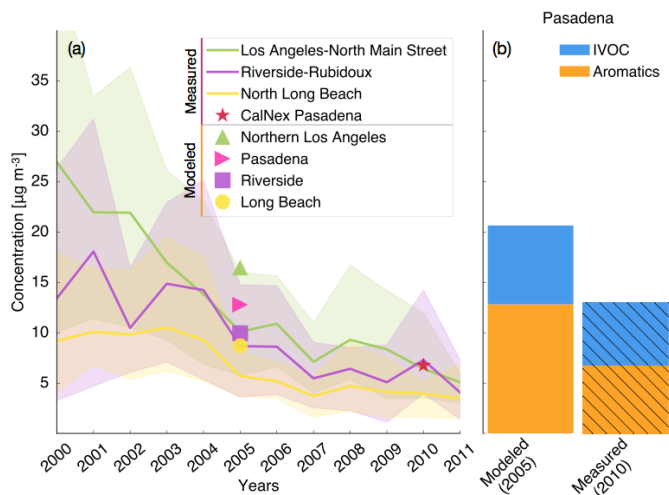


Figure 7: (a) Mass concentrations of single-ring aromatics in southern California at different sites between 2000 and 2011. Measurements show the temporal trend in the summertime mean (solid line) and 10th-90th percentile (bands) at Los Angeles, Riverside, and Long Beach from 2000 to 2011 (ARB, 2017) and the campaign-averaged measurement from CalNex at the Pasadena ground site in 2010 (Zhao et al., 2014). Model predictions show the 14-day averaged concentration simulated in this work at four different sites (solid symbols) in 2005. (b) Mass concentrations of single-ring aromatics and IVOCs compared between the model predictions from 2005 (this work) to measurements in 2010

(Zhao et al., 2014).

In Figure 7(b), model predictions of aromatics and IVOCs in Pasadena in 2005 are compared against measurements made at the Pasadena ground site in 2010. The model predictions in Pasadena were calculated by averaging predictions from the grid cell that contained the Pasadena ground site and the grid cell immediately to the south. This was done because the ground site location was very close to the cell boundary to the south and the grid cell containing the Pasadena ground site included mountains to the north of Pasadena that tended to dilute the concentrations in that grid cell. The measurements in Figure 7(b) included primary IVOCs but did not include the oxygenated IVOCs measured by Zhao et al. (2014) since the primary IVOCs, according to the authors, relate most closely to IVOC emissions from mobile sources. The IVOCs included in this work were mostly (>95%) from mobile sources (see Figure 1) and the hence the comparison with primary IVOCs was appropriate. The model predicted aromatic concentrations at Pasadena in 2005 were twice the measured aromatic concentrations at Pasadena in 2010. This 2005(modeled)-to-2010(measured) ratio was slightly higher but still consistent with the measured 2005-to-2010 ratio in aromatic concentrations at the Los Angeles-North Main Street site (1.67). That the 2005(modeled)-to-2010(measured) ratio for IVOCs in Pasadena was ~1.0 is some evidence that the model predictions of IVOCs might be underpredicted in 2005, assuming that the ambient IVOC-to-aromatic ratio did not change between 2005 and 2010. The IVOC_{max} sensitivity simulation (the only sensitivity simulation that modeled an increase in IVOC emissions) predicted a 2005(modeled)-to-2010(measured) ratio of 3.15 for IVOCs in Pasadena, which was closer to the measured aromatic concentrations ratios between 2005 and 2010 at the Los Angeles-North Main Street site. This provides additional evidence for higher IVOC emissions to be included in the model and it is possible that these additional IVOC emissions might come from volatile chemical products such as pesticides, coatings, cleaning agents, and personal care products (McDonald et al., 2018). While this model-measurement comparison validates the aromatic SOA precursors and to some extent the mobile source IVOC SOA precursors, our model does not account for the oxygenated IVOCs that Zhao et al. (2014) measured and we recommend that future work investigate the sources, composition, and the SOA potential for these IVOCs.

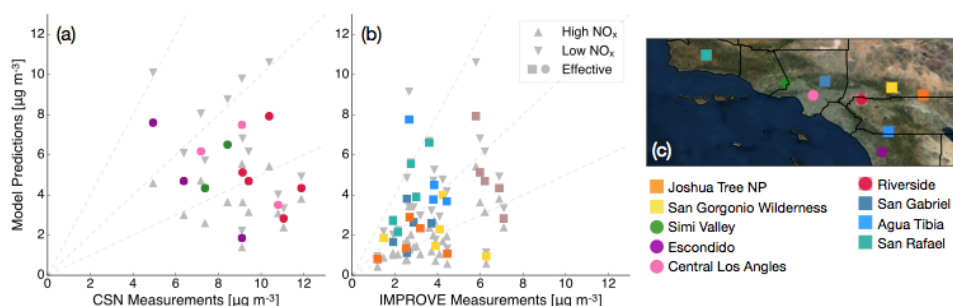


Figure 8: Model-measurement comparison for daily-averaged OA mass concentrations at (a) CSN and (b) IMPROVE sites in southern California. Panel (c) shows the geographic locations where the comparisons were made.

4.2 OA Mass Concentrations

Scatter plots comparing model predictions of OA from the Base simulations to (a) CSN and (b) IMPROVE measurements in southern California are shown in Figure 8(a) and (b). Predictions from the low and high NO_x simulations are presented in grey while predictions accounting for the influence of NO_x are shown in color. The colors

denote different sites and the site locations are shown in Figure 8(c). The model-measurement performance is also captured using statistical metrics of fractional bias, fractional error, and the coefficient of determination in Table 4. At all CSN sites, model predictions of OA that included SOA mass concentrations adjusted for the influence of NO_x were in-between those predicted between the low and high NO_x simulations. As explained earlier, this was because the VOC:NO_x ratios at all these sites (see Figure S9(a)) were always higher than those in the high NO_x chamber experiments (see Table 2) and hence the SOA mass concentrations calculated using equation 2 were always higher than those predicted in the high NO_x simulations. At all the CSN sites, correcting for NO_x improved model performance compared to the high NO_x experiments but was still inferior compared to the predictions from the low NO_x simulations (see Table 4). The mean predicted OA mass concentration across all the CSN sites was about 30% lower than the measurements (5.96 versus 8.86 µg m⁻³). Model predictions of OA were very similar to those predicted in the low NO_x simulations at the IMPROVE sites where the VOC:NO_x ratios were higher (e.g., San Rafael–green square). But, similar to the finding at the CSN sites, model predictions of OA were in-between the predictions between the low and high NO_x simulations at the IMPROVE sites where the VOC:NO_x ratios were lower as a result of their proximity to urban areas (e.g., Agua Tibia–blue square and Riverside–brown square). Accounting for NO_x seemed to improve the model performance at the IMPROVE sites when compared to predictions from the high NO_x simulations and were slightly inferior to those from the low NO_x simulations (see Table 4). Of the 27 IMPROVE measurements available for comparison, 22 or ~80% of the model predictions corrected for NO_x were within a factor of two of measurements with little bias (fractional bias = -16.63%). The model skill, captured by the R^2 values, for all model simulations at both the CSN and IMPROVE sites was quite poor, but still slightly better than that found in earlier work for the southern California region with the CMAQ model (Baker et al., 2015). However, the model skill was much worse than that reported in earlier work with CMAQ (e.g., Murphy et al. (2017)) and WRF-Chem (e.g., Ahmadov et al. (2012)) over regions other than southern California, suggesting that there might be missing emissions sources and/or chemical pathways or meteorological considerations that contribute to the poor model skill in southern California.

Given the differences in the model-measurement comparison between the CSN (or urban) and IMPROVE (rural/remote continental) sites, the underprediction at the CSN sites might be indicative of a missing urban source or pathway of OA formation. Recently, McDonald et al. (2018) found that volatile chemical products such as pesticides, coatings, cleaning agents, and personal care products may contribute substantially to IVOC emissions and account for more than half of the anthropogenic SOA formation in southern California. Our underprediction at urban sites might be evidence of missing SOA from volatile chemical product-related IVOC emissions. However, it is also possible that the urban versus rural/remote continental difference is an artifact of how the SOM models the oxidation chemistry and/or accounts for the influence of vapor wall losses. Within the CSN and IMPROVE sites, we did not find the model-measurement comparison to vary systematically by location. The model-measurement comparison over all of California using the 24 km simulations produced a similar result (Figure S10).

Table 4: Statistical metrics of averages, fractional bias, fractional error, and R^2 for the model-measurement comparison in southern California.

Simulation	CSN					IMPROVE				
	Measured Average (µg m ⁻³)	Modeled Average (µg m ⁻³)	Fractional Bias	Fractional Error	R^2	Measured Average (µg m ⁻³)	Modeled Average (µg m ⁻³)	Fractional Bias	Fractional Error	R^2
Base - Low NO _x	8.86	7.96	-31.5%	46.0%	0.16	3.72	4.87	-1.38 %	41.8%	0.116
Base -	8.86	5.96	-53.4%	49.2%	0.13	3.72	4.02	-16.6 %	44.8%	0.079

Formatted: Font: Italic

Formatted: Font: Italic, Superscript

Deleted: (Baker et al., 2015)

Deleted: (e.g., Murphy et al., 2017) and WRF-Chem (e.g., Ahmadov et al., 2012)

Formatted: Font color: Black

Deleted:

Moved (insertion) [1]

Deleted: 1

Moved up [1]: Recently, McDonald et al. (2018) found that volatile chemical products such as pesticides, coatings, cleaning agents, and personal care products may contribute substantially to IVOC emissions and account for more than half of the anthropogenic SOA formation in southern California. Our underprediction at urban sites might be evidence of missing SOA from volatile chemical product-related IVOC emissions.

Effective										
Base - High NO _x	8.86	3.97	-83.1%	83.1%	0.013	3.72	2.00	-74.1 %	75.9%	0.317

Model predictions of the OA:ΔCO diurnal profile and daytime OA versus CO (between 10 am and 8 pm local time) are compared against measurements made at the Riverside site during the SOAR-1 campaign in Figure 9(a) and (b); SOA mass concentrations have been adjusted for the influence of NO_x using equation (2). The ΔCO for the measurements was calculated by assuming a background concentration of 105 ppbv (Hayes et al., 2013) while the ΔCO for the model predictions was calculated by using the model predicted background concentration of CO over the ocean to the west of Los Angeles. This model-measurement comparison was not completely coincident in time since the model results were between July 20 and August 2 while the SOAR-1 campaign spanned from July 15 to August 15. The measurements did not point to any substantial differences in results between the coincident and non-coincident time and hence we did not anticipate any issues in our comparisons here. The model predictions were able to capture the general trends in the measured diurnal profile in Figure 9(a) with low ratios during the night, high ratios attributed to photochemistry in the mid-afternoon, and a peak between 1 and 2 pm (local time). However, the modeled OA:ΔCO ratios at all times in the diurnal profile in Figure 9(a) and the slope of the OA:CO ratios in Figure 9(b) was approximately a factor of 2 to 3 lower than the measured ratios, indicating a significant underprediction of urban SOA, which was consistent with the much higher POA/SOA ratios predicted by the model compared to the observations, as discussed above. This underprediction cannot be blamed on the model grid resolution since a ratio with CO should to first order account for the influence of dilution in the grid cell. Cappa et al. (2016) showed much better model performance than this work when they assumed a non-volatile POA and SOA formed under low NO_x conditions. In this work, despite forming additional SOA from SVOCs and IVOCs, the evaporation of the POA mass and an SOA estimate adjusted for NO_x meant that the model performance was worse in comparison to Cappa et al. (2016). The sensitivity simulations of IVOC_{max} and S-IVOC_{aromatic} produced slightly higher OA mass concentrations (~10-15%) compared to the Base simulations but not dramatically different to influence the comparison in Figure 9(a) and (b). As mentioned earlier, SOA formation from IVOC emissions from volatile chemical products, or other future improvements in the SOM, have the potential to reduce the model underprediction at Riverside during the SOAR-1 campaign.

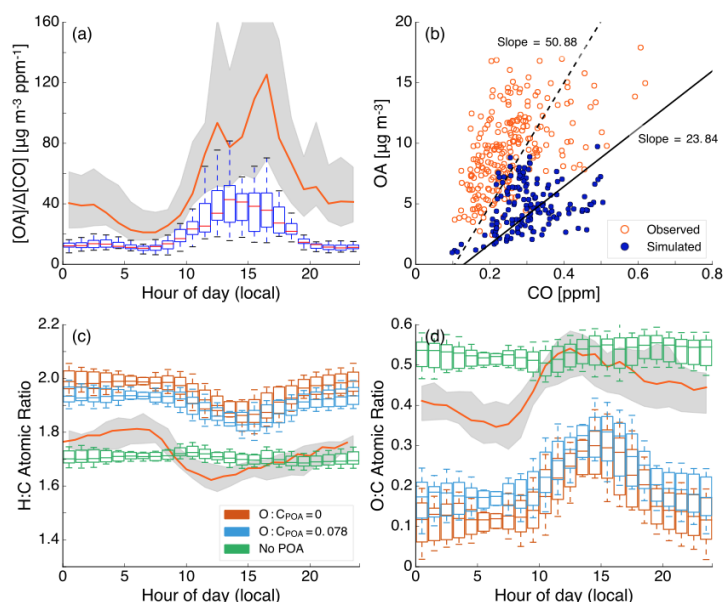


Figure 9: (a) Diurnal profile of the modeled and measured OA/ΔCO ratios at Riverside, CA. The box plots capture the 10th-25th-50th-75th-90th in model predictions over the simulated episode while the gray bands and solid orange line represent the 10th and 90th percentile and median of the measured data. (b) Modeled and measured OA mass concentrations plotted against CO concentrations between 10 am and 8 pm local time. The solid and dashed black lines represent lines fitted to the modeled and measured data by forcing the X-intercept to be the corresponding modeled and measured background CO concentration. Diurnal profiles of the modeled and measured (c) H:C and (d) O:C ratios of the OA (corrected as per Canagaratna et al. (2015)). The three different predictions show results from the Base simulations for OA assuming no change, the POA O:C was fixed to 0.078 *based on the measurements of Docherty et al. (2011)*, and no POA.

4.3 POA and SOA Mass Concentrations

The 14-day averaged results predicted POA and SOA mass concentrations of 3.4 and 2.2 μg m⁻³ and an approximate 60:40 POA-SOA split at Riverside. Docherty et al. (2011) estimated average POA and SOA mass concentrations of 1.9 and 7.0 μg m⁻³ and a POA-SOA split of 20:80 at Riverside during the SOAR-1 campaign. On an absolute basis model predictions of POA mass concentrations were overpredicted by ~80%. A sensitivity simulation that turned sea spray emissions off suggested that the 14-day averaged marine POA mass concentrations at Riverside were ~0.8 μg m⁻³, which are very likely to be overestimated (Hayes et al., 2013). If the emissions of marine POA were updated to align better with the observations and in the limiting case where the marine POA mass concentrations at Riverside were negligible, model predicted POA mass concentrations at Riverside (3.4-0.8=2.6 μg m⁻³) would compare well with the measured values (1.9 μg m⁻³). *As the POA mass concentrations in the SVOC_{cooking} simulations increased and the SOA mass concentrations remained the same compared to the Base simulations, a low volatility and more realistic treatment of the POA from food cooking sources increased the discrepancy in the modeled and measured POA:SOA ratio at Riverside.* It is also possible that the model might be over predicting POA because we only considered POA from certain sources

Deleted: 2.2

Formatted: Subscript

Deleted:

(gasoline and diesel use, woodsmoke, and food cooking) to be semi-volatile.

Figure 1 shows that more than half of the partitioned POA (that excludes marine POA) in southern California belonged to other sources (e.g., road and construction dust) and this POA was treated as non-volatile in the Base simulations. Model predictions from the SVOC_{max} simulations that treated all POA except marine POA as semi-volatile predicted a 14-day averaged POA mass concentration of 2.1 $\mu\text{g m}^{-3}$, which was much closer to the measured value of 1.9 $\mu\text{g m}^{-3}$. This suggests that all POA, regardless of source, might be semi-volatile and could be modeled so in atmospheric models. While these results are in better agreement with measurements, $\text{PM}_{2.5}$ from road and construction dust sources is not created in a high temperature process followed by rapid cooling and so it is unknown whether the POA portion in it would evaporate with atmospheric dilution. We also compared the hydrocarbon-like OA (HOA) estimate from the measurements, which was more representative of POA from mobile sources, against model predictions of POA from mobile sources. We did not model POA from mobile sources separately but if we assumed that mobile sources only accounted for about a quarter of the partitioned POA mass in southern California (based on Figure 1), our estimated Base model predictions of POA mass concentrations from mobile sources of 0.85 $\mu\text{g m}^{-3}$ ($=3.4 \times 0.25$) would compare reasonably with the measured HOA mass concentrations of 1.20 $\mu\text{g m}^{-3}$.

Formatted: Subscript

Deleted: be ~30% lower

Deleted: than the

On an absolute basis, SOA mass concentrations were underpredicted by a factor of 3 compared to measurements. Based on the discussion in the previous paragraph, if we added the non-mobile source POA to SOA, the net SOA mass concentration ($3.4 \times 0.75 + 2.2 = 4.75 \mu\text{g m}^{-3}$) was still 33% lower than the measured value. The SOA mass concentrations in the IVOC_{max} simulations – sensitivity simulations that modeled a fixed IVOC:NMOG ratio of 20% for all sources except biogenic sources, assumed IVOCs formed SOA similar to a C_{15} linear alkane, and which produced the maximum SOA mass concentrations amongst all the simulations – were 33% higher than those in the Base simulation but still ~60% lower than the measured SOA mass concentration of 7 $\mu\text{g m}^{-3}$. A combination of the two, i.e., adding the non-mobile source POA to the SOA formation in the IVOC_{max} simulations, resulted in a net SOA mass concentration that was only 22% lower than the measured SOA value. Since the IVOC_{max} simulations produced ambient IVOC concentrations that were more in line with the measurement trends (see Section 4.1), it is likely that the IVOC_{max} simulations were better in predicting IVOC concentrations and their contribution to SOA. However, there are no bottom up (i.e., source) or top down (i.e., atmospheric) data to directly constrain the emissions of and SOA formation from IVOCs in the IVOC_{max} simulations and hence this finding provides motivation for more detailed studies of IVOCs in the future.

4.4 OA Elemental Composition

The SOM tracks the carbon and oxygen numbers for the OA species and hence we were able to compare model predictions of the diurnal profiles for the OA H:C and O:C ratios to measurements made at the Riverside site during the SOAR-1 campaign. The comparisons are shown in Figure 9(c) and (d). For the Base simulations (shown as orange box plots), model predictions of H:C were significantly overpredicted and those for O:C were significantly underpredicted although the predictions did capture dips in the H:C and the peaks in the O:C ratios in the mid-afternoon, coincident with peak photochemical activity. The model predictions did not capture the slight increase in H:C and the decrease in O:C in the early morning attributed to emissions from rush hour traffic. The high H:C and low O:C predictions were a result of OA being dominated by POA (~60%), which in this work was modeled as a hydrocarbon distribution that had an H:C slightly larger than 2.0 and an O:C of 0. Docherty et al. (2011) found that POA had a campaign-averaged H:C of 1.92 and an O:C of 0.078. If the POA O:C were fixed to the values estimated by Docherty et al. (2011), model

predictions (shown as blue box plots) improved – as shown in Figure 9(c) and (d) – but still over and under predicted the H:C and O:C, respectively; since SOM only tracks carbon and oxygen numbers for an organic species and determines the hydrogen number based on the remaining valence, specifying the O:C dictates the H:C. To assess the ability of the model to predict the elemental composition of SOA, we plot the diurnal profile of H:C and O:C of the SOA in Figure 9(c) and (d). Model predictions of SOA H:C and O:C (shown as green box plots) compared well with the measured range of values but did not reproduce the diurnal changes. Docherty et al. (2011) argued that the H:C and O:C of OA at Riverside was mostly controlled by the SOA composition, which did not change dramatically during the day, and was modified by POA at certain times when POA emissions dominated over SOA production (e.g., nights, rush-hour traffic). This suggests that if absolute predictions of the SOA mass concentrations and the POA-SOA splits were improved, our model would be able to predict both the magnitude and diurnal changes in OA H:C and O:C ratios. We found that the SOA H:C and O:C ratio predictions did not vary significantly and produced similarly flat diurnal profiles across a subset of sensitivity simulations performed (Figure S11), suggesting that the modeled elemental composition of SOA was not very sensitive to the distribution of precursor contributions to SOA.

Deleted: under and over

5 Summary and Discussion

Organic aerosol (OA) is an important contributor to urban fine particle pollution yet remains one of its most uncertain components. In this work, we updated the organic aerosol treatment in the UCD/CIT chemical transport model to include a semi-volatile and reactive treatment of POA, emissions and SOA formation from IVOCs, the NO_x influence on SOA formation, and SOA parameterizations for SVOCs and IVOCs that were corrected for vapor wall loss artifacts during chamber experiments. All updates were implemented in the statistical oxidation model (SOM), which simulates the multigenerational aging and gas/particle partitioning of organic aerosol and is embedded in the UCD/CIT model (Cappa et al., 2016; Jathar et al., 2015, 2016). POA, SVOC, and IVOC updates were based on an interpretation of a comprehensive set of source measurements. The influence of NO_x on SOA formation was estimated offline using methods based on the VOC:NO_x ratios/NO_x concentrations.

Despite treating the POA from gasoline, diesel, biomass burning, and food cooking sources as semi-volatile, the updated model only predicted a 30-50% decrease in POA mass concentrations in the urban airshed even when the volatility data used to simulate POA projected a much larger decrease (45 to 80%). The primary reason for the weaker response was that a large fraction of the POA mass came from sources other than those modeled as semi-volatile, e.g., road and construction dust, marine. When all POA, except for marine POA, was modeled as semi-volatile, more than 60% of the POA mass evaporated and the POA mass concentrations under this scenario compared well with measurements made in Riverside, CA as part of the SOAR-1 field campaign. While this sensitivity analysis was informative, it is unlikely that the POA from sources such as road and construction dust is semi-volatile and recent measurements suggest that POA from food cooking sources has much lower volatility than assumed in the Base simulations in this work. These findings indicate that model predictions continue to overestimate POA relative to measured concentrations. Sea spray emissions accounted for a quarter of the POA mass concentrations in the urban airshed but more recent observations suggest that the sea spray emissions or the organic fraction attributed to the sea spray emissions might be overestimated (Hayes et al., 2013). This needs to be examined in future applications of the UCD/CIT model. Atmospheric oxidation of the evaporated POA vapors or SVOCs did not contribute significantly to the SOA burden (<0.1 µg m⁻³), even after accounting for the influence of vapor wall loss artifacts, since the timescales for SOA production appeared to be longer than the timescales for transport out of the urban airshed.

Deleted: shorter

2
3
4
5
6
7
8
9
0
1
2
3
4
5
6
7
8
9
0
1
2
3
4
5
6
7
8
9
0
1
2
3
4
5
6
7
8
9
0
1
2
3

We found IVOCs to be more important than SVOCs but less important than traditional VOCs such as single-ring aromatics and biogenics in forming SOA. IVOCs accounted for less than 0.5 $\mu\text{g m}^{-3}$ of SOA while single-ring aromatics and biogenics each contributed to approximately 1 $\mu\text{g m}^{-3}$ in the Base simulations. The IVOC contribution to SOA was smaller than that for aromatics partly because IVOC SOA was relatively less sensitive to corrections of vapor wall loss artifacts in chamber experiments. Another reason for the small IVOC contribution to SOA was that we only considered IVOC emissions from gasoline, diesel, and biomass burning. On analyzing trends in SOA precursor concentrations in southern California, the modeled IVOC concentrations in this scenario appeared to be underpredicted by a factor of ~2. Allowing all sources that emit non-methane organic gases (NMOG) to emit IVOCs (using an IVOC:NMOG ratio of 0.2) and form SOA similar to a C_{15} linear alkane seemed to increase the IVOC contribution to SOA ($\frac{1}{3}$ of total SOA) and produced better comparisons against ambient measurements of IVOC concentrations, OA composition, and SOA mass concentrations. This might be indicative of missing IVOC emissions in the model. These missing emissions might be from volatile chemical products such as pesticides, coatings, cleaning agents, and personal care products, which have been found to contribute substantially to urban SOA burdens (McDonald et al., 2018). It is also likely that the missing IVOC emissions are from sources considered in this work (i.e., gasoline, diesel, and biomass burning sources) but were not accounted in the emissions inventories because they have been shown to be very easily lost to sampling tubes (Pagonis et al., 2017). The IVOCs in this work were modeled using a linear alkane surrogate despite recent evidence that IVOCs in combustion emissions are a mixture of branched and cyclic alkanes, aromatics, and oxygenated compounds with very few linear alkanes (Koss et al., 2018; Zhao et al., 2016, 2017). A more chemically appropriate representation of the IVOCs would not have substantially changed the findings in this work since the linear alkane surrogates were chosen to reproduce the SOA formation in chamber experiments performed on combustion emissions. However, future work should incorporate the more detailed speciation available to model the emissions and SOA formation from IVOCs.

Loss of vapors to the Teflon walls has been shown to significantly bias SOA formation in environmental chamber experiments (Krechmer et al., 2016; Zhao et al., 2014). Cappa et al. (2016) studied the influence of vapor wall loss artifacts on ambient SOA mass concentrations from VOC precursors. In this work, we extended the work of Cappa et al. (2016) by considering additional precursors of SOA, i.e., S/IVOCs. Correcting for vapor wall loss artifacts seemed to increase SOA mass concentrations for all precursors but the enhancement varied by precursor. With a few exceptions, the SOA enhancements correlated with carbon number where larger carbon number precursors had lower enhancements and vice versa. The reason for this inverse relationship was that larger precursors and their oxidation products have shorter chemical lifetimes and undergo fewer chemical reactions to form SOA, which made them less susceptible to being lost to the chamber walls. Recent work suggests that the vapor wall loss rates to the Teflon wall might be two or more times larger than the rates used in this work to develop the SOM parameters (Huang et al., 2018; Krechmer et al., 2016). The use of these faster rates will tend to increase the model predicted SOA mass concentrations and help explain the underpredictions with ambient measurements.

The total SOA enhancement was modified by the NO_x level where low NO_x regions might see higher enhancements compared to high NO_x regions. In southern California where urban SOA mass concentrations might be higher than rural/remote continental SOA mass concentrations, the NO_x -mediated enhancement will tend to reduce the spatial gradients in SOA mass concentrations and make SOA a regional pollutant like O_3 . Accounting for the influence of NO_x seemed to improve OA model performance against routine measurements in rural/remote environments (i.e.,

Deleted: (
Deleted: Zhao et al., 2016; Zhao et al., 2017; Koss et al., 2018)...
Field Code Changed
Formatted: Font: Not Italic

Field Code Changed
Formatted: Font: Not Italic
Deleted: (Zhang et al., 2014; Krechmer et al., 2016)
Deleted: in chamber experiments

Deleted: (Krechmer et al., 2016; Huang et al., 2018)
Deleted:
Deleted: Furthermore, t

Interagency Monitoring of Protected Visual Environments network) where OA model predictions were within a factor of 2 with very little bias (e.g., fractional bias of -16.6%). However, model predictions of OA at routine monitoring sites in urban environments (i.e., Chemical Speciation Network) and at the Riverside site during the SOAR-1 field campaign were still underpredicted by at least a factor of 2 (e.g., fractional bias of -49.2%). This suggested a missing emissions or chemical source of OA in urban areas.

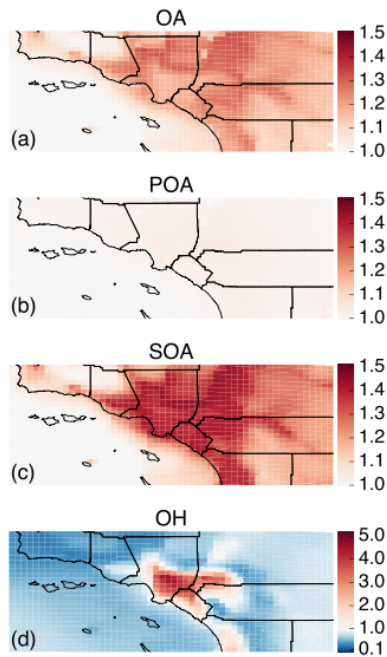


Figure 10: Ratios of 14-day averaged model predictions of (a) OA, (b) POA, (c) SOA, and (d) OH from 2035 to those from 2005. The 2035 simulations were performed with 2005 meteorological inputs but scaling the anthropogenic emissions for CO, NO_x, VOC, PM_{2.5}, SO₂, and NH₃ based on changes projected by the California Emission Projections and Analysis Model (CARB, 2018).

The future OA burden in southern California will depend not only on reductions in POA and SOA precursor emissions but also on changes in oxidant concentrations and VOC:NO_x ratios. We used the Base model to simulate the same time period, July 20 to August 2, for the year 2035 to determine how emissions reductions and atmospheric conditions may change in a future year to influence ambient OA-POA-SOA mass concentrations. The same meteorology and environmental conditions were assumed, with the understanding that climatological changes in the future may alter the findings presented here. Emissions reductions in CO, NO_x, VOC, PM_{2.5}, SO₂, and NH₃ were informed by net reductions in statewide emissions between 2005 and 2035 as projected by the California Emission Projections and Analysis Model (CARB, 2018). The 2005 inventory was scaled based on these emissions reductions for anthropogenic sources but the biogenic emissions and VOC emissions profiles were kept the same. We did not resolve the emissions reductions in these pollutants by source or by region since the goal was to examine the general trend in the OA-POA-SOA system and not to predict future air quality; heterogeneity in the reduction in pollutant emissions by source and geography may alter the results. Statewide emissions reductions in CO, NO_x, and VOC of 78%, 83%, and 33% resulted in approximately

5 50%, 75%, 75%, and 30% reductions in ambient concentrations of CO, NO, NO₂, and VOC in the urban airshed (Figure
6 S12 plots the ratio of CO, NO, NO₂, and VOC concentrations in 2035 to those in 2005). Here, VOC is the sum of all
7 organic species tracked in the SAPRC-11 gas-phase chemical mechanism (excludes methane). Since the NO_x reduction
8 was much more dramatic than that for VOCs, the VOC:NO_x ratio in the urban airshed increased from ~1 to ~5 between
9 2005 and 2035, which was in line with recent modeled estimates by Fujita et al. (2016).

1 We plot the ratio of the mass concentrations for OA, POA, and SOA in 2035 to those in 2005 in Figure 10(a), (b), and
2 (c) respectively. SOA mass concentrations have been adjusted for the influence of NO_x using equation 2. POA mass
3 concentrations in the urban airshed in 2035 were slightly higher (~5%) than those in 2005 primarily because PM_{2.5}
4 emissions were higher in 2035 compared to 2005; according to CEPAM, increases in PM_{2.5} emissions were mostly from
5 increases in area source emissions and not mobile source emissions. Surprisingly, SOA mass concentrations in the urban
6 airshed were 30-40% higher in 2035 compared to 2005 despite a 30% reduction in VOC emissions and concentrations.
7 Some of the increase in the SOA mass concentrations was from a shifting VOC:NO_x ratio that produced more SOA via
8 the low-NO_x pathway. However, the primary reason for the SOA increase was that OH concentrations in the urban area
9 had increased by a factor of 2 to 4 (see Figure 10(d)) and had reacted more of the SOA precursors. The OH
0 concentrations were presumably higher in 2035 because lower NO_x emissions resulted in a higher OH lifetime since
1 the NO₂+OH reaction is the primary sink for OH in polluted environments (Jacob, 1999), including the Los Angeles
2 area (Griffith et al., 2016). These findings suggest that the SOA and OA mass concentrations may not necessarily
3 respond linearly to reductions in VOC and NO_x emissions in the future but rather will be strongly influenced by the
4 changes in chemical regime. Similarly, Praske et al. (2018) argue that dramatic reductions in NO_x emissions and
5 concentrations in urban environments may increasingly lead to SOA formation through autooxidation pathways and
6 alter the rate and quantity of SOA formed. Hence, attention needs to be paid to appropriately simulate the chemical
7 regime (e.g., oxidant concentrations, VOC:NO_x ratios, autooxidation reactions) if we are to accurately simulate the
8 SOA burden in urban environments in the future.

Deleted: quantify

6 Author Contributions

SHJ and AA developed the model and designed the configurations of the numerical simulations with some help from
MJK. AA performed the numerical simulations and post-processed and analyzed the model outputs. AA and SHJ wrote
the paper with contributions from all co-authors.

Formatted: Font: 14 pt, Bold

7 Acknowledgements

We thank Nehzat Motallebi for sharing the VOC data gathered by the California Air Resources Board in southern
California. AA and SHJ were partially supported by National Oceanic and Atmospheric Administration
(NA17OAR4310003). JLJ was supported by the Environmental Protection Agency (EPA) STAR program (83587701-
0). EPA has not reviewed this manuscript and thus no endorsement should be inferred. SMG, SD, PSS, and CDC were
supported by the National Science Foundation (AGS-0612738, AGS-1104880 and AGS-1523500).

Formatted: Normal

Deleted: 6

8 References

Ahmadv, R., McKeen, S. A., Robinson, A. L., Bahreini, R., Middlebrook, A. M., de Gouw, J. A., Meagher, J., Hsie,
E.-Y., Edgerton, E., Shaw, S. and Trainer, M.: A volatility basis set model for summertime secondary organic aerosols

Deleted: 7

over the eastern United States in 2006, J. Geophys. Res., 117(D6), D06301, 2012.

American Lung Association: State of the Air 2017, <https://www.lung.org/local-content/california/our-initiatives/state-of-the-air/2017/state-of-the-air-2017.html>, 2017.

Baker, K. R., Carlton, A. G., Kleindienst, T. E., Offenberg, J. H., Beaver, M. R., Gentner, D. R., Goldstein, A. H., Hayes, P. L., Jimenez, J. L., Gilman, J. B., Gouw, J. A. de, Woody, M. C., Pye, H. O. T., Kelly, J. T., Lewandowski, M., Jaoui, M., Stevens, P. S., Brune, W. H., Lin, Y.-H., Rubitschun, C. L. and Surratt, J. D.: Gas and aerosol carbon in California: comparison of measurements and model predictions in Pasadena and Bakersfield, Atmos. Chem. Phys., 15(9), 5243–5258, 2015.

Bergström, R., Denier Van Der Gon, H., Prévôt, A., Yttri, K. E. and Simpson, D.: Modelling of organic aerosols over Europe (2002–2007) using a volatility basis set (VBS) framework: application of different assumptions regarding the formation of secondary organic aerosol, Atmos. Chem. Phys., 12(18), 8499–8527, 2012.

Bond, T. C., Streets, D. G., Yarber, K. F., Nelson, S. M., Woo, J.-H. and Klimont, Z.: A technology-based global inventory of black and organic carbon emissions from combustion, J. Geophys. Res. D: Atmos., 109(D14) [online] Available from: <http://onlinelibrary.wiley.com/doi/10.1029/2003JD003697/full>, 2004.

Borbon, A., Gilman, J. B., Kuster, W. C., Grand, N., Chevaillier, S., Colomb, A., Dolgorouky, C., Gros, V., Lopez, M., Sarda-Esteve, R. and Others: Emission ratios of anthropogenic volatile organic compounds in northern mid-latitude megacities: Observations versus emission inventories in Los Angeles and Paris, J. Geophys. Res. D: Atmos., 118(4), 2041–2057, 2013.

Brandenberger, S., Mohr, M., Grob, K. and Neukom, H. P.: Contribution of unburned lubricating oil and diesel fuel to particulate emission from passenger cars, Atmos. Environ., 39(37), 6985–6994, 2005.

Camredon, M., Aumont, B., Lee-Taylor, J. and Madronich, S.: The SOA/VOC/NO_x system: an explicit model of secondary organic aerosol formation, Atmos. Chem. Phys., 7(21), 5599–5610, 2007.

Canagaratna, M. R., Jimenez, J. L., Kroll, J. H., Chen, Q., Kessler, S. H., Massoli, P., Hildebrandt Ruiz, L., Fortner, E., Williams, L. R., Wilson, K. R., Surratt, J. D., Donahue, N. M., Jayne, J. T. and Worsnop, D. R.: Elemental ratio measurements of organic compounds using aerosol mass spectrometry: characterization, improved calibration, and implications, Atmos. Chem. Phys., 15(1), 253–272, 2015.

Cappa, C. D. and Wilson, K. R.: Multi-generation gas-phase oxidation, equilibrium partitioning, and the formation and evolution of secondary organic aerosol, Atmos. Chem. Phys., 12(20), 9505–9528, 2012.

Cappa, C. D., Zhang, X., Loza, C. L., Craven, J. S., Lee, Y. D. and Seinfeld, J. H.: Application of the Statistical Oxidation Model (SOM) to Secondary Organic Aerosol formation from photooxidation of C₁₂ alkanes, Atmos. Chem. Phys., 13(3), 1591–1606, 2013.

Cappa, C. D., Jathar, S. H., Kleeman, M. J., Docherty, K. S., Jimenez, J. L., Seinfeld, J. H. and Wexler, A. S.: Simulating secondary organic aerosol in a regional air quality model using the statistical oxidation model—Part 2: Assessing the influence of vapor wall losses, Atmos. Chem. Phys., 16(5), 3041–3059, 2016.

Caravaggio, G. A., Charland, J.-P., Macdonald, P. and Graham, L.: n-alkane profiles of engine lubricating oil and particulate matter by molecular sieve extraction, Environ. Sci. Technol., 41(10), 3697–3701, 2007.

Carlton, A. G., Bhawe, P. V., Napelenok, S. L., Edney, E. O., Sarwar, G., Pinder, R. W., Pouliot, G. A. and Houyoux, M.: Model representation of secondary organic aerosol in CMAQv4.7, Environ. Sci. Technol., 44(22), 8553–8560, 2010.

Carter, W. P. L.: Development of the SAPRC-07 chemical mechanism, Atmos. Environ., 44(40), 5324–5335, 2010.

Chacon-Madrid, H. J. and Donahue, N. M.: Fragmentation vs. functionalization: chemical aging and organic aerosol formation, Atmos. Chem. Phys., 11(20), 10553–10563, 2011.

Chan, A. W. H., Kautzman, K. E., Chhabra, P. S., Surratt, J. D., Chan, M. N., Crounse, J. D., Kürten, A., Wennberg, P. O., Flagan, R. C. and Seinfeld, J. H.: Secondary organic aerosol formation from photooxidation of naphthalene and alkylnaphthalenes: implications for oxidation of intermediate volatility organic compounds (IVOCs), Atmos. Chem. Phys., 9(9), 3049–3060, 2009.

Deleted: Association, A. L. and Others: State of the Air 2017, Fort Collins, CO. <http://www.lung.org/our-initiatives/healthy-air/sota/cityrankings/msas/fort-collins-co.html#ozone>, 2017.

Formatted: Space After: 11 pt, Widow/Orphan control, Border: Top: (No border), Bottom: (No border), Left: (No border), Right: (No border), Between : (No border)

Formatted: Font: 12 pt

Formatted: Space After: 11 pt, Widow/Orphan control, Border: Top: (No border), Bottom: (No border), Left: (No border), Right: (No border), Between : (No border)

Deleted: Camredon, M., Aumont, B. and Lee-Taylor, J.: The SOA/VOC/NO_x system: an explicit model of secondary organic aerosol formation, Atmospheric [online] Available from: <https://www.atmos-chem-phys.net/7/5599/2007/acp-7-5599-2007.pdf>, 2007.

Formatted: Font: 12 pt

- 3 Chhabra, P. S., Flagan, R. C. and Seinfeld, J. H.: Elemental analysis of chamber organic aerosol using an aerodyne
4 high-resolution aerosol mass spectrometer, *Atmos. Chem. Phys.*, 10(9), 4111–4131, 2010.
- 5 Chhabra, P. S., Ng, N. L., Canagaratna, M. R., Corrigan, A. L., Russell, L. M., Worsnop, D. R., Flagan, R. C. and
6 Seinfeld, J. H.: Elemental composition and oxidation of chamber organic aerosol, *Atmos. Chem. Phys.*, 11(17), 8827–
7 8845, 2011.
- 8 Docherty, K. S., Stone, E. A., Ulbrich, I. M., DeCarlo, P. F., Snyder, D. C., Schauer, J. J., Peltier, R. E., Weber, R. J.,
9 Murphy, S. M., Seinfeld, J. H., Grover, B. D., Eatough, D. J. and Jimenez, J. L.: Apportionment of primary and
0 secondary organic aerosols in southern California during the 2005 study of organic aerosols in riverside (SOAR-1),
1 *Environ. Sci. Technol.*, 42(20), 7655–7662, 2008.
- 2 Docherty, K. S., Aiken, A. C., Huffman, J. A., Ulbrich, I. M., DeCarlo, P. F., Sueper, D., Worsnop, D. R., Snyder, D.
3 C., Peltier, R. E., Weber, R. J., Grover, B. D., Eatough, D. J., Williams, B. J., Goldstein, A. H., Ziemann, P. J. and
4 Jimenez, J. L.: The 2005 Study of Organic Aerosols at Riverside (SOAR-1): instrumental intercomparisons and fine
5 particle composition, *Atmospheric Chemistry and Physics*; Katlenburg-Lindau, 11(23), 12387, 2011.
- 6 Dzepina, K., Volkamer, R. M., Madronich, S., Tulet, P., Ulbrich, I. M., Zhang, Q., Cappa, C. D., Ziemann, P. J. and
7 Jimenez, J. L.: Evaluation of recently-proposed secondary organic aerosol models for a case study in Mexico City,
8 *Atmos. Chem. Phys.*, 9(15), 5681–5709, 2009.
- 9 Dzepina, K., Cappa, C. D., Volkamer, R. M., Madronich, S., Decarlo, P. F., Zaveri, R. A. and Jimenez, J. L.:
0 Modeling the multiday evolution and aging of secondary organic aerosol during MILAGRO 2006, *Environ. Sci.*
1 *Technol.*, 45(8), 3496–3503, 2011.
- 2 Ehn, M., Thornton, J. A., Kleist, E., Sipilä, M., Junninen, H., Pullinen, I., Springer, M., Rubach, F., Tillmann, R., Lee,
3 B., Lopez-Hilfiker, F., Andres, S., Acir, I.-H., Rissanen, M., Jokinen, T., Schobesberger, S., Kangasluoma, J.,
4 Kontkanen, J., Nieminen, T., Kurtén, T., Nielsen, L. B., Jørgensen, S., Kjaergaard, H. G., Canagaratna, M., Maso, M.
5 D., Berndt, T., Petäjä, T., Wahner, A., Kerminen, V.-M., Kulmala, M., Worsnop, D. R., Wildt, J. and Mentel, T. F.: A
6 large source of low-volatility secondary organic aerosol, *Nature*, 506(7489), 476–479, 2014.
- 7 Eluri, S., Cappa, C. D., Friedman, B., Farmer, D. K. and Jathar, S. H.: Modeling the formation and composition of
8 secondary organic aerosol from diesel exhaust using parameterized and semi-explicit chemistry and thermodynamic
9 models, Colorado State University. [online] Available from: [https://www.atmos-chem-phys-discuss.net/acp-2017-](https://www.atmos-chem-phys-discuss.net/acp-2017-1060/acp-2017-1060.pdf)
0 [1060/acp-2017-1060.pdf](https://www.atmos-chem-phys-discuss.net/acp-2017-1060/acp-2017-1060.pdf), 2017.
- 1 Emmons, L. K., Walters, S., Hess, P. G., Lamarque, J.-F., Pfister, G. G., Fillmore, D., Granier, C., Guenther, A.,
2 Kinnison, D., Laepple, T., Orlando, J., Tie, X., Tyndall, G., Wiedinmyer, C., Baughcum, S. L. and Kloster, S.:
3 Description and evaluation of the Model for Ozone and Related chemical Tracers, version 4 (MOZART-4), , 3(1), 43–
4 67, 2010.
- 5 Ensberg, J. J., Hayes, P. L., Jimenez, J. L., Gilman, J. B., Kuster, W. C., de Gouw, J. A., Holloway, J. S., Gordon, T.
6 D., Jathar, S., Robinson, A. L. and Seinfeld, J. H.: Emission factor ratios, SOA mass yields, and the impact of
7 vehicular emissions on SOA formation, *Atmos. Chem. Phys.*, 14(5), 2383–2397, 2014.
- 8 Fountoukis, C., Megaritis, A. G., Skyllakou, K., Charalampidis, P. E., Denier van der Gon, H. A. C., Crippa, M.,
9 Prévôt, A. S. H., Fachinger, F., Wiedensohler, A., Pilinis, C. and Pandis, S. N.: Simulating the formation of
0 carbonaceous aerosol in a European Megacity (Paris) during the MEGAPOLI summer and winter campaigns, *Atmos.*
1 *Chem. Phys.*, 16(6), 3727–3741, 2016.
- 2 Fujita, E. M., Campbell, D. E., Stockwell, W. R., Saunders, E., Fitzgerald, R. and Perea, R.: Projected ozone trends
3 and changes in the ozone-precursor relationship in the South Coast Air Basin in response to varying reductions of
4 precursor emissions, *J. Air Waste Manage. Assoc.*, 66(2), 201–214, 2016.
- 5 Fuzzi, S., Baltensperger, U., Carslaw, K., Decesari, S., Denier van der Gon, H., Facchini, M. C., Fowler, D., Koren, I.,
6 Langford, B., Lohmann, U., Nemitz, E., Pandis, S., Riipinen, I., Rudich, Y., Schaap, M., Slowik, J. G., Spracklen, D.
7 V., Vignati, E., Wild, M., Williams, M. and Gilardoni, S.: Particulate matter, air quality and climate: lessons learned
8 and future needs, *Atmos. Chem. Phys.*, 15(14), 8217–8299, 2015.
- 9 Gentner, D. R., Isaacman, G., Worton, D. R., Chan, A. W. H., Dallmann, T. R., Davis, L., Liu, S., Day, D. A., Russell,
0 L. M., Wilson, K. R., Weber, R., Guha, A., Harley, R. A. and Goldstein, A. H.: Elucidating secondary organic aerosol
1 from diesel and gasoline vehicles through detailed characterization of organic carbon emissions, *Proc. Natl. Acad. Sci.*
2 *U. S. A.*, 109(45), 18318–18323, 2012.

Formatted: Space After: 11 pt, Widow/Orphan control,
Border: Top: (No border), Bottom: (No border), Left: (No
border), Right: (No border), Between : (No border)

Formatted: Font: 12 pt

Gentner, D. R., Jathar, S. H., Gordon, T. D., Bahreini, R., Day, D. A., El Haddad, I., Hayes, P. L., Pieber, S. M., Platt, S. M., de Gouw, J., Goldstein, A. H., Harley, R. A., Jimenez, J. L., Prévôt, A. S. H. and Robinson, A. L.: Review of Urban Secondary Organic Aerosol Formation from Gasoline and Diesel Motor Vehicle Emissions, *Environ. Sci. Technol.*, 51(3), 1074–1093, 2017.

Gong, S. L.: A parameterization of sea-salt aerosol source function for sub-and super-micron particles, *Global Biogeochem. Cycles*, 17(4) [online] Available from: <http://onlinelibrary.wiley.com/doi/10.1029/2003GB002079/full>, 2003.

Gordon, T. D., Presto, A. A., May, A. A., Nguyen, N. T., Lipsky, E. M., Donahue, N. M., Gutierrez, A., Zhang, M., Maddox, C., Rieger, P. and Others: Secondary organic aerosol formation exceeds primary particulate matter emissions for light-duty gasoline vehicles, *Atmos. Chem. Phys.*, 14(9), 4661–4678, 2014a.

Gordon, T. D., Presto, A. A., Nguyen, N. T., Robertson, W. H., Na, K., Sahay, K. N., Zhang, M., Maddox, C., Rieger, P., Chattopadhyay, S., Maldonado, H., Maricq, M. M. and Robinson, A. L.: Secondary organic aerosol production from diesel vehicle exhaust: impact of aftertreatment, fuel chemistry and driving cycle, *Atmos. Chem. Phys.*, 14(9), 4643–4659, 2014b.

Grieshop, A. P., Logue, J. M., Donahue, N. M. and Robinson, A. L.: Laboratory investigation of photochemical oxidation of organic aerosol from wood fires 1: measurement and simulation of organic aerosol evolution, *Atmos. Chem. Phys.*, 9(4), 1263–1277, 2009a.

Grieshop, A. P., Donahue, N. M. and Robinson, A. L.: Laboratory investigation of photochemical oxidation of organic aerosol from wood fires 2: analysis of aerosol mass spectrometer data, *Atmos. Chem. Phys.*, 9(6), 2227–2240, 2009b.

Griffith, S. M., Hansen, R. F., Dusanter, S., Michoud, V., Gilman, J. B., Kuster, W. C., Veres, P. R., Graus, M., Gouw, J. A., Roberts, J. and Others: Measurements of hydroxyl and hydroperoxy radicals during CalNex-LA: Model comparisons and radical budgets, *J. Geophys. Res. D: Atmos.*, 121(8), 4211–4232, 2016.

Guenther, A., Karl, T., Harley, P., Wiedinmyer, C., Palmer, P. I. and Geron, C.: Estimates of global terrestrial isoprene emissions using MEGAN (Model of Emissions of Gases and Aerosols from Nature), *Atmos. Chem. Phys.*, 6(11), 3181–3210, 2006.

Hatch, L. E., Luo, W., Pankow, J. F., Yokelson, R. J., Stockwell, C. E. and Barsanti, K. C.: Identification and quantification of gaseous organic compounds emitted from biomass burning using two-dimensional gas chromatography--time-of-flight mass spectrometry, *Atmos. Chem. Phys.*, 15(4), 1865–1899, 2015.

Hayes, P. L., Ortega, A. M., Cubison, M. J., Froyd, K. D., Zhao, Y., Cliff, S. S., Hu, W. W., Toohey, D. W., Flynn, J. H., Lefer, B. L. and Others: Organic aerosol composition and sources in Pasadena, California, during the 2010 CalNex campaign, *J. Geophys. Res. D: Atmos.*, 118(16), 9233–9257, 2013.

Hayes, P. L., Carlton, A. G., Baker, K. R., Ahmadvov, R., Washenfelter, R. A., Alvarez, S., Rappenglück, B., Gilman, J. B., Kuster, W. C., de Gouw, J. A., Zotter, P., Prévôt, A. S. H., Szidat, S., Kleindienst, T. E., Offenberg, J. H., Ma, P. K. and Jimenez, J. L.: Modeling the formation and aging of secondary organic aerosols in Los Angeles during CalNex 2010, *Atmos. Chem. Phys.*, 15(10), 5773–5801, 2015.

Hays, M. D., Preston, W., George, B. J., George, I. J., Snow, R., Faircloth, J., Long, T., Baldauf, R. W. and McDonald, J.: Temperature and Driving Cycle Significantly Affect Carbonaceous Gas and Particle Matter Emissions from Diesel Trucks, *Energy Fuels*, 31(10), 11034–11042, 2017.

Hennigan, C. J., Miracolo, M. A., Engelhart, G. J., May, A. A., Presto, A. A., Lee, T., Sullivan, A. P., McMeeking, G. R., Coe, H., Wold, C. E., Hao, W.-M., Gilman, J. B., Kuster, W. C., Gouw, J. de, Schichtel, B. A., Collett, J. L., Jr., Kreidenweis, S. M. and Robinson, A. L.: Chemical and physical transformations of organic aerosol from the photo-oxidation of open biomass burning emissions in an environmental chamber, *Atmos. Chem. Phys.*, 11(15), 7669–7686, 2011.

Henze, D. K., Seinfeld, J. H., Ng, N. L., Kroll, J. H., Fu, T.-M., Jacob, D. J. and Heald, C. L.: Global modeling of secondary organic aerosol formation from aromatic hydrocarbons: high- vs. low-yield pathways, *Atmos. Chem. Phys.*, 8(9), 2405–2420, 2008.

Heo, J., de Foy, B., Olson, M. R., Pakbin, P., Sioutas, C. and Schauer, J. J.: Impact of regional transport on the anthropogenic and biogenic secondary organic aerosols in the Los Angeles Basin, *Atmos. Environ.*, 103, 171–179, 2015.

- 2 Hodzic, A., Kasibhatla, P. S., Jo, D. S., Cappa, C. D., Jimenez, J. L., Madronich, S. and Park, R. J.: Rethinking the
3 global secondary organic aerosol (SOA) budget: stronger production, faster removal, shorter lifetime, Atmospheric
4 Chemistry and Physics; Katlenburg-Lindau, 16(12), 7917–7941, 2016.
- 5 Hodzic, A. and Jimenez, J. L.: Modeling anthropogenically controlled secondary organic aerosols in a megacity: a
6 simplified framework for global and climate models, Geoscientific Model Development, 4(4), 901–917, 2011.
- 7 Hofzumahaus, A., Rohrer, F., Lu, K., Bohn, B., Brauers, T., Chang, C.-C., Fuchs, H., Holland, F., Kita, K., Kondo,
8 Y., Li, X., Lou, S., Shao, M., Zeng, L., Wahner, A. and Zhang, Y.: Amplified trace gas removal in the troposphere,
9 Science, 324(5935), 1702–1704, 2009.
- 0 Huang, Y., Zhao, R., Charan, S. M., Kenseth, C. M., Zhang, X. and Seinfeld, J. H.: Unified Theory of Vapor–Wall
1 Mass Transport in Teflon-Walled Environmental Chambers, Environ. Sci. Technol., 52(4), 2134–2142, 2018.
- 2 Huffman, J. A., Docherty, K. S., Aiken, A. C., Cubison, M. J., Ulbrich, I. M., DeCarlo, P. F., Sueper, D., Jayne, J. T.,
3 Worsnop, D. R., Ziemann, P. J. and Jimenez, J. L.: Chemically-resolved aerosol volatility measurements from two
4 megacity field studies, Atmos. Chem. Phys., 9(18), 7161–7182, 2009.
- 5 Hu, J., Zhang, H., Chen, S., Ying, Q., Wiedinmyer, C., Vandenbergh, F. and Kleeman, M. J.: Identifying PM2.5 and
6 PM0.1 sources for epidemiological studies in California, Environ. Sci. Technol., 48(9), 4980–4990, 2014.
- 7 Hu, J., Zhang, H., Ying, Q., Chen, S.-H., Vandenbergh, F. and Kleeman, M. J.: Long-term particulate matter
8 modeling for health effect studies in California--Part 1: Model performance on temporal and spatial variations, Atmos.
9 Chem. Phys., 15(6), 3445–3461, 2015.
- 0 Jacob, D.: Introduction to Atmospheric Chemistry, Princeton University Press., 1999.
- 1 Jathar, S. H., Gordon, T. D., Hennigan, C. J., Pye, H. O. T., Pouliot, G., Adams, P. J., Donahue, N. M. and Robinson,
2 A. L.: Unspeciated organic emissions from combustion sources and their influence on the secondary organic aerosol
3 budget in the United States, Proc. Natl. Acad. Sci. U. S. A., 111(29), 10473–10478, 2014.
- 4 Jathar, S. H., Cappa, C. D., Wexler, A. S., Seinfeld, J. H. and Kleeman, M. J.: Multi-generational oxidation model to
5 simulate secondary organic aerosol in a 3-D air quality model, Geoscientific Model Development; Katlenburg-Lindau,
6 8(8), 2553–2567, 2015.
- 7 Jathar, S. H., Cappa, C. D., Wexler, A. S., Seinfeld, J. H. and Kleeman, M. J.: Simulating secondary organic aerosol in
8 a regional air quality model using the statistical oxidation model--Part 1: Assessing the influence of constrained multi-
9 generational ageing, Atmos. Chem. Phys., 16(4), 2309–2322, 2016.
- 0 Jathar, S. H., Woody, M., Pye, H. O. T., Baker, K. R. and Robinson, A. L.: Chemical transport model simulations of
1 organic aerosol in southern California: model evaluation and gasoline and diesel source contributions, Atmos. Chem.
2 Phys., 17(6), 4305–4318, 2017a.
- 3 Jathar, S. H., Heppding, C., Link, M. F., Farmer, D. K., Akherati, A., Kleeman, M. J., Gouw, J. A. de, Veres, P. R.
4 and Roberts, J. M.: Investigating diesel engines as an atmospheric source of isocyanic acid in urban areas, Atmos.
5 Chem. Phys., 17(14), 8959–8970, 2017b.
- 6 Jimenez, J. L., Canagaratna, M. R., Donahue, N. M., Prevot, A. S. H., Zhang, Q., Kroll, J. H., DeCarlo, P. F., Allan, J.
7 D., Coe, H., Ng, N. L., Aiken, A. C., Docherty, K. S., Ulbrich, I. M., Grieshop, A. P., Robinson, A. L., Duplissy, J.,
8 Smith, J. D., Wilson, K. R., Lanz, V. A., Hueglin, C., Sun, Y. L., Tian, J., Laaksonen, A., Raatikainen, T., Rautiainen,
9 J., Vaattovaara, P., Ehn, M., Kulmala, M., Tomlinson, J. M., Collins, D. R., Cubison, M. J., Dunlea, E. J., Huffman, J.
0 A., Onasch, T. B., Alfarra, M. R., Williams, P. I., Bower, K., Kondo, Y., Schneider, J., Drewnick, F., Borrmann, S.,
1 Weimer, S., Demerjian, K., Salcedo, D., Cottrell, L., Griffin, R., Takami, A., Miyoshi, T., Hatakeyama, S., Shimono,
2 A., Sun, J. Y., Zhang, Y. M., Dzepina, K., Kimmel, J. R., Sueper, D., Jayne, J. T., Herndon, S. C., Trimborn, A. M.,
3 Williams, L. R., Wood, E. C., Middlebrook, A. M., Kolb, C. E., Baltensperger, U. and Worsnop, D. R.: Evolution of
4 organic aerosols in the atmosphere, Science, 326(5959), 1525–1529, 2009.
- 5 Kaltsonoudis, C., Kostenidou, E., Louvaris, E., Psichoudaki, M., Tsiligiannis, E., Florou, K., Liangou, A. and Pandis,
6 S. N.: Characterization of fresh and aged organic aerosol emissions from meat charbroiling, Atmos. Chem. Phys.,
7 17(11), 7143–7155, 2017.
- 8 Kim, P. S., Jacob, D. J., Fisher, J. A., Travis, K., Yu, K., Zhu, L., Yantosca, R. M., Sulprizio, M. P., Jimenez, J. L.,
9 Campuzano-Jost, P. and Others: Sources, seasonality, and trends of southeast US aerosol: an integrated analysis of

Formatted: Space After: 11 pt, Widow/Orphan control,
Border: Top: (No border), Bottom: (No border), Left: (No
border), Right: (No border), Between : (No border)

Formatted: Font: 12 pt

0 surface, aircraft, and satellite observations with the GEOS-Chem chemical transport model, *Atmos. Chem. Phys.*,
1 15(18), 10411–10433, 2015.

2 Kleeman, M. J. and Cas, G. R.: A 3D Eulerian source-oriented model for an externally mixed aerosol, *Environ. Sci.*
3 *Technol.*, 35(24), 4834–4848, 2001.

4 Kleeman, M. J., Ying, Q., Lu, J., Mysliwiec, M. J., Griffin, R. J., Chen, J. and Clegg, S.: Source apportionment of
5 secondary organic aerosol during a severe photochemical smog episode, *Atmos. Environ.*, 41(3), 576–591, 2007.

6 Koo, B., Knipping, E. and Yarwood, G.: 1.5-Dimensional volatility basis set approach for modeling organic aerosol in
7 CAMx and CMAQ, *Atmos. Environ.*, 95, 158–164, 2014.

8 [Koss, A. R., Sekimoto, K., Gilman, J. B., Selimovic, V., Coggon, M. M., Zarzana, K. J., Yuan, B., Lerner, B. M.,
9 Brown, S. S., Jimenez, J. L., Krechmer, J., Roberts, J. M., Warneke, C., Yokelson, R. J. and Gouw, J. de: Non-
10 methane organic gas emissions from biomass burning: identification, quantification, and emission factors from PTR-
11 ToF during the FIREX 2016 laboratory experiment, *Atmos. Chem. Phys.*, 18\(5\), 3299–3319, 2018.](#)

2 Krechmer, J. E., Pagonis, D., Ziemann, P. J. and Jimenez, J. L.: Quantification of Gas-Wall Partitioning in Teflon
3 Environmental Chambers Using Rapid Bursts of Low-Volatility Oxidized Species Generated in Situ, *Environ. Sci.*
4 *Technol.*, 50(11), 5757–5765, 2016.

5 Kroll, J. H. and Seinfeld, J. H.: Chemistry of secondary organic aerosol: Formation and evolution of low-volatility
6 organics in the atmosphere, *Atmos. Environ.*, 42(16), 3593–3624, 2008.

7 Kroll, J. H., Smith, J. D., Che, D. L., Kessler, S. H., Worsnop, D. R. and Wilson, K. R.: Measurement of
8 fragmentation and functionalization pathways in the heterogeneous oxidation of oxidized organic aerosol, *Phys.*
9 *Chem. Chem. Phys.*, 11(36), 8005–8014, 2009.

0 Kuwayama, T., Collier, S., Forestieri, S., Brady, J. M., Bertram, T. H., Cappa, C. D., Zhang, Q. and Kleeman, M. J.:
1 Volatility of Primary Organic Aerosol Emitted from Light Duty Gasoline Vehicles, *Environ. Sci. Technol.*, 49(3),
2 1569–1577, 2015.

3 Lim, Y. B. and Ziemann, P. J.: Effects of Molecular Structure on Aerosol Yields from OH Radical-Initiated Reactions
4 of Linear, Branched, and Cyclic Alkanes in the Presence of NO_x, *Environ. Sci. Technol.*, 43(7), 2328–2334, 2009.

5 Lipsky, E. M. and Robinson, A. L.: Effects of dilution on fine particle mass and partitioning of semivolatile organics
6 in diesel exhaust and wood smoke, *Environ. Sci. Technol.*, 40(1), 155–162, 2006.

7 Liu, T., Li, Z., Chan, M. and Chan, C. K.: Formation of secondary organic aerosols from gas-phase emissions of
8 heated cooking oils, *Atmos. Chem. Phys.*, 17(12), 7333–7344, 2017.

9 Louvaris, E. E., Florou, K., Karnezi, E., Papanastasiou, D. K., Gkatzelis, G. I. and Pandis, S. N.: Volatility of source
0 apportioned wintertime organic aerosol in the city of Athens, *Atmos. Environ.*, 158, 138–147, 2017.

1 [Louvaris, E. E., Karnezi, E., Kostenidou, E., Kaltsonoudis, C. and Pandis, S. N.: Estimation of the volatility
2 distribution of organic aerosol combining thermodenuder and isothermal dilution measurements, *Atmospheric
3 Measurement Techniques*, 10\(10\), 3909–3918, 2017.](#)

4 Loza, C. L., Craven, J. S., Yee, L. D., Coggon, M. M., Schwantes, R. H., Shiraiwa, M., Zhang, X., Schilling, K. A.,
5 Ng, N. L., Canagaratna, M. R., Ziemann, P. J., Flagan, R. C. and Seinfeld, J. H.: Secondary organic aerosol yields of
6 12-carbon alkanes, *Atmos. Chem. Phys.*, 14(3), 1423–1439, 2014.

7 Ma, P. K., Zhao, Y., Robinson, A. L., Worton, D. R., Goldstein, A. H., Ortega, A. M., Jimenez, J. L., Zotter, P.,
8 Prévôt, A. S. H., Szidat, S. and Others: Evaluating the impact of new observational constraints on PS/IVOC
9 emissions, multi-generation oxidation, and chamber wall losses on SOA modeling for Los Angeles, CA, *Atmos.*
0 *Chem. Phys.*, 17(15), 9237–9259, 2017.

1 May, A. A., Presto, A. A., Hennigan, C. J., Nguyen, N. T., Gordon, T. D. and Robinson, A. L.: Gas-particle
2 partitioning of primary organic aerosol emissions: (1) Gasoline vehicle exhaust, *Atmos. Environ.*, 77, 128–139,
3 2013a.

4 May, A. A., Presto, A. A., Hennigan, C. J., Nguyen, N. T., Gordon, T. D. and Robinson, A. L.: Gas-particle
5 partitioning of primary organic aerosol emissions: (2) diesel vehicles, *Environ. Sci. Technol.*, 47(15), 8288–8296,

Formatted: Space After: 11 pt, Widow/Orphan control,
Border: Top: (No border), Bottom: (No border), Left: (No
border), Right: (No border), Between : (No border)

Formatted: Font: 12 pt

Formatted: Space After: 11 pt, Widow/Orphan control,
Border: Top: (No border), Bottom: (No border), Left: (No
border), Right: (No border), Between : (No border)

Formatted: Font: 12 pt

- 2013b.
- May, A. A., Levin, E. J. T., Hennigan, C. J., Riipinen, I., Lee, T., Collett, J. L., Jimenez, J. L., Kreidenweis, S. M. and Robinson, A. L.: Gas-particle partitioning of primary organic aerosol emissions: 3. Biomass burning, *J. Geophys. Res. D: Atmos.*, 118(19) [online] Available from: <http://onlinelibrary.wiley.com/doi/10.1002/jgrd.50828/full>, 2013c.
- May, A. A., Nguyen, N. T., Presto, A. A., Gordon, T. D., Lipsky, E. M., Karve, M., Gutierrez, A., Robertson, W. H., Zhang, M., Brandow, C., Chang, O., Chen, S., Cicero-Fernandez, P., Dinkins, L., Fuentes, M., Huang, S.-M., Ling, R., Long, J., Maddox, C., Massetti, J., McCauley, E., Miguel, A., Na, K., Ong, R., Pang, Y., Rieger, P., Sax, T., Truong, T., Vo, T., Chattopadhyay, S., Maldonado, H., Maricq, M. M. and Robinson, A. L.: Gas- and particle-phase primary emissions from in-use, on-road gasoline and diesel vehicles, *Atmos. Environ.*, 88, 247–260, 2014.
- McDonald, B. C., Gentner, D. R., Goldstein, A. H. and Harley, R. A.: Long-term trends in motor vehicle emissions in US urban areas, *Environ. Sci. Technol.*, 47(17), 10022–10031, 2013.
- McDonald, B. C., de Gouw, J. A., Gilman, J. B., Jathar, S. H., Akherati, A., Cappa, C. D., Jimenez, J. L., Lee-Taylor, J., Hayes, P. L., McKeen, S. A., Cui, Y. Y., Kim, S.-W., Gentner, D. R., Isaacman-VanWertz, G., Goldstein, A. H., Harley, R. A., Frost, G. J., Roberts, J. M., Ryerson, T. B. and Trainer, M.: Volatile chemical products emerging as largest petrochemical source of urban organic emissions, *Science*, 359(6377), 760–764, 2018.
- Miracolo, M. A., Presto, A. A., Lambe, A. T., Hennigan, C. J., Donahue, N. M., Kroll, J. H., Worsnop, D. R. and Robinson, A. L.: Photo-Oxidation of Low-Volatility Organics Found in Motor Vehicle Emissions: Production and Chemical Evolution of Organic Aerosol Mass, *Environ. Sci. Technol.*, 44(5), 1638–1643, 2010.
- Murphy, B. N., Woody, M. C., Jimenez, J. L., Carlton, A. M. G., Hayes, P. L., Liu, S., Ng, N. L., Russell, L. M., Setyan, A., Xu, L., Young, J., Zaveri, R. A., Zhang, Q. and Pye, H. O. T.: Semivolatile POA and parameterized total combustion SOA in CMAQv5.2: impacts on source strength and partitioning, *Atmos. Chem. Phys.*, 17(18), 11107–11133, 2017.
- Murphy, B. N. and Pandis, S. N.: Simulating the formation of semivolatile primary and secondary organic aerosol in a regional chemical transport model, *Environ. Sci. Technol.*, 43(13), 4722–4728, 2009.
- Murphy, B. N., Donahue, N. M., Robinson, A. L. and Pandis, S. N.: A naming convention for atmospheric organic aerosol, *Atmos. Chem. Phys.*, 14(11), 5825–5839, 2014.
- Ng, N. L., Kroll, J. H., Chan, A. W. H., Chhabra, P. S., Flagan, R. C. and Seinfeld, J. H.: benzene, *Atmos. Chem. Phys.*, 7, 3909–3922, 2007a.
- Ng, N. L., Chhabra, P. S., Chan, A., Surratt, J. D., Kroll, J. H., Kwan, A. J., McCabe, D. C., Wennberg, P. O., Sorooshian, A., Murphy, S. M. and Others: Effect of NO_x level on secondary organic aerosol (SOA) formation from the photooxidation of terpenes, *Atmos. Chem. Phys.*, 7(19), 5159–5174, 2007b.
- Pachauri, R. K., Allen, M. R., Barros, V. R., Broome, J., Cramer, W., Christ, R., Church, J. A., Clarke, L., Dahe, Q., Dasgupta, P., Dubash, N. K., Edenhofer, O., Elgizouli, I., Field, C. B., Forster, P., Friedlingstein, P., Fuglestad, J., Gomez-Echeverri, L., Hallegatte, S., Hegerl, G., Howden, M., Jiang, K., Jimenez Cisneros, B., Kattsov, V., Lee, H., Mach, K. J., Marotzke, J., Mastrandrea, M. D., Meyer, L., Minx, J., Mulugetta, Y., O'Brien, K., Oppenheimer, M., Pereira, J. J., Pichs-Madruga, R., Plattner, G.-K., Pörtner, H.-O., Power, S. B., Preston, B., Ravindranath, N. H., Reisinger, A., Riahi, K., Rusticucci, M., Scholes, R., Seyboth, K., Sokona, Y., Stavins, R., Stocker, T. F., Tschakert, P., van Vuuren, D. and van Ypersele, J.-P.: Climate Change 2014: Synthesis Report. Contribution of Working Groups I, II and III to the Fifth Assessment Report of the Intergovernmental Panel on Climate Change, edited by R. K. Pachauri and L. Meyer, IPCC, Geneva, Switzerland., 2014.
- Pagonis, D., Krechmer, J. E., de Gouw, J., Jimenez, J. L. and Ziemann, P. J.: Effects of gas–wall partitioning in Teflon tubing and instrumentation on time-resolved measurements of gas-phase organic compounds, *Atmospheric Measurement Techniques*, Katlenburg-Lindau, 10(12), 4687–4696, 2017.
- Praske, E., Otkjær, R. V., Crounse, J. D., Hethcox, J. C., Stoltz, B. M., Kjaergaard, H. G. and Wennberg, P. O.: Atmospheric autoxidation is increasingly important in urban and suburban North America, *Proc. Natl. Acad. Sci. U. S. A.*, 115(1), 64–69, 2018.
- Presto, A. A., Miracolo, M. A., Donahue, N. M. and Robinson, A. L.: Secondary Organic Aerosol Formation from High-NO_x Photo-Oxidation of Low Volatility Precursors: n-Alkanes, *Environ. Sci. Technol.*, 44(6), 2029–2034, 2010.

Formatted: Space After: 11 pt, Widow/Orphan control, Border: Top: (No border), Bottom: (No border), Left: (No border), Right: (No border), Between : (No border)

Formatted: Font: 12 pt

- Presto, A. A. and Donahue, N. M.: Investigation of α -pinene+ ozone secondary organic aerosol formation at low total aerosol mass, *Environ. Sci. Technol.* [online] Available from: <https://pubs.acs.org/doi/abs/10.1021/es052203z>, 2006.
- Pye, H. O. T. and Pouliot, G. A.: Modeling the role of alkanes, polycyclic aromatic hydrocarbons, and their oligomers in secondary organic aerosol formation, *Environ. Sci. Technol.*, 46(11), 6041–6047, 2012.
- Pye, H. O. T. and Seinfeld, J. H.: A global perspective on aerosol from low-volatility organic compounds, *Atmos. Chem. Phys.*, 10(9), 4377–4401, 2010.
- Robinson, A. L., Donahue, N. M., Shrivastava, M. K., Weitkamp, E. A., Sage, A. M., Grieshop, A. P., Lane, T. E., Pierce, J. R. and Pandis, S. N.: Rethinking organic aerosols: semivolatile emissions and photochemical aging, *Science*, 315(5816), 1259–1262, 2007.
- Robinson, A. L., Grieshop, A. P., Donahue, N. M. and Hunt, S. W.: Updating the Conceptual Model for Fine Particle Mass Emissions from Combustion Systems Allen L. Robinson, *J. Air Waste Manage. Assoc.*, 60(10), 1204–1222, 2010.
- Schauer, J. J., Kleeman, M. J., Cass, G. R. and Simoneit, B. R. T.: Measurement of Emissions from Air Pollution Sources. 2. C1 through C30 Organic Compounds from Medium Duty Diesel Trucks, *Environ. Sci. Technol.*, 33(10), 1578–1587, 1999.
- Schauer, J. J., Kleeman, M. J., Cass, G. R. and Simoneit, B. R. T.: Measurement of Emissions from Air Pollution Sources. 3. C1–C29 Organic Compounds from Fireplace Combustion of Wood, *Environ. Sci. Technol.*, 35(9), 1716–1728, 2001.
- Schauer, J. J., Kleeman, M. J., Cass, G. R. and Simoneit, B. R. T.: Measurement of Emissions from Air Pollution Sources. 4. C1–C27 Organic Compounds from Cooking with Seed Oils, *Environ. Sci. Technol.*, 36(4), 567–575, 2002a.
- Schauer, J. J., Kleeman, M. J., Cass, G. R. and Simoneit, B. R. T.: Measurement of Emissions from Air Pollution Sources. 5. C1–C32 Organic Compounds from Gasoline-Powered Motor Vehicles, *Environ. Sci. Technol.*, 36(6), 1169–1180, 2002b.
- Shrivastava, M. K., Lane, T. E., Donahue, N. M., Pandis, S. N. and Robinson, A. L.: Effects of gas particle partitioning and aging of primary emissions on urban and regional organic aerosol concentrations, *J. Geophys. Res. D: Atmos.*, 113(D18) [online] Available from: <http://onlinelibrary.wiley.com/doi/10.1029/2007JD009735/full>, 2008.
- Stockwell, C. E., Veres, P. R., Williams, J. and Yokelson, R. J.: Characterization of biomass burning emissions from cooking fires, peat, crop residue, and other fuels with high-resolution proton-transfer-reaction time-of-flight mass spectrometry, *Atmos. Chem. Phys.*, 15(2), 845–865, 2015.
- Subramanian, R., Khlystov, A. Y., Cabada, J. C. and Robinson, A. L.: Positive and negative artifacts in particulate organic carbon measurements with denuded and undenuded sampler configurations special issue of aerosol science and technology on findings from the fine particulate matter supersites program, *Aerosol Sci. Technol.*, 38(S1), 27–48, 2004.
- Sunol, A. M., Charan, S. M. and Seinfeld, J. H.: Computational simulation of the dynamics of secondary organic aerosol formation in an environmental chamber, *Aerosol Sci. Technol.*, 52(4), 470–482, 2018.
- Tkacik, D. S., Presto, A. A., Donahue, N. M. and Robinson, A. L.: Secondary Organic Aerosol Formation from Intermediate-Volatility Organic Compounds: Cyclic, Linear, and Branched Alkanes, *Environ. Sci. Technol.*, 46(16), 8773–8781, 2012.
- Tkacik, D. S., Robinson, E. S., Ahern, A., Saleh, R., Stockwell, C., Veres, P., Simpson, I. J., Meinardi, S., Blake, D. R., Yokelson, R. J., Presto, A. A., Sullivan, R. C., Donahue, N. M. and Robinson, A. L.: A dual-chamber method for quantifying the effects of atmospheric perturbations on secondary organic aerosol formation from biomass burning emissions, *J. Geophys. Res. D: Atmos.*, 122(11), 2016JD025784, 2017.
- Tsimpidi, A. P., Karydis, V. A., Zavala, M., Lei, W., Molina, L., Ulbrich, I. M., Jimenez, J. L. and Pandis, S. N.: Evaluation of the volatility basis-set approach for the simulation of organic aerosol formation in the Mexico City metropolitan area, *Atmos. Chem. Phys.*, 10(2), 525–546, 2010.
- Turpin, B. J. and Lim, H.-J.: Species Contributions to PM_{2.5} Mass Concentrations: Revisiting Common Assumptions

Formatted: Space After: 11 pt, Widow/Orphan control, Border: Top: (No border), Bottom: (No border), Left: (No border), Right: (No border), Between : (No border)

Formatted: Font: 12 pt

for Estimating Organic Mass, *Aerosol Sci. Technol.*, 35(1), 602–610, 2001.

Volkamer, R., Jimenez, J. L., San Martini, F., Dzepina, K., Zhang, Q., Salcedo, D., Molina, L. T., Worsnop, D. R. and Molina, M. J.: Secondary organic aerosol formation from anthropogenic air pollution: Rapid and higher than expected, *Geophys. Res. Lett.*, 33(17), 4407, 2006.

Warneke, C., de Gouw, J. A., Holloway, J. S., Peischl, J., Ryerson, T. B., Atlas, E., Blake, D., Trainer, M. and Parrish, D. D.: Multiyear trends in volatile organic compounds in Los Angeles, California: Five decades of decreasing emissions: TRENDS IN VOCS IN LOS ANGELES, *J. Geophys. Res.*, 117(D21), doi:10.1029/2012JD017899, 2012.

Wiedinmyer, C., S. K. Akagi, University of Montana-Missoula, Robert J. Yokelson, University of Montana-Missoula, Emmons, L. K., Al-Saadi, J. A., Orlando, J. J., Soja, A. J. and Authors: The Fire INventory from NCAR (FINN): A High Resolution Global Model to Estimate the Emissions from Open Burning, *Geoscientific Model Development*, 4(3), 625, 2011.

Woody, M. C., Baker, K. R., Hayes, P. L., Jimenez, J. L., Koo, B. and Pye, H. O. T.: Understanding sources of organic aerosol during CalNex-2010 using the CMAQ-VBS, *Atmos. Chem. Phys.*, 16(6), 4081–4100, 2016.

Worton, D. R., Isaacman, G., Gentner, D. R., Dallmann, T. R., Chan, A. W. H., Ruehl, C., Kirchstetter, T. W., Wilson, K. R., Harley, R. A. and Goldstein, A. H.: Lubricating oil dominates primary organic aerosol emissions from motor vehicles, *Environ. Sci. Technol.*, 48(7), 3698–3706, 2014.

Xu, L., Guo, H., Boyd, C. M., Klein, M., Bougiatioti, A., Cerully, K. M., Hite, J. R., Isaacman-VanWertz, G., Kreisberg, N. M., Knote, C., Olson, K., Koss, A., Goldstein, A. H., Hering, S. V., de Gouw, J., Baumann, K., Lee, S.-H., Nenes, A., Weber, R. J. and Ng, N. L.: Effects of anthropogenic emissions on aerosol formation from isoprene and monoterpenes in the southeastern United States, *Proc. Natl. Acad. Sci. U. S. A.*, 112(1), 37–42, 2015.

Zhang, Q., Jimenez, J. L., Canagaratna, M. R., Allan, J. D., Coe, H., Ulbrich, I., Alfarra, M. R., Takami, A., Middlebrook, A. M., Sun, Y. L. and Others: Ubiquity and dominance of oxygenated species in organic aerosols in anthropogenically-influenced Northern Hemisphere midlatitudes, *Geophys. Res. Lett.*, 34(13) [online] Available from: <https://agupubs.onlinelibrary.wiley.com/doi/abs/10.1029/2007GL029979>, 2007.

Zhang, Q. J., Beekmann, M., Freney, E., Sellegri, K., Pichon, J. M., Schwarzenboeck, A., Colomb, A., Bourrianne, T., Michoud, V. and Borbon, A.: Formation of secondary organic aerosol in the Paris pollution plume and its impact on surrounding regions, *Atmos. Chem. Phys.*, 15(24), 13973–13992, 2015.

Zhang, Q. J., Beekmann, M., Drewnick, F., Freutel, F., Schneider, J., Crippa, M., Prevot, A. S. H., Baltensperger, U., Poulain, L., Wiedensohler, A., Sciare, J., Gros, V., Borbon, A., Colomb, A., Michoud, V., Doussin, J.-F., Denier van der Gon, H. A. C., Haeffelin, M., Dupont, J.-C., Siour, G., Petetin, H., Bessagnet, B., Pandis, S. N., Hodzic, A., Sanchez, O., Honoré, C. and Perrussel, O.: Formation of organic aerosol in the Paris region during the MEGAPOLI summer campaign: evaluation of the volatility-basis-set approach within the CHIMERE model, *Atmos. Chem. Phys.*, 13(11), 5767–5790, 2013.

Zhang, X., Cappa, C. D., Jathar, S. H., McVay, R. C., Ensberg, J. J., Kleeman, M. J. and Seinfeld, J. H.: Influence of vapor wall loss in laboratory chambers on yields of secondary organic aerosol, *Proc. Natl. Acad. Sci. U. S. A.*, 111(16), 5802–5807, 2014.

Zhao, Y., Hennigan, C. J., May, A. A., Tkacik, D. S., de Gouw, J. A., Gilman, J. B., Kuster, W. C., Borbon, A. and Robinson, A. L.: Intermediate-Volatility Organic Compounds: A Large Source of Secondary Organic Aerosol, *Environ. Sci. Technol.*, 48(23), 13743–13750, 2014.

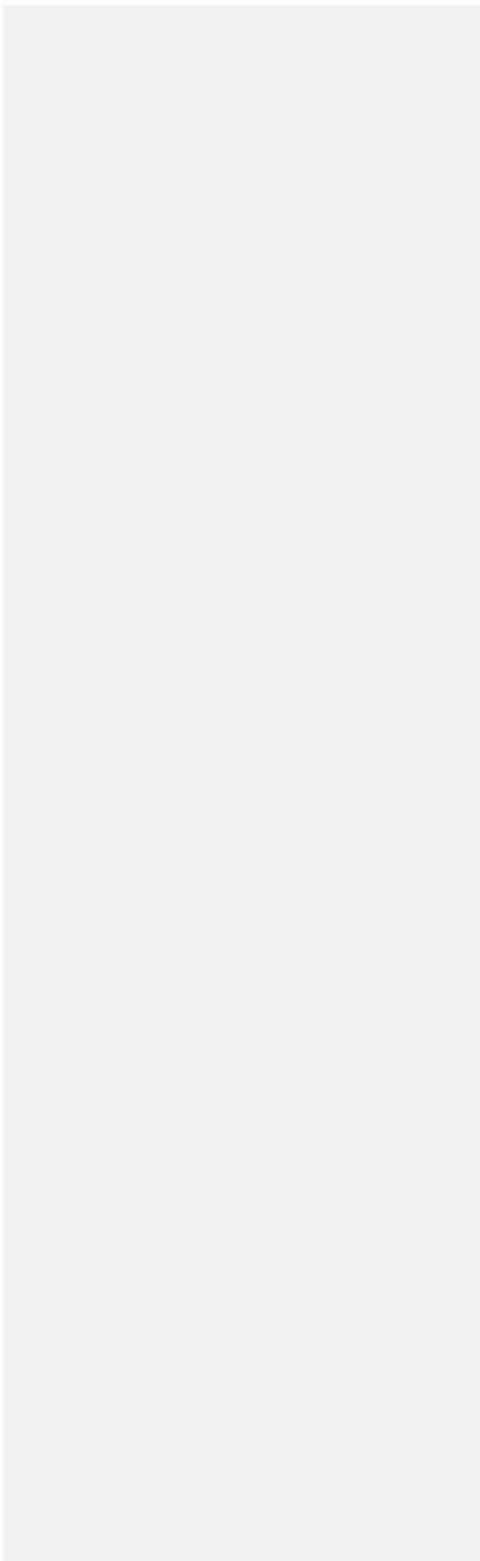
Zhao, Y., Nguyen, N. T., Presto, A. A., Hennigan, C. J., May, A. A. and Robinson, A. L.: Intermediate volatility organic compound emissions from on-road diesel vehicles: chemical composition, emission factors, and estimated secondary organic aerosol production, *Environ. Sci. Technol.*, 49(19), 11516–11526, 2015.

Zhao, Y., Nguyen, N. T., Presto, A. A., Hennigan, C. J., May, A. A. and Robinson, A. L.: Intermediate Volatility Organic Compound Emissions from On-Road Gasoline Vehicles and Small Off-Road Gasoline Engines, *Environ. Sci. Technol.*, 50(8), 4554–4563, 2016.

Zhao, Y., Saleh, R., Saliba, G., Presto, A. A., Gordon, T. D., Drozd, G. T., Goldstein, A. H., Donahue, N. M. and Robinson, A. L.: Reducing secondary organic aerosol formation from gasoline vehicle exhaust, *Proc. Natl. Acad. Sci. U. S. A.*, 114(27), 6984–6989, 2017.

Formatted: Space After: 11 pt, Widow/Orphan control, Border: Top: (No border), Bottom: (No border), Left: (No border), Right: (No border), Between : (No border)

Formatted: Font: 12 pt



Subscript

Subscript

Subscript

▲